# Turgor regulation in species of *Vaucheria* (Xanthophyceae, Heterokontophyta) from habitats of contrasting salinities

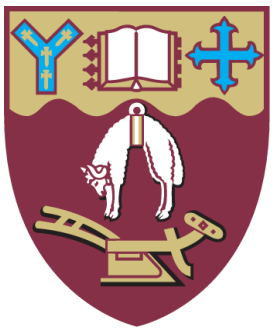

A thesis
submitted in partial fulfilment
of the requirements for the Degree
of

Doctor of Philosophy

at the
University of Canterbury
New Zealand

---

Abishek Muralidhar

2014

**Dedicated to the memory of Pati and Thata**

# Contents

## List of figures

## List of tables

## Acknowledgements

Words cannot express my gratitude to Dr. Ashley Garrill and Dr. Paul Broady, who have been the most wonderful supervisors. I can't thank Ashley enough for putting up with me these last three years. He has been a great mentor who has encouraged me, thought me how to think critically and is responsible for my development as a researcher. I am indebted to Paul for giving me an opportunity to carry out this study and for his enthusiasm and approachability.

I would also like to thank my associate supervisors - Dr. David Collings for his support and advice and Dr. Phil Novis for his expertise and guidance with the molecular study. Special thanks to Prof. Sergey Shabala and Dr. Lana Shabala for being gracious hosts during my visit to their laboratory for the MIFE experiments. I am also grateful for technical assistance and advice from Dr. Matt Polson, Manfred Ingerfeld, Alan Woods, Reijel Gardener, Craig Galillee, Dr. Krithika Yogeshwaran, Dr. Chris Glover, Nic Bolteridge, Dr. Rob Smissen and Matt Walters. Thanks are also in order to my labmates- Faradina, Francine, Freddie, Pat, Sitara, Aliaa, Gloria, Emma and Gonda for keeping me sane.

I could not have got to this stage without my parents, who have been my pillars of strength. This thesis is as much theirs as it is mine. I owe it all to their unconditional support. I can't thank my girlfriend, Nirupama enough for being so patient and backing me over the last four years. She has been with me through this entire rollecoaster ride and I wouldn't be here without her. I would also like to thank my sister, Aparna, for motivating me and being one of my biggest well-wishers. I am indebted to my grandma and grandpa (pati and thata), who were around when I started off on this journey. They had a big influence on me and live on in my memory. I would also like to thank my extended family in Chennai, Dehi, Cochin and North Carolina, for their undying love and affection and my friends back home for giving me regular updates of happenings.

# ABSTRACT

Turgor regulation is the process by which walled organisms alter their internal osmotic potential to adapt to osmotic changes in the environment. Much of what we know regarding turgor regulation and osmotic adjustment in algae is limited to the green characean and chlorphytan algae. This thesis is an investigation of turgor regulation in two species of the yellow-green xanthophycean alga, *Vaucheria*.

The first part of this study involved the collection and identification of species of *Vaucheria* from contrasting habitats in New Zealand. Seven species of *Vaucheria* were identified based on the morphology of their reproductive structures. Two were described as new species (*V. aestuarii* and *V. edaphica*) and two others were reported for the first time from New Zealand (*V. erythrospora* and *V. litorea*). The genetic variation and phylogenetic position of these species were studied using phylogenetic analyses of *rbc*L sequences.

Two of the species from contrasting habitats were selected for a comparative study on turgor regulation. These were *Vaucheria erythrospora,* isolated from an estuarine habitat, and *Vaucheria repens*, isolated from a freshwater habitat. Using a single cell pressure probe to directly measure turgor after hyperosmotic shock, *V. erythrospora* was found to recover turgor after a larger shock than *V. repens*. Threshold shock values for this ability were > 0.5 MPa for *V. erythrospora* and < 0.5 MPa for *V. repens*. Recovery was more rapid in *V. erythrospora* than *V. repens* after comparable shocks. Growth studies showed that *V. erythrospora* was able to grow and maintain turgor over a wider range of NaCl concentrations. These responses are thought to underlie the ability of *V. erythrospora* to survive in an estuarine habitat and restrict *V. repens* to freshwater.

The final part of this study investigated the mechanisms underlying turgor regulation in *V. erythrospora*. Different responses were observed depending on whether NaCl or sorbitol was used to elicit the shock. Membrane potential ($E_m$) measurements showed a rapid depolarization of the plasma membrane in response to a NaCl-induced hyperosmotic shock, followed by a slower repolarization, and recovery almost back to the resting $E_m$. MIFE recordings indicate a net $K^+$ efflux, a response that has been reported in other systems. While recordings of $Na^+$ fluxes were not possible due to the high external $Na^+$, these may account for the depolarisation and recovery of turgor as turgor recovery was inhibited by the non-selective cation channels (NSCCs) inhibitor $Gd^{3+}$ and was dependant on the external $Na^+$ concentration. An equivalent sorbitol-induced hyperosmotic shock hyperpolarized the $E_m$, followed by depolarization and recovery back to the resting $E_m$. Net flux recordings showed that both $K^+$ and $Na^+$ were taken up in response to a sorbitol shock when there was a low external $Na^+$ concentration (1mM). $K^+$ was possibly taken up through inward rectifying $K^+$ channels activated by membrane hyperpolarization. The ability of *V. erythrospora* to rapidly regulate turgor by taking up ions during hyperosmotic stress is the possible reason for its survival in an estuarine habitat.

Deputy Vice-Chancellor's Office
Postgraduate Office

UNIVERSITY OF CANTERBURY
Te Whare Wānanga o Waitaha
CHRISTCHURCH NEW ZEALAND

# Co-Authorship Form

This form is to accompany the submission of any PhD thesis that contains research reported in co-authored work that has been published, accepted for publication, or submitted for publication. A copy of this form should be included for each co-authored work that is included in the PhD thesis. Completed forms should be included at the front (after the thesis abstract) of each copy of the thesis submitted for examination and library deposit (including electronic copy).

Please indicate the chapter/section/pages of this thesis that are extracted from co-authored work and provide details of the publication or submission from the extract comes:

Chapter 2:

Muralidhar, A, Broady, PA, MacIntyre DP, Wilcox, MD, Garrill, A, .Novis, PM, (2014) Morphological and phylogenetic characterization of seven species of *Vaucheria*, including two new species, from contrasting habitats in New Zealand. Phytotaxa (under review)

Chapter 3 and some of inhibitor studies from Chapter 4:

Muralidhar, A, Novis, PM, Broady, PA, Collings, DA, Garrill, A. (2013) An estuarine species of the alga *Vaucheria* (Xanthophyceae) displays an increased capacity for turgor regulation when compared to a freshwater species. Journal of Phycology 49: 967-978.

Please detail the nature and extent (%) of contribution by the PhD candidate:
Abishek Muralidhar was involved in much of the experimental design, carried out all of the experiments and wrote both of the manuscripts. Overall contribution ~85%.

**Certification by Co-authors:**

If there is more than one co-author then a single co-author vcan sign on behalf of all

The undersigned certifies that:

- The above statement correctly reflects the nature and extent of the PhD candidate's contribution to this co-authored work
- In cases where the PhD candidate was the lead author of the co-authored work he or she wrote the text

| | | |
|---|---|---|
| Name: Ashley Garrill | Signature:  | Date: 1st February 2014 |

# ABBREVIATIONS

ATP - Adenosine triphosphate

bp - Base pairs

*cf.* - Confer/compare to

cst - Centistokes

$E_m$ - Membrane potential

GC-MS - Gas chromatography-mass spectrometry

mOsmol - Milliosmols

MPa - Megapascal

mV - Millivolts

p-distance - Proportion (p) of nucleotide sites which differ between two sequences

ppt - Parts per thousand

*rbc*L - Ribulose bisphosphate carboxylase large chain

SE - Standard error of the mean

SD - Standard deviation

w/v - Weight/volume

# Chapter 1

# Introduction

This thesis investigates the responses of species of the yellow-green alga *Vaucheria* to osmotic stress. This introductory chapter is intended as an overview to set the other chapters in context. Each individual chapter has its own detailed introduction. Section 1.1 explains key concepts such as water potential, osmotic potential and turgor and the impact of osmotic stress on algae from different environments. Section 1.2 describes why this study is of relevance and relates it to comparable studies in other algae. Section 1.3 provides a description of the morphology and ecology of *Vaucheria*. Osmotic adaptations and mechanisms underlying turgor regulation in algae, plants and fungi are reviewed in sections 1.4 and 1.5. Finally, section 1.6 summarises the key aims of this thesis and outlines the content of the other chapters.

## 1.1. The impact of varying osmotic potential

The ability to respond to changes in external osmotic potential is likely to be a key determinant in the distribution of organisms in different aquatic habitats. In such habitats, osmotic potential is determined by the concentration of dissolved salts or salinity of water. Sodium and chloride are the major dissolved ions contributing to salinity. Because the concentration of dissolved salts can differ between different aquatic habitats, the osmotic potential also varies. In marine habitats, the salinity varies only slightly, for example, the open ocean has a salinity of 33-37 ppt. This sets the osmotic potential of these habitats at around - 2.5 MPa. Freshwater habitats such as lakes and rivers have lower concentrations of dissolved salts with a salinity of < 0.5 ppt and an osmotic potential of about - 0.005 MPa. These two habitats are similar in that they exhibit little or no variation in osmotic potential. In contrast, brackish habitats like estuaries, and lagoons, typically exhibit fluctuations in

osmotic potential. In estuarine habitats, fluctuations in osmotic potential can be attributed to a combination of different factors. The biggest factor is the difference in the mixing of freshwater and seawater governed by the tidal cycle (Karsten et al. 1991, Bisson and Kirst 1995). Salinity can vary from < 0.05 ppt, due to dilution caused by freshwater, to that of full strength seawater (35 ppt) during high tides (Kirst 1990). This can result in osmotic potential fluctuations of the range of 2 MPa over a tidal cycle. Contributing to these fluctuations are dilution due to rainfall and concentration due to evaporation. Stratification of freshwater and saline layers in some estuaries may also govern the duration and magnitude of these fluctuations (Young et al. 1987a). Figure 1.1 shows the fluctuations in salinity and volume of water flowing through a model estuary over a tidal cycle.

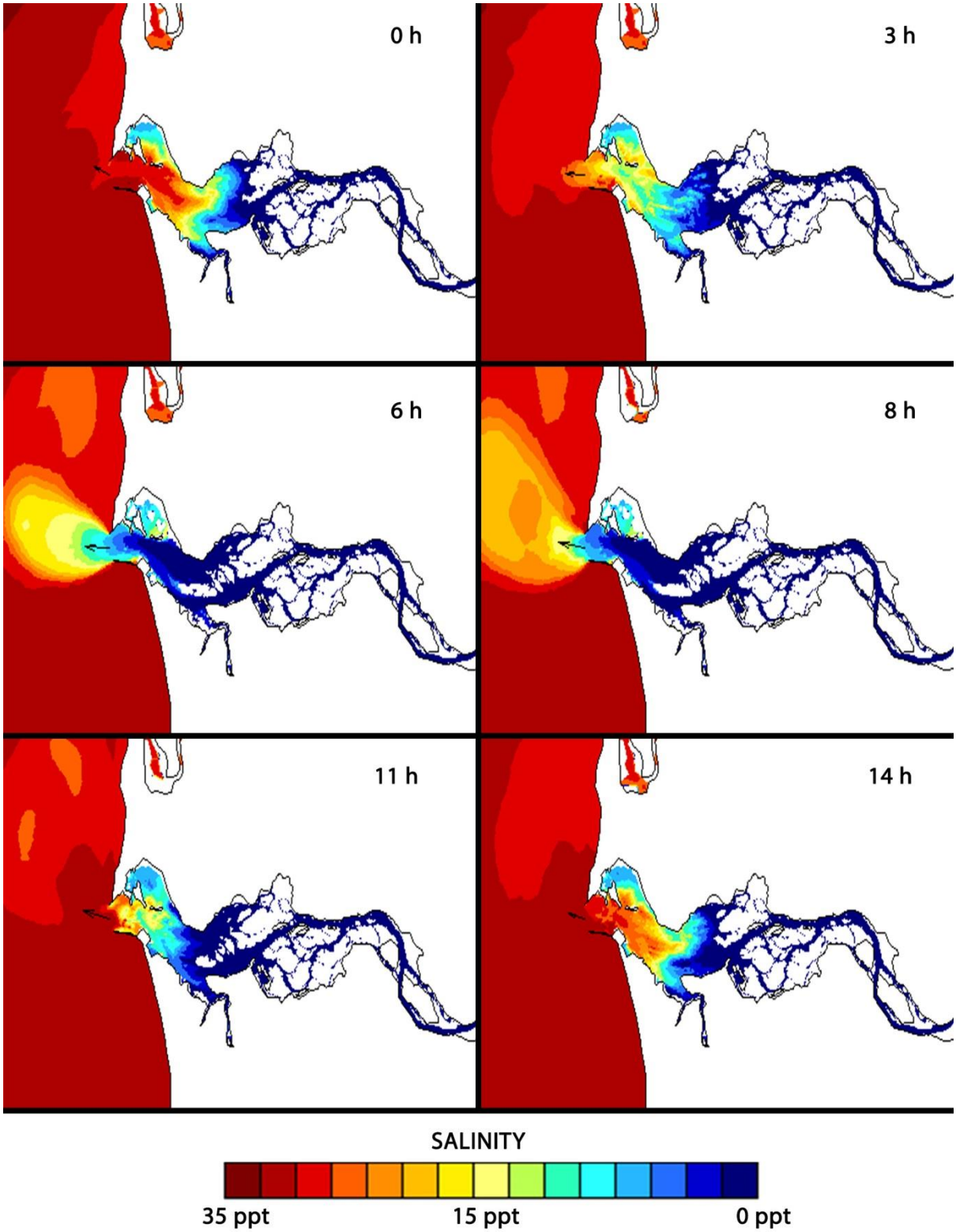


**Fig 1.1.** Model showing salinity fluctuations in an estuary over time. The red colour represents high salinity (seawater) and the blue represents low salinity. Notice in addition to the salinity changes, there are changes in the volume of water flowing through the estuary. Figure adapted from animation obtained from : http://www.sciencebuzz.org/image/animation-estuary-salinity ; retrieved on 2.10.2013

These fluctuations in osmotic potential can have a direct bearing on the water status of organisms and can prove to be stressful, especially for sessile plants and algae. Algae in particular are found in habitats with widely different osmotic potentials (Kirst 1990). Algae that colonize habitats that are consistently freshwater, e.g. rivers, or are consistently saline, e.g. the open ocean, are usually stenohalinic, i.e. they are unable to survive in wide fluctuations of salinity and osmotic potential. For example stenohaline charophyte algae include *Chara corallina*, which is restricted to freshwater, and the chlorophyte *Dunaliella salina* which is restricted to waters of high salinity (Cowan et al. 1992; Kiegle & Bisson 1996).

In contrast, algae found in brackish habitats such as estuaries, are termed euryhaline as they are adapted to a wide range of salinities. These include the chlorophyte microalgae *Chlorella autotrophica* and *Tetraselmis subcordiformis*, and the macroalgae *Enteromorpha intestinalis* and *Chara longifolia* (Kirst 1977; Ahmad & Hellebust 1984; Young et al. 1987b; Kiegle & Bisson 1996). Macroalgae are the dominant flora in intertidal and estuarine habitats worldwide (Schiel & Foster 2006). The most common among these include the brown algae, belonging to the orders Laminariales (true kelps) and Fucales (fucoids). Wilkinson et al. (1995) have shown that the spatial distribution of macroalgae is dependent on the salinity gradients created by the mixing of freshwater and seawater and is similar in estuaries worldwide. This observation was based on a comparative analysis of algal species from estuaries over a wide latitudinal range in different continents. This study identified three algal zones in estuaries- Zone A includes the mouth of the estuary with a large number of macroalgal species and is dominated by fucoids; Zone B is further up the estuary, which has fewer species and fucoids still dominate; Zone C is more greatly affected

by freshwater river inflow and is characterized by mat-forming brackish species such as the xanthophycean *Vaucheria* and the chlorophyte *Enteromorpha*.

### 1.1.1. Water potential, turgor and its significance

Diverse groups of algae have presumably evolved physiological strategies to successfully colonise the habitats described above. Though the exact mechanistic details of the strategies may differ between algae, central to all is the ability to move water into and out of cells as the need arises. Water is important for most physiological and biochemical processes in all organisms. It constitutes the majority of the fresh weight of living cells. It acts as a solvent and medium for transport of organic and mineral nutrients as well as gases and is also vital as an electron provider in photosynthesis. Turgor also provides structural integrity to cells and drives growth through hydrostatic pressure or turgor. Osmotic potential directly impacts the water status of these organisms, thereby governing their growth in these habitats. This can be explained using the concepts of water potential and turgor.

Water potential is a term that describes the potential energy of water per unit volume and it is this that governs its tendency to move from one location to another (Boyer 1969). Water always moves from a region of high water potential to one of low water potential. Water potential is denoted by the Greek letter psi (Ψ) and is measured in terms of pressure in megapascals (MPa). It is influenced by many forces acting on water, expressed in the following equation (Boyer 1969; Duniway 1979):

$$\mathbf{\Psi = \Psi_g + \Psi_m + \Psi_s + \Psi_p,}$$

where **g**, **m**, **s** and **p** refer to the gravity, matrix, solutes and pressure components of water potential.

Gravity potential ($\Psi_g$) describes the movement of water due to gravity. $\Psi_g$ is negligible at the cellular level, but may be a critical component of the water potential in tall trees (Boyer 1969). In such a situation, it is a limiting force which a plant must overcome to move water upwards.

Matric potential ($\Psi_m$) is brought about by the adsorption of water molecules to interfaces in solid substrates. This matrix for the adhesion of water is provided by hydrophilic molecules (for example cellulose) that make up the cell wall or substrates like soil (Duniway 1979). The binding of water reduces its potential energy as it limits its movement. Matric potential is thought to be more relevant in dry terrestrial habitats, where water is scarce. It is negligible in aquatic habitats saturated with water and in plant tissues composed of highly vacuolated cells. In these cases the term is left out of water potential measurements (Boyer 1969).

Osmotic potential or solute potential ($\Psi s$) represents the effect of dissolved solutes and has the biggest impact on water potential. Pure water has an osmotic potential of zero. As the amount of solutes in water increases, the $\Psi_s$ becomes more negative. This relationship can be explained in terms of the van't Hoff equation:

$$\Psi s = - M i RT,$$

where,

**M** = concentration of solute in moles (molarity)

***i*** **=** van't Hoff factor- this is the ratio between the actual concentration of particles when solute is dissolved, and concentration of solute estimated from its mass

**R =** ideal gas constant (8.31 J. mol $^{-1}$. K$^{-1}$)

**T**= absolute temperature (Kelvin)

Cells have a greater concentration of solutes than the outside, i.e., a more negative osmotic potential ($\Psi_s$) with respect to the external environment. This creates an osmotic gradient between the outside of the cell (higher $\Psi_w$) to the inside (lower $\Psi_w$) that causes water to move into the cell through the plasma membrane. The inward movement of water directly raises the pressure potential or hydrostatic pressure of the cell ($\Psi_p$). For example, in walled algal cells with a rigid outer wall, an increase in $\Psi_p$ will cause the plasma membrane to push against the wall. In this state, the cells are said to be turgid, and the pressure exerted on the cell wall is called turgor.

The rigidity of the cell wall enables algal, plant and fungal cells to establish high turgor pressures in ranges that can be equivalent to the pressure of tyres of cars and bicycles (Sanati Nezhad & Geitmann 2013). Turgor is thought to be the driving force for the growth of walled cells. This growth occurs due to the yielding of the plastic cell wall to the turgor (Cleland 1967; Ray et al. 1972; Taiz 1984; Bisson & Kirst 1995). Turgor provides form and rigidity to cells which is vital for their proper physiological functioning (Bisson & Kirst 1995). A loss of turgor can lead to distortion to the membrane and membrane bound proteins and also organelles (Bisson & Kirst 1995).

### 1.1.2. What makes an estuarine habitat stressful?

To drive water uptake and maintain turgor, cells need to maintain a negative osmotic potential with respect to the environment. Achieving this under conditions of constantly varying osmotic potential such as in estuaries, is a challenge (Fig 1.1). The movement of seawater into an estuary concentrates the water with salts, making it hyperosmotic for an organism. The $\Psi_s$ of seawater is about -2.5 MPa, which would generate a gradient for the water to move out of the cell towards the more negative $\Psi$ on the outside (Duniway 1979).

This would lead to plasmolysis, the retraction of the protoplast away from the cell wall. A prolonged plasmolysis can cause irreversible damage to the plasma membrane and subcellular structures (Oparka 1994). To survive an organism has to adapt by raising its internal solute concentration sufficiently to take in water and restore turgor. These conditions essentially reverse when the seawater is diluted by fresh water from a river, making it hypoosmotic relative to the inside of the cell. The inside of the cell would now have a more negative $\Psi$ with respect to the outside, causing water to move into the cell. The turgor pressure under this condition would rise rapidly, pushing the protoplast harder against the cell wall, which has a threshold level of turgor it can withstand. The organism therefore has to lower its internal solute concentration, to move water out and lower the turgor.

As these changes happen frequently in an estuary, for an organism to survive, it not only has to constantly adjust to the changes in osmotic potential but also needs to ensure that normal cellular processes like growth and photosynthesis are functioning optimally in the face of any mechanisms that maintain the turgor at a constant value. Therefore organisms have evolved mechanisms for osmotic adjustment that retain turgor, under stressful conditions. This process of alteration of the internal osmotic potential in response to changes in the external osmotic potential to restore turgor is termed as turgor regulation. This ability to regulate turgor has been observed widely in algae, plants, fungi and bacteria. The mechanisms involved in turgor regulation in these organisms are covered in section 1.3.

### 1.2. Responses of algae to osmotic stress - turgor regulation and volume regulation

The ability to generate and sustain turgor varies between different algae and is dependent on properties of their cell envelopes (Zimmermann 1978). Algae which lack cell walls, for example, species of *Dunaliella* and the chrysophycean, *Poterioochromonas malhemensis* and

algae which are covered with loosely-held scales, for example the chlorophyte *Tetraselmis* function like osmometers under osmotic stress (Hellebust 1976). They regulate their volume by shrinking and swelling under hyper- and hypoosmotic stress, respectively, due to rapid fluxes of water. These cells rely predominantly on the synthesis of organic osmolytes to drive water movement. *Dunaliella tertiolecta, D. viridis* and *D. parva* are euryhaline and tolerate a wide range of osmotic potentials by adjusting their intracellular glycerol concentration in response to osmotic stress (Hellebust 1976; Wegmann 1986). The enzymes of *D. viridis* are able to withstand glycerol concentrations of up to 4M (Yancey et al. 1982). The freshwater alga, *P. malhamensis* only tolerates small changes in external osmotic potential. It regulates its volume by adjusting the intracellular concentration of isofloridoside (galactosylglycerol) in response to osmotic stress. Isofloridoside is produced by the reaction between glycerol-3-phosphate and galactose catalyzed by the enzyme isofloridoside-phosphate synthase (Kauss 1983). This response is relatively rapid with isofloridoside production reaching a constant rate in 1–3 min (Stone and Clarke 1992). Excess isofloridoside is then converted to osmotically inactive chrysolaminarin when normal conditions return. This is also produced as a storage product of photosynthesis. Chrysolaminarin is thought to be again broken down under hyperosmotic stress to osmotically active isofloridoside (Wegmann 1986).

In contrast to algae that lack walls, those with rigid cell walls are capable of sustaining high turgor pressures. The rigidity of the cell wall dictates that turgor pressure is the key parameter which needs to be regulated under osmotic stress (Zimmermann 1978). Most studies investigating turgor regulation and electrophysiology in algae are limited to the green algae, Chlorophyta and Charophyta. Members of Charophyta are the closest relatives of the land plants and are grouped together under Streptophyta. Chlorophyta encompasses the rest of the green algae (Bisson et al. 2006). The Charophyta include the characean algae which have been most extensively studied and have served as models used to understand the membrane

transport processes and electrical properties of algal cells. They have large cells with rigid walls and large vacuoles. Osmotic adjustment is mostly brought about by inorganic ion uptake. Most are found in freshwater and lack the ability to turgor regulate under an imposed osmotic stress (Stento et al. 2000). Two salt tolerant species, *Lamprothamnium succinctum* and *Chara longifolia* are however able to turgor regulate and grow in both freshwater and seawater salinities (Okazaki 1996; Stento et al. 2000). In these two species, $K^+$ and $Cl^-$ are the main solutes involved in turgor regulation with $Na^+$ playing only a minor role. The internal $Na^+$ concentration is always found to be lower than that of $K^+$ (Bisson and Kirst 1980). *C. longifolia* exhibits enhanced $Na^+$ extrusion under hyperosmotic stress to maintain a low cytosolic $Na^+$ concentration (Kiegle and Bisson 1996). A $Na^+/H^+$ antiporter is thought to mediate this process, similar to that observed in various plant studies (see later sections). Efflux is greater than in *C. corallina*, a non-turgor regulating freshwater species (Whittington and Bisson 1994). However, both species have been shown to exhibit similar tolerance levels to $Na^+$, suggesting that the ability / inability to regulate turgor enables *C.longifolia* to survive in estuarine habitats and restricts *C. corallina* to freshwater (Hoffmann and Bisson 1988; Tufariello et al. 1988).

Among the chlorophytes, the giant-celled siphonous, coenocytic *Ventricaria* and *Valonia* are the most extensively studied. Like the salt tolerant characeans, they regulate turgor in response to hyperosmotic stress by mediating $K^+$ and $Cl^-$ uptake, but have a different electrophysiology. The membrane potential depolarizes (becomes more positive) in response to NaCl-induced hyperosmotic shock in the chlorophyceans. $K^+$ uptake at the tonoplast has been shown to cause this depolarisation (Hastings & Gutknecht 1976; Bisson and Beilby 2002).

There have been conflicting reports regarding the responses of the characean algae to NaCl hyperosmotic shock. Some studies report hyperpolarization of membrane potential (more

negative), while others report transient depolarization followed by hyperpolarization (Okazaki et al. 1984; Reid et al. 1984; Al Khazaaly and Beilby 2007). The hyperpolarization of membrane potential in these studies is mediated by activation of the proton pump. This is thought to drive $K^+$ uptake through inward rectifying $K^+$ channels and $Cl^-$ uptake by $H^+$ symport (Bisson et al. 2006). In the siphonous chlorophytes however, membrane potential becomes more positive, this is thought to be caused by active $K^+$ uptake at the tonoplast.

Euryhaline *Enteromorpha intestinalis*, *E. prolifera* and *Codium decorticatum* are other examples of turgor regulating chlorophytes (Black & Weeks 1972; Bisson & Gutknecht 1975, 1977; Young et al. 1987a, b; Edwards et al. 1988). These algae extrude $Na^+$ and take up $K^+$ and $Cl^-$ under hyperosmotic stress, similar to the other green algae investigated. *Enteromorpha* also accumulates the organic osmolyte, dimethylsulfoniopropionate under long-term exposure to hyperosmotic stress (Young et al. 1987a). A freshwater chlorophyte, *Eremosphaera viridis* lacks the ability to regulate turgor, as do the freshwater charophytes studied (Frey et al. 1988).

Algae appear to accumulate a wide range of organic compounds as osmolytes and osmoprotectants under osmotic stress, irrespective of whether they regulate turgor or volume. Often these compounds are derivatives of photosynthetic products and different compounds are used by different taxonomic groups. For example, mannitol is used in the Phaeophyceae and Prasinophyceae, proline in the Bacillariophyceae and Chlorophyceae, heterosides in the Rhodophyceae and Chrysophyceae and sucrose in the Chlorophyceae and Charophyceae (Ben-Amotz & Avron 1983; Kirst 1990). While the synthesis and regulation of metabolites under osmotic stress have been studied in great detail in unicellular algae, our knowledge of these processes in macroalgae is limited (Kirst 1990).

### 1.2.1 Responses of stramenopiles to osmotic stress

Stramenopila is one of the major phylogenetic groups of the eukaryotes. It includes organisms as diverse as large multicellular seaweeds, unicellular diatoms, fungi-like plant pathogens, parasites of both animals and marine alga and free living flagellates. Photosynthetic stramenopiles are placed within the Heterokontophyta. These heterogeneous organisms are grouped together on the basis of molecular analyses of their gene sequences and on their flagellar characteristics (Massana et al. 2004). While only a few species have been studied, the diversity of their physiological responses to osmotic stress is becoming apparent.

A halotolerant, raphidophycean alga, *Heterosigma akashiwo* accumulates inorganic ions to adjust the internal osmotic potential under high salinity. In addition it has a $Na^+$ ATPase for active extrusion of $Na^+$ under high salinity, unlike the $Na^+/H^+$ antiporter that is found in most plants and algae (Wada et al. 1989; Gimmler 2000; Shono et al. 2001; Hara et al. 2003). Among algae and plants, this type of pump has been found in one other organism, a halotolerant green chlorophyte, *Tetraselmis viridis*, which has the ability to regulate its volume (Gimmler 2000). A heterotrophic marine stramenopile *Thraustochytrium* also adjusts its internal osmotic potential by regulating inorganic ion transport (Shabala et al. 2009). $Na^+$ and $Cl^-$ are the major ions in osmotic adjustment whereas $K^+$ is found to have only a minor role.

Oomycetes, commonly referred to as water molds are fungi-like stramenopiles. Although they share many morphological characters with fungi, cell ultrastructural studies and gene sequence comparisons have placed them within the stramenopiles (Latijnhouwers et al. 2003). Most true fungi respond to hyperosmotic stress by taking up inorganic ions and synthesizing organic osmolytes to regain turgor back to the original value. The freshwater

oomycetes, *Achlya bisexualis* and *Saprolegnia ferax* appear to lack a mechanism for turgor regulation (Money and Harold 1993; Lew et al. 2004). This would be consistent with organisms living in an environment where there is little change in external osmotic potential.

### 1.2.2. Investigating turgor regulation in *Vaucheria*

Given the paucity of studies on the Stramenopiles and the various responses that have been shown thus far, in this thesis, turgor regulation and mechanisms of osmotic adjustment will be investigated in species of the alga, *Vaucheria*. *Vaucheria* is a genus of yellow green alga (class Xanthophyceae, phylum Heterokontophyta; Graham et al. 2009). It is characterized by siphonous (aseptate), coenocytic, tip-growing filaments (siphons) which are similar to the hyphae of oomycetes (Ott & Brown 1974; Hulvey et al. 2007; Fig 1.2). While many species are stenohaline, restricted to either freshwater or fully marine conditions, a considerable number are euryhaline, found in brackish habitats that are subject to salinity variations (Christensen 1988). Species are also found in terrestrial habitats, for example, in soil, where salinities are also likely to vary substantially through desiccation-hydration cycles.

The diversity of habitats occupied by *Vaucheria* makes it an intriguing experimental system for investigations of turgor regulation. As *Vaucheria* shares a common lineage and several morphological traits with the Oomycota, this raises the question of whether, like the oomycetes tested, the freshwater species are unable to turgor regulate. This would have consequences for any species that live in brackish environments, as they would have to contend with fluctuations in external osmotic potential. It also raises the question of whether estuarine species have the ability to regulate their turgor in response to a change in external osmotic potential.

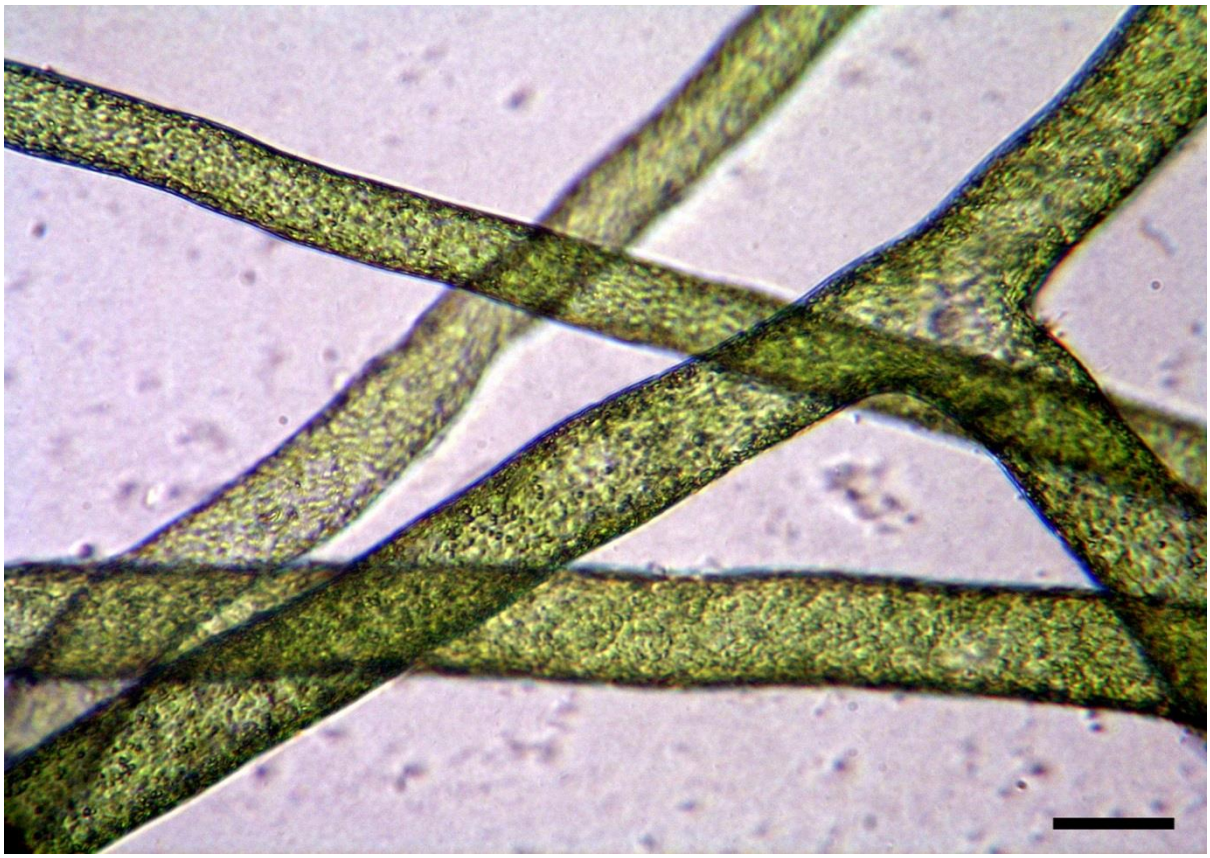

**Figure 1.2.** Vegetative siphons of *Vaucheria*. Notice the characteristic yellow green, aseptate, branching filaments.

## 1.3. Description of *Vaucheria*

### 1.3.1. Morphology and reproduction

Filaments of *Vaucheria* are typically siphonous (= aseptate) and coenocytic, with a vegetative cell potentially containing several thousand nuclei (Ott & Brown 1974; Ott 1992; Fig. 1.2). Siphons are cylindrical, up to 100 µm in diameter and form cushion-like mats which are felt-like in texture, earning them the name 'water felt' (Taylor et al. 2008). Siphon growth is restricted to the apex, similar to the hyphae of fungi and oomycetes and to pollen tubes. Siphons are partitioned with a septum only during development of reproductive structures or mechanical injury. The cell wall ranges from 0.5 µm wide along the apical dome to 1 µm along other parts of the siphon (Kataoka 1975). The cytoplasm is restricted to the periphery by a large central vacuole and forms a thin layer between the plasma membrane and the tonoplast (Ott & Brown 1974).

The life cycle of *Vaucheria* includes sexual, asexual and vegetative stages. Vegetative reproduction occurs via the fragmentation of vegetative filaments (Gavrilova & Rudanova 1999). Asexual reproduction is by means of the germination of multiflagellate zoospores, called synzoospores or non-motile spores called aplanospores (Gavrilova & Rudanova 1999; Lee 2008). Germination results in formation of typical siphons. Sexual reproduction in *Vaucheria* is oogamous, involving the male antheridia and female oogonia. These are either adjacent to each other on a common branch or are on adjacent branches. A septum cuts off each gametangium from the siphon. Spermatozooids are released through apertures in the antheridia and fertilize a single egg produced by each female oogonium through the aperture in the oogonium. The zygote, termed an oospore is released from the oogonium through decay of the oogonial wall and germinates into a new siphon. Taxonomy of the genus is

predominantly based on morphology and arrangement of sexual structures and sometimes on the morphology of vegetative siphons (Entwisle 1988).

### 1.3.2. Ecology

*Vaucheria* has a cosmopolitan distribution with 75 accepted species worldwide (Guiry & Guiry 2013). Their habitats range from freshwater, through brackish to fully marine. They are also prevalent in terrestrial habitats. Marine and brackish water species are epipelic (growing on surface of sediments) on mud flats and salt marshes, on banks of estuaries and other marine and intertidal waterbodies. There have also been a few reports of *Vaucheria* growing as epiphytes on mangroves, for example *V. karachiensis* which occurs as dense compact mats on the pneumatophores of the mangrove, *Avicennia marina*. Freshwater species are most often epilithic (attached to rock surfaces) or epipelic and submerged in shallow water of lentic and lotic waterbodies or attached to moist soil around the periphery of waterbodies. They are sometimes metaphytic (entangled amongst littoral vegetation)

As they are found in freshwater, brackish and marine waters, species of *Vaucheria* grow in widely different osmolalities. Most species are stenohalinic, growing in either freshwater or seawater. *V. conifera*, *V. piloboloides*, *V. subsimplex* and *V. medusa* are restricted to seawater, whereas *V. schleicheri*, *V. bursata*, *V. dillwynii* are restricted to freshwater. Many species are euryhalinic, often tolerating great variations in salinity over a short period of time, for example, *V. compacta*, *V. dichotoma*, *V. erythrospora* and *V. velutina* (Simons 1974; Christensen 1988). Ecotypic variations between strains of the same species is common, for example, the species *V. coronata* and *V. dichotoma* have been shown to have both stenohalinic freshwater strains and euryhalinic brackish water strains (Christensen 1988; Andersen & Bailey 2002). They are known to survive a variety of drastic changes in the environment. For instance, a strain of *V. dichotoma* has been shown to thrive in a shallow bay

in the Baltic Sea which is subject to large changes in salinity, pH, pollutants and levels of $H_2S$, an environment where other algae and seaweeds struggle to survive (Åberg & Fries 1976).

*Vaucheria* has been widely reported in Australia with an abundance of species from different habitats (Entwisle 1988). 25 different species have been reported from South Australia alone. The distribution of *Vaucheria* in New Zealand however, is poorly known. There are eleven species reported in total, of which seven are freshwater species and the rest have been collected from marine and intertidal habitats (Hooker 1867; Chapman 1956; Chapman et al. 1957; Sarma 1973, 1974; Adams 1994; Wilcox 2001). Most of these records are from the North Island.

The *Vaucheria* strains for this study were collected from different habitats in Canterbury, which is New Zealand's largest region in terms of land area. It is part of New Zealand's South Island. The Southern Alps form the region's western boundary, and the Conway River and Waitaki River the northern and southern boundaries respectively. The region has diverse aquatic habitats including glacial rivers, lakes, groundwater discharges, brackish lagoons and estuaries. The diversity and distribution of *Vaucheria* in Canterbury, like the rest of New Zealand (and especially the South Island), is poorly known. Figure 1.3 shows the location of Canterbury in New Zealand and the different lakes and river systems in the region.

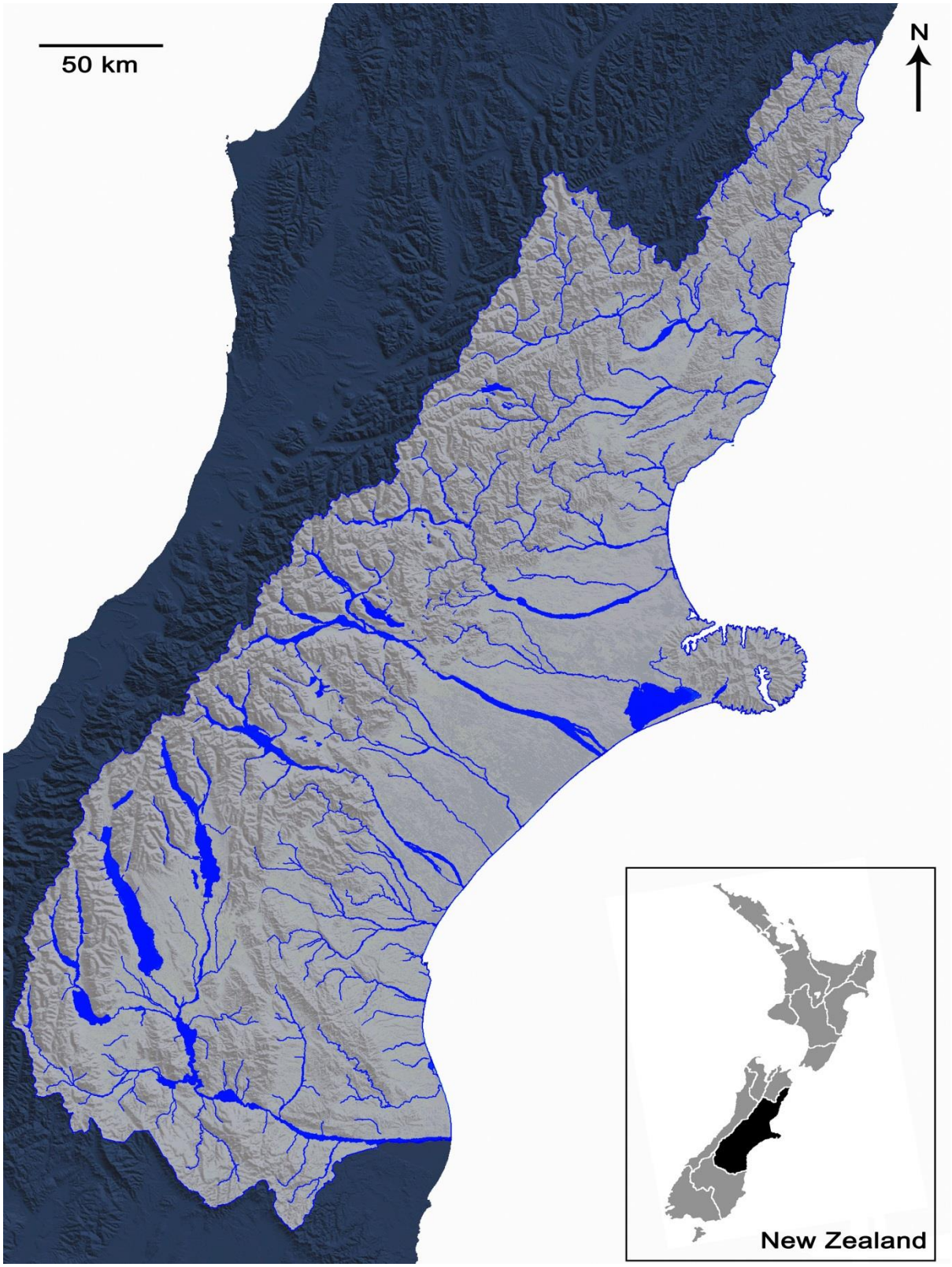


**Figure 1.3.** Map of Canterbury showing all the rivers, estuaries and lakes. Inset map shows location of Canterbury in New Zealand.

## 1.4. Turgor regulation and mechanisms of osmotic adjustment

The ability to regulate turgor has been observed widely in algae, plants, fungi and bacteria. Although these organisms are morphologically and phylogenetically diverse, many of the strategies employed in osmotic adjustment and turgor regulation appear to have been conserved. There are two main players in the regulatory process which appear common to turgor regulating organisms - inorganic ions and organic solutes. Under hyperosmotic stress, there is an influx or uptake of inorganic ions and the accumulation of low-molecular-weight organic compounds in order to increase the internal osmotic potential and facilitate uptake of water into the cell. Under hypoosmotic stress, inorganic ions and organic osmolytes are released out of the cell to decrease the internal osmotic potential.

The turgor regulation process is thought to be a highly regulated bi-phasic process (Kirst 1990). The first phase is thought to involve rapid variations in turgor as the external osmotic potential changes, resulting in water movement into and out of the cell. This change in turgor is thought to be detected by a sensor which in turn is thought to trigger the second phase of the process. The second phase involves the osmotic changes that happen in the cell in the form of influx and efflux of inorganic and organic osmolytes leading to restoration of turgor back to the original value. As these processes involve the movement of charged molecules into and out of the cell, they have electrophysiological consequences. In this section I will review the possible mechanisms of sensing and initial change in external osmotic potential and the resultant adjustment of internal osmotic potential through ion movements into/out of the cell.

### 1.4.1 Sensing pressure

The pressure sensing mechanism in walled cells exposed to osmotic stress is the most poorly understood step in the process. Various hypotheses have been suggested, most of which are

based on pressure differential and proximity between components of the cell wall and the plasma membrane (Bisson et al. 2006). Studies on the electrical properties of *Arabidopsis thaliana* root hairs (Lew 1996) and the algae *Valonia*, *Codium* and *Halicystis* (cited in Kirst 1990) suggest that osmotic gradients may be involved in the pressure sensing mechanism rather than absolute changes in turgor. This may imply the presence of an osmo-sensor rather than a turgor-sensor which is activated under osmotic stress (Lew 1996). As substantial osmotic gradients may be unlikely within the cytoplasm, the sensor is thought to be located in the plasma membrane (Kirst 1990). The osmo-sensor is thought to activate a $H^+$-ATPase, which generates an electrochemical gradient across the plasma membrane. The mechanism by which the osmo-sensor activates the $H^+$-ATPase is also poorly understood. A study on the HOG1 and PBS2 genes in the yeast *Saccaromyces cerevesiae*, which encode members of the mitogen-activated kinase (MAPK) has shown a possible transduction pathway in response to hyperosmotic stress, involving a tyrosine phosphorylation of the HOG1 (High Osmolarity Glycerol) protein (Brewster et al. 1993). Two transmembrane kinases are thought to function as a cell wall bound polypeptide ligand and a plasma membrane bound receptor respectively - their interaction is thought to be pivotal in the sensor/ transduction pathway and the activation of the $H^+$ ATPase. In *S. cerevisiae,* HOG1 accumulation in the nucleus activates transcription factors responsible for increased expression of enzymes in glycerol biosynthesis (Rep et al. 1999).

It is known that the $H^+$-ATPase requires, and is regulated by, membrane lipids (Kasamo 1987, 1990; Palmgren 1991; Kasamo 2003), which suggests that membrane tension changes could directly activate the protein. Mechanosensitive channels activated and inactivated by stretching of the membrane during osmotic stress may also act as osmosensors. Studies on the electrical properties of *Arabidopsis thaliana* suspension cultures under hyperosmotic stress suggest an indirect mechanism of $H^+$-ATPase activation involving stretch-inactivated $Cl^-$

channels (Teodoro et al. 1998; Zingarelli et al. 1999). These channels are thought to be inactivated by membrane tension changes caused by hyperosmotic stress, resulting in inhibition of $Cl^-$ efflux. Hyperpolarization of internal membrane due to inhibition of $Cl^-$ efflux was found to precede the activation of the $H^+$ ATPase, suggesting its role in the activation (Zingarelli et al. 1999). The inhibition of $Cl^-$ efflux has also been shown to occur concurrently with an independent $Cl^-$ influx, further adding to the polarization (Teodoro et al. 1998). Mechanosensitive $Ca^{2+}$ channels in guard cells are thought to play a role in sensing changes in turgor pressure and mediate turgor regulation (Garrill et al. 1996; Zhang et al. 2007). Studies of turgor regulation in guard cells have also suggested the possible role of the actin cytoskeleton in osmo-sensing and triggering $K^+$ channels (Liu & Luan 1998).

### 1.4.2. $H^+$- ATPase

As detailed above the plasma membrane $H^+$-ATPase is thought to play an important role in turgor regulation and osmotic stress tolerance. Pump-mediated $H^+$ efflux has been observed in hyperosmotically stressed *Arabidopsis thaliana* root epidermal cells, leading to hyperpolarization of membrane potential. This hyperpolarization then triggers $K^+$ influx through voltage-gated $K^+$ channels (Curti et al. 1993; Shabala & Lew 2002). Salt-dependent activation of the $H^+$-ATPase is thought to be regulated both at the translational and post-translational level (Portillo 2000; Janicka-Russak 2011).

The $H^+$-ATPase also plays a vital role in the cell turgor changes in guard cells. Various environmental stimuli like $CO_2$, light and humidity can activate the proton pump. For example, blue light receptors, called phototropins, which are auto-phosphorylating Serine/Threonine protein kinases, activate the proton pump which hyperpolarizes the plasma membrane. This triggers the opening of $K^+$ channels, leading to $K^+$ and anion influx. With the resultant water influx turgor increases causing the guard cells to swell and the stomata to

open (Morsomme & Boutry 2000; Schroeder et al. 2001; Janicka-Russak 2011). Stomatal closure is mediated by $Cl^-$, $K^+$ and malate efflux through $Ca^{2+}$ and voltage-gated anion channels and KORCs (Zhang et al. 2004). This process is induced by abscisic acid.

In addition to turgor regulation the pump has been attributed with many other physiological functions including nutrient uptake, xylem and phloem loading in plants, intracellular pH regulation, cell expansion and salt stress tolerance (Michelet & Boutry 1995; Morsomme & Boutry 2000; Janicka-Russak 2011).

The $H^+$-ATPase belongs to a large family of membrane proteins, the P-type ATPases, so-called because they form an aspartyl phosphate intermediate during their catalytic cycle (Morsomme & Boutry 2000). It couples ATP hydrolysis to the transport of protons against their electrochemical gradient, and hence it acts as a proton pump (Morsomme & Boutry 2000; Portillo 2000). $H^+$-ATPases have been identified genetically and biochemically in fungal, plant and algal plasma membranes, with homologous sequences also detected in protozoa and archaebacteria (Portillo 2000). They are encoded by several genes, the number varying between organisms - one in *Zostera marina* and *Phaseolus vulgaris*, two in *Saccaromyces cerevisiae*, *Zea mays* and *Oryza sativa*, eleven in *Arabidopsis thaliana*, seven in tomato and four genes in tobacco (Michelet & Boutry 1995; Portillo 2000).

Secondary transport processes, either via symport or antiport with a proton, powered by the electrochemical gradient created by the $H^+$-ATPase, are also involved in turgor regulation and in salt stress tolerance. For example, a $H^+$/ $K^+$ symport functions in plants under low soil $K^+$ concentrations of < 27nM, enabling high affinity uptake of 1 $K^+$ coupled with 1 $H^+$ (Michelet & Boutry 1995; Briskin & Gawienowski 1996). This symport is also thought to function as an alternative pathway for influx of $K^+$ ions during turgor regulation under hyperosmotic stress (Shabala & Lew 2002). A plasma membrane $Na^+/H^+$ antiporter in plants

is thought to aid in salt stress tolerance by extruding toxic $Na^+$ ions from cells (Shi et al. 2002). This antiporter, termed SOS1 is part of an SOS (salt-overly sensitive) network of proteins controlling $Na^+$ efflux (dealt with in detail in later sections). Vacuolar $H^+$-ATPases (V-type) operate in the tonoplast membrane, where the electrochemical gradient created is thought to be vital in the extruding $Na^+$ ions from the cytosol using a vacuolar $Na^+/H^+$ antiporter (Barkla et al. 1995; Morsomme & Boutry 2000; Aharon et al. 2003). This process helps keep the toxic $Na^+$ ions away from the cytosol and compartmentalizes them in the vacuole. Apart from the SOS family of $Ca^{2+}$ sensitive proteins, $Ca^{2+}$/ calmodulin- dependent protein kinases can also detect transient increases in cytosolic calcium concentration caused by exposure to salt stress. These kinases are able to couple $Ca^{2+}$ increase to the phosphorylation of different proteins, aiding in salt stress tolerance (Zhu 2003b; Janicka-Russak 2011).

### 1.4.3. Ion movements

The main cations involved in turgor regulation are $K^+$ and $Na^+$, with $Ca^{2+}$ thought to play a role in signalling. Movements of these ions in walled cells are best characterized in higher plants (Maathuis & Amtmann 1999; Krol & Trebacz 2000; Cushman 2001; Zhu 2003b).

#### 1.4.3.1. Inward rectifying channels

$K^+$ inward rectifying channels (KIRCs) are voltage-dependent channels which conduct current into the cytoplasm, facilitating uptake of $K^+$ into the cell (Cushman 2001). They are involved in what is called 'low-affinity $K^+$ uptake', or the uptake of $K^+$ ions when the external concentration of $K^+$ is > 0.3 mM (Latorre et al. 2003). The driving force of this uptake is the substantial negative membrane potential created by the proton pump. The gating characteristics of these channels are such that they are activated when the membrane voltage is more negative than the equilibrium potential of $K^+$ (Maathuis & Amtmann 1999). KIRCs

operate over a fixed voltage range on activation at negative voltages and are independent of the concentration of the $K^+$ ion (Hedrich 2012). These were the first plant ion channels identified at the molecular level and are homologous to Shaker channels found in animal cells, though the Shaker channels are outward rectifying. They are highly selective for $K^+$ ions over other monovalent and divalent cations (Bentrup 1990; Tester 1990; Gassmann et al. 1993). Though KIRCs have been reported in algae and fungi (Sauer et al. 1993; Roberts 2003), detailed characterization studies on the structures and physiological functions have been performed mostly on plant systems like *Arabidopsis thaliana*, *Solanum tuberosum* and *Hordeum vulgare* (Zimmermann et al. 1998; Amtmann et al. 1999; Latorre et al. 2003).

AKT1 is an example of a KIRC expressed in *Arabidopsis thaliana* roots, which functions in uptake of $K^+$ from the soil (Maathuis & Amtmann 1999). The KAT1 channel is expressed in guard cells and is involved in guard cell turgor regulation and the stomatal opening process. The expression of KMT1, another KIRC belonging to the AKT/KAT family of inward rectifying $K^+$ channels is known to be upregulated under salinity and osmotic stress (Zhu 2003b). KIRCs are thought to play only a minor role in the uptake of $Na^+$ (Maathuis & Amtmann 1999; Cushman 2001). A study on an AKT1 gene knockout mutant, akt1-1 has shown that this mutant is as sensitive to salt stress as the wild type, adding weight to the argument that KIRCs may not have much of a role in $Na^+$ uptake (Blumwald 2000). However, a more recent study on $Na^+$ uptake in the halophyte *Suaeda maritima*, has suggested the involvement of a low-affinity channel resembling AKT1 in $Na^+$ uptake (Wang et al. 2007). Another study comparing $Na^+$ uptake in salt tolerant and salt sensitive rice cultivars has shown that while $K^+$ channels mediated $Na^+$ uptake in the salt sensitive cultivar, they did not in the tolerant one (Kader & Lindberg 2005; Brini & Masmoudi 2012). These studies suggest that mechanisms for $Na^+$ uptake may vary between salt tolerant and sensitive

plants and this may determine whether an organism can tolerate salt stress and may contribute to effective turgor regulation.

### 1.4.3.2. Outward rectifying channels

$K^+$ outward rectifying channels (KORCs) are a class of ion channel that are involved in the efflux of $K^+$ ions from the cell (Cushman 2001). GORK is a KORC which has been shown to play a major role in turgor regulation of guard cells through depolarization-induced $K^+$ release (Liu & Luan 1998; Ache et al. 2000). The gating characteristics of these channels are such that they are activated by depolarization of the membrane potential. KORCs differ from KIRC in that they are affected by both voltage and the extracellular $K^+$ concentration (Hedrich 2012).

Turgor regulation under hyperosmotic stress may involve close regulation of KIRCs and KORCs. Though they are thought to be highly selective for $K^+$ efflux, KORCs have been shown to be permeable to $Na^+$ and hence may have a role in $Na^+$ uptake (Maathuis & Amtmann 1999; Krol & Trebacz 2000). Zingarelli et al. (1999) reported that hyperpolarization brought about by hyperosmotic stress in cultured *Arabidopsis* cells partially shuts down KORCs, rather than facilitating $K^+$ influx through KIRCs. This is thought to limit $K^+$ efflux and contribute to depolarization.

The primary function of KORCs is thought to be the stabilization of membrane potential against excessive depolarization, while also providing a pathway for the release of $K^+$ ions (Maathuis & Amtmann 1999). SKOR (Shaker-type $K^+$ outward rectifying), another KORC expressed in *A. thaliana* roots and xylem parenchyma is involved in the transport of $K^+$ ions from the xylem to the shoots (Cushman 2001).

### 1.4.3.3. Non-selective cation channels

Non-selective cation channels (NSCC) are a large, heterogeneous group of ion channels which facilitate the passive fluxes of a range of different cations in plant membranes, for which they show similar permeability levels (Demidchik et al. 2002; Demidchik & Maathuis 2007). In addition to monovalent cations, some NSCC are also permeable to divalent cations like $Ca^{2+}$. The fact that NSCCs can allow large amounts of cationic charge to flow due to their non-selectivity could suggest that they have a crucial role in turgor regulation and also in restoring cytosolic charge ratios. NSCCs are classified into various types based on their response to membrane potential changes and response to ligands and physical stimuli. These include depolarization-activated, voltage-independent, hyperpolarization-activated, membrane stretch-activated, amino acid-gated and cyclic nucleotide-gated NSCCs (Demidchik & Maathuis 2007; Kronzucker & Britto 2011). As indicated above they demonstrate low $Na^+/K^+$ selectivity compared to KIRCs and KORCs (Cushman 2001) and have been characterized in different plant cell types like roots, leaf epidermis, guard cells, mesophyll cells and pollen tubes (Demidchik & Maathuis 2007). Various electrophysiological and modelling-based studies have suggested that NSCCs are a major pathway for $Na^+$ entry into plants during salinity stress (Amtmann & Sanders 1999; Davenport & Tester 2000; Demidchik & Tester 2002; Murthy & Tester 2006; Demidchik & Maathuis 2007). They are thought to exhibit a wide range of physiological functions including rapid adaptation to salinity and hyperosmotic stress by facilitating $Na^+$ influx, $Ca^{2+}$ uptake for growth, $Ca^{2+}$ signalling and stabilization of membrane potential (Maathuis & Amtmann 1999; Demidchik & Maathuis 2007). NSCCs found in the peribacterial membrane between legumes and nitrogen fixing bacteria are thought to facilitate the flux of fixed $NH_4^+$ to the host cell (Roberts & Tyerman 2002; Obermeyer & Tyerman 2005).

### 1.4.3.4. Other means of cation transport

High affinity $K^+$ transport is the uptake of $K^+$ under external $K^+$ concentrations of 1-200 µM (Latorre et al. 2003). Uptake under micromolar external concentrations of $K^+$ would typically occur against a concentration gradient and hence needs to be mediated by a carrier energized by coupling to an electrochemical gradient (Maathuis & Amtmann 1999). Two families of such carriers have been identified in plants. HKT1 belonging to the HKT family (High-affinity $K^+$ transporters), is a $Na^+$-$K^+$ symport which moves two $K^+$ ions per one $Na^+$. Both HKT1 binding sites are thought to be occupied by $Na^+$ ions under high external $Na^+$ concentrations and hence HKT1 may have more relevance in terms of $Na^+$ rather than $K^+$ uptake (Maathuis & Amtmann 1999). Though HKT1 mediates uptake of both $K^+$ and $Na^+$, its role in the process is thought to be less significant compared to that of selective ion channels like KIRCs (Maathuis & Amtmann 1999). A second family of high-affinity $K^+$ transporters are the KUP/HAK family ($K^+$ uptake/ High affinity $K^+$ uptake) which mediate $K^+$ uptake at micromolar external concentrations (Quintero & Blatt 1997; Kim et al. 1998; Rodríguez-Navarro & Rubio 2006). They are thought to function by coupling to a $H^+$ gradient rather than a $Na^+$ gradient as used by HKTs (Cushman 2001). They are up regulated under low external $K^+$ concentrations and are blocked by millimolar concentrations of $Na^+$ (Maathuis & Amtmann 1999). Members of the KUP/HAK family and related transporters are conserved over different phyla (Quintero & Blatt 1997). An HKT1 homologue from *Arabidopsis*, AtHKT1, has been shown to preferentially mediate the uptake of $Na^+$ and has very limited $K^+$ uptake activity. AtHKT1 does not couple cation uptake to either $H^+$ or $Na^+$ gradients and therefore is thought to be a pathway for low-affinity $Na^+$ uptake (Cushman 2001). LCT1 is another low-affinity carrier in wheat which has been shown to facilitate non-selective uptake of monovalent cations including calcium and cadmium which may also have a role in $Na^+$ uptake under high salinity (Maathuis & Amtmann 1999; Cushman 2001).

### 1.4.3.5. Anion channels and transporters

Anions are also likely to play an important role in turgor regulation. Plant cells contain a complex mixture of diverse anions including chloride, nitrate, sulfate, phosphate and organic anions like malate and citrate, each one having their own physiological roles (Barbier-Brygoo et al. 2011). Because of the wide range of physiological functions of different anions, anion channels and transporters are thought to be involved in many physiological processes in addition to turgor regulation, these include salinity tolerance, plant nutrition, acquisition and compartmentalization of metabolites, stomatal movements (through changes in turgor), metal tolerance and signal transduction and propagation (Schroeder 1995; Kollist et al. 2011). In addition to this, they are important for counterbalancing the charges of cations, and hence are closely regulated in the cell. Anion channels can be divided into different classes based on their activation - hyperpolarization-activated, depolarization-activated, stretch-activated, $Ca^{2+}$-, $Cl^-$- and cyclic nucleotide-activated (Schroeder 1995). Anion channels were identified in characean algae (these are $C1^-$ channels) before they were in plants and found to contribute to transient depolarization during action potentials (Tyerman 1992; Schroeder 1995). The role of stretch-activated $Cl^-$ channels in turgor and osmotic sensing has been discussed earlier (Teodoro et al. 1998; Zingarelli et al. 1999).

There are four families of anion transporter genes that have been identified in plants, SLAC1 (slow anion channel 1), ALMT1 (aluminum-activated malate transporter 1)/ QUAC (quick anion channel), TMEM (Transmembrane anion channel) and CLC (chloride channel) which encode different anion channels and transporters (Barbier-Brygoo et al. 2011; Hedrich 2012). SLAC1 encodes the S-type (Slow-type) anion channel which has slow activation/ deactivation kinetics in the 10 sec range and has low dependency to voltage. It is thought to be involved in the stomatal turgor regulation and closure process (Barbier-Brygoo et al. 2011). QUAC/AMLT1 family encodes the R-type (Rapid-type) anion channel which has

rapid activation/ deactivation kinetics of a milliseconds and is highly voltage dependent. Its precise role is unclear. The CLC gene family encodes $Cl^-/H^+$ antiporters located in different endomembranes of plant cells and $Cl^-$/cation symporters ($K^+$, $H^+$) participating in $Cl^-$ uptake with a possible role in osmotic adjustment and turgor regulation. Other $Cl^-$ channels, activated by high external $Cl^-$ concentrations brought about by high salinity have also been reported, which are thought to regulate membrane potential and $Cl^-$ uptake (Skerrett & Tyerman 1994; Tyerman et al. 1997).

#### 1.4.3.6. $Na^+$ stress

An increase in external NaCl can impose two types of stresses on a cell. Change in osmotic potential due to an increase in NaCl can lead to osmotic stress resulting in water and turgor loss. A high extracellular $Na^+$ concentration generates a large electrochemical gradient for the passive influx of $Na^+$ into the cell through KIRCs, KORCs and NSCCs as discussed in earlier sections. Once inside the cell, $Na^+$ can impose an ionic stress affecting ion homeostasis which can be toxic to cells (Zhu 2003b; Affenzeller et al. 2009)**.** $K^+$ is a major inorganic nutrient for plants and $K^+$ homeostasis and is important for balancing the negative charge of DNA and proteins, for the activation of enzymes, for contributing to osmotic potential, cell turgidity and expansion (Maathuis & Amtmann 1999; Zhu 2003a). Because of similar physiochemical structures of $Na^+$ and $K^+$, $Na^+$ can thwart vital metabolic processes by either inhibiting $K^+$ activated enzymes or competing for enzyme binding sites in the cytoplasm with $K^+$ (Maathuis & Amtmann 1999; Shi et al. 2002). A $Na^+$ excess can also lead to $K^+$ deficiency in the cytosol brought about by competition for transport sites. Dealing with $Na^+$ is therefore vital for a cell to tolerate and survive the stresses imposed by NaCl. The mechanisms of dealing with $Na^+$ differ between different cells but they can be broadly classified into three strategies- minimizing influx, maximizing extrusion/ efflux, and translocation and compartmentalization (Tester & Davenport 2003).

The first strategy of translocation of $Na^+$ and compartmentalization in the vacuole ensures that the cytosol $Na^+$ concentration is kept below toxic levels (Blumwald 2000). It also provides the cell with a cheap and abundant osmoticum to restore the osmotic potential and turgor. Both halophytes and glycophytes have been shown to accumulate $Na^+$ in the vacuole (Shi et al. 2002). $Na^+/H^+$ antiporters in the tonoplast are involved in this process of vacuolar compartmentalization and have been identified in different organisms (Barkla et al. 1995; Morsomme & Boutry 2000; Aharon et al. 2003). AtNHX1 is a vacuolar $Na^+/H^+$ antiporter in *Arabidopsis*, whose overexpression has been shown to confer salt tolerance in transgenic *Arabidopsis* (Apse et al. 1999) and more recently in buck wheat (Chen et al. 2008). Apart from $Na^+$ compartmentalization, other NHXs have been shown to play a role in $K^+$ homeostasis, endomembrane protein trafficking and regulation of growth (Bassil et al. 2011; Bassil et al. 2012).

The second strategy is the efflux or extrusion of $Na^+$ from the cytosol into the external medium. This process is mediated by $Na^+/ H^+$ antiporters in the plasma membrane, which couple $Na^+$ efflux with the proton influx energised by the proton gradient created by the proton pump (Blumwald 2000). A plasma membrane $Na^+/H^+$ antiporter was identified which was encoded by the *Arabidopsis* SOS1 (salt overly sensitive 1) gene part of SOS transduction pathway involved in $Na^+$ extrusion (Shi et al. 2000). $Na^+$ efflux through SOS1 is mediated by a salt-induced increase in cytosolic calcium which is detected by an SOS3 protein. This then phosphorylates an SOS2 protein, a Serine/Threonine protein kinase, which activates the antiporter activity (Shi et al. 2002; Janicka-Russak 2011). This SOS signal transduction pathway is thought to play a significant role in salt tolerance and maintaining intracellular ion homeostasis through $Na^+$ extrusion. $Na^+/H^+$ antiporters involved in $Na^+$ extrusion have been identified in different organisms including salt tolerant algae (Katz et al. 1991; Uji et al. 2012). $Na^+$ extrusion is also carried out in some bacteria, fungi and cyanobacteria by $Na^+$-

ATPase pumps. As mentioned earlier, a few marine algae have been reported to have $Na^+$-ATPases for $Na^+$ extrusion (Gimmler 2000).

Limiting the influx of $Na^+$ is another strategy which could lessen salinity stress. Very few studies have investigated this strategy of dealing with $Na^+$. A study on the protoplasts of rice cultivars reported that a salt tolerant variety was able to maintain a lower $Na^+$ influx (thereby accumulating less $Na^+$ in their cytosol), than the sensitive variety (Kader & Lindberg 2005). It was also found to have a greater capacity for $Na^+$ extrusion. This study also suggested that $Na^+$ influx maybe mediated by a different set of ion channels in the two varieties.

### 1.4.3.7. Aquaporins

In addition to ion channels and transporters, water channels or aquaporins are thought to play a vital role in regulation of water movement in and out of the cell, a process that is essential for osmotic balance (Cushman 2001). Aquaporins are highly conserved membrane proteins belonging to the major intrinsic protein (MIPs) superfamily with molecular masses of between 26 and 30 kDa, capable of mediating bidirectional flow of water (Tyerman et al. 1999; Cushman 2001). The activity and physiological implications of aquaporins are only beginning to be understood. Studies on *Chara* have shown that water permeability decreases under increasing osmotic pressure due to dehydration of pores in the membrane (Tyerman et al. 2002). Ye et al. (2004) have shown an inhibition of aquaporin activity in *Chara*, both under increasing concentration and size of osmotic solute. A study on PM28A, a MIP from spinach leaf plasma membrane, has shown that an increase in water potential results in the phosphorylation and subsequent activation of the protein, whereas decreasing water potential causes a dephosphorylation-mediated inactivation (Johansson et al. 1998). Some plant aquaporins have been reported to be upregulated and others downregulated under salinity and osmotic stress (Cushman 2001). Others have been shown to facilitate the movement of

molecules like glycerol, ammonia and gases like carbon-dioxide and even ions, in addition to water (Tyerman et al. 2002). In the yeast *Saccharomyces cerevisiae*, glycerol accumulates under hyperosmotic stress as an osmoticum to raise the internal osmotic potential. Under hypoosmotic shock, it regulates turgor by releasing glycerol through a MIP, Fpslp (Tyerman et al. 2002). These studies on changes in gating and expression of MIPs, suggest a possible role for aquaporins in mediating water fluxes and also osmolyte transport under osmotic stress.

### 1.4.4. Organic osmolytes

In addition to inorganic ions, algae, plants, fungi and bacteria can accumulate certain low molecular weight organic compounds in response to wide range of abiotic stresses. These are responsible for the second part of the overall strategy for turgor regulation mentioned above. These organic compounds are thought to perform a dual role under hyperosmotic stress, functioning both as osmolytes and as osmoprotectants. As osmolytes they are synthesized under hyperosmotic stress to restore cytosolic osmotic potential which drives water uptake and turgor regulation. Hyperosmotic stress leads to an immediate uptake of inorganic ions from the external solution. This results in an increase in the concentration of inorganic ions in the cytosol which can affect proteins and nucleic acids, thereby impairing cellular function. In contrast, some of these organic compounds can accumulate at high concentrations in the cytosol. Such organic osmolytes are termed ‘compatible solutes’ (Yancey et al. 1982; Yancey 2001, 2005). However, in most cases the turgor regulation process is too quick to be explained simply by *de novo* synthesis of organic compounds functioning as osmolytes (Shabala & Lew 2002). In addition, these compounds are often produced at too low a concentration to contribute to complete osmotic adjustment (Cushman 2001).

In cases where inorganic ions act as the predominant osmolytes, organisms may rely on efficient transport mechanisms to compartmentalize these ions in organelles like the vacuole. This strategy makes use of cheaply available ions as osmolytes, while keeping their cytosolic concentrations at levels where the structural integrity and function of proteins is maintained. Compatible solutes, in these situations may be synthesized solely to mitigate the adverse effects of these inorganic ions. For example, glycine betaine and proline have been found to mitigate the effects of salt stress in barley (Chen et al. 2007). Thus some of these compounds may function as osmoprotectants, protecting the water shell around proteins, stabilizing protein complexes and membranes and protecting against oxidative stress (Cushman 2001; Cuin & Shabala 2007).

Compatible solutes can be chemically categorized into polyols (eg., glycerol, sorbitol, arabitol), sugars (e.g., sucrose, fructose, trehalose), heterosides (eg., floridoside, isofloridoside), amino acids and amino acid derivatives (eg., proline, glycine betaine) and tertiary sulfonium compounds (eg., dimethylsulfoniopropionate) (Bisson & Kirst 1995).

Polyols are the most common organic compounds synthesized by algae, plants and fungi under hyperosmotic stress. The salt tolerant alga, *Dunaliella viridis* tolerates a wide range of salinities by adjusting its intracellular glycerol concentration as has been discussed earlier (Yancey et al. 1982). Glycerol production is also up-regulated and its efflux is limited under hyperosmotic stress in *Saccharomyces cerevisiae*, *Neurospora crassa* and *Arabidopsis thaliana* (Brewster et al. 1993; Zhang et al. 2002; Reiser et al. 2003; Burg & Ferraris 2008). Mannitol is another common polyol functioning as an osmolyte in algae, plants and fungi (Tarczynski et al. 1993; Iwamoto & Shiraiwa 2005). Polyols are thought to function as osmoprotectants by forming an artificial water sphere around macromolecules (Kirst 1990).

Heterosides are used as osmolytes in various algal classes. For example, the synthesis of isofloridoside, a heteroside, is rapidly increased under hyperosmotic stress and reduced after volume regulation in the unicellular alga *Poterioochramonas malhemensis* (Bisson & Kirst 1995). Isofloridoside is also the osmolyte of choice in salt tolerant estuarine red alga, *Porphyra columbina* (Karsten et al. 1993).

Amino acids and their derivatives are also employed by different organisms as osmolytes and osmoprotectancts. Among these, proline is the most common, found in diverse groups of plants including some halophytes like *Spartina* and *Mesembryanthemum sp.* and glycophytes like rice, tobacco, spinach, potato, tomato, *Arabidopsis*, field bean, soybean, wheat, barley and rice (Delauney & Verma 1993). It is also involved in turgor regulation and osmoprotection in some green algae, bacteria and diatoms (Yancey et al. 1982; Kirst 1990; Delauney & Verma 1993). It is thought to protect protein complexes by associating with hydrophobic portions and making them hydrophilic (Kirst 1990).

In many plants and algae, these organic compounds are identical to, or derivatives of, photosynthetic products (Bisson and Kirst 1995). Because of this, there is a preference for certain compounds in certain taxonomic classes, especially in the algae. Taxonomic preferences for compatible solutes are also observed in halophytic plant species (Flowers & Colmer 2008). As mentioned earlier, some compounds are employed as osmolytes by a wide range of organisms from different habitats and taxonomic classes suggesting either convergent evolution or conservation of certain metabolic pathways (Somero & Yancey 2010).

## 1.5. Osmotic adjustment and turgor regulation in other organisms

### 1.5.1. Higher plants

Plants are both structurally and functionally more complex than algae, fungi and bacteria, which translates into complexity in the mechanisms of osmotic adjustment (Hellebust 1976). This complexity stems from the existence of different types of tissues in plants with different physiological roles, and exposure to different levels of stress. Salinity can be defined as the presence of a high concentration of soluble salts in the soil. Soils are considered saline when they have more than 40mM NaCl (0.2 MPa). Based on their tolerance to salinity, higher plants are divided into two groups- halophytes which can tolerate high salt concentrations and glycophytes which cannot.

#### 1.5.1.1. Halophytes

Halophytes make up about 1% of the world's flora and grow in salinized coastal soils and arid regions (Flowers & Colmer 2008). They are defined as plants which are capable of completing their life cycle under an external NaCl concentration of 200 mM or greater. While dicotyledonous halophytes show optimal growth under 50-250 mM NaCl, monocots grow optimally in the absence of NaCl or at low concentrations (< 50 mM). Irrespective of their growth optima, all halophytes have to accumulate solutes to combat the osmotic stress imposed by their habitats to generate turgor. Cytosolic enzymes in halophytes are not adapted to function under high cytosolic salt concentrations, unlike in halophilic bacteria, which have specially modified proteins (Yancey et al. 1982; Kosová et al. 2013). Therefore, a build-up of $Na^+$ and $Cl^-$ in the cytosol is as toxic to halophytes as it is to other organisms, with the exception of halophilic bacteria. Halophytes therefore have to be efficient at compensating for the passive cation influx through non-selective cation channels under salinity stress. They do this by both active exclusion and compartmentalization. In the halophyte

*Mesembryanthemum crystallinum*, increasing salinity results in increased activity of the tonoplast ATPase and $Na^+/H^+$ exchanger in the leaves and in suppression of activity in roots (Flowers & Colmer 2008). This suggests an increased compartmentalization of $Na^+$ in the leaves. The halophyte *Thallungiella halophila*, has been shown to express greater levels of the SOS1 encoded plasma membrane $Na^+/H^+$ antiporter than *A. thaliana*, which is a glycophyte. This differential gene expression of plasma membrane transporters is thought to contribute to greater salinity tolerance in halophytes (Kant et al. 2006).

Halophytes also efficiently use compatible organic solutes both as osmolytes and osmoprotectants. There have been numerous studies that show the synthesis of a wide range of compatible solutes under increasing salinity (Flowers & Colmer 2008) and increased expression levels of enzymes involved in their synthesis (Kosová et al. 2013). In many halophytes, these compatible solutes are synthesized to high concentrations (40 mM in the leaves) contributing to osmotic pressure values of over 0.1 MPa (Munns & Tester 2008).

Many halophytes also have specialized structures such as salt glands in their leaves to deal with salt stress. These structures help move salt away from shoots and compartmentalize it in the leaves, where they are separated from living cells by a cuticle (Tester & Davenport 2003). The concentration of salts in the salt glands is thought to draw water away from the living cells of the leaf. Halophytes with salt glands are therefore found in habitats with abundant water like salt marshes (Plett et al. 2010). Other halophytes have salt-secreting bicellular glands and microhairs which perform a similar function and help halophytes tolerate high salinity (Tester & Davenport 2003).

Patch clamp studies on the halophytic gymnosperm, *Zostera muelleri* have suggested net $K^+$, and $Cl^-$ uptake under hyperosmotic stress mediated by inward and outward rectifying $K^+$ channels and stretch activated $K^+$ and $Cl^-$ channels (Garrill et al. 1994).

*Z. marina*, another halophytic species from the genus, has been shown to mediate $Na^+$ efflux under high salinity via a $Na^+/H^+$ antiporter, maintaining a low cytosolic $Na^+$ concentration (Fernández et al. 1999). Muramatsu et al. (2002) compared the activity of $H^+$-ATPases from *Vallisneria gigantea*, a freshwater grass, *Oryza sativa* (rice, a terrestrial plant) and *Z. marina*, under differing high salinities. They found that while activity in *Vallisneria* and rice was inhibited, it was not in *Z. marina* suggesting that its $H^+$-ATPase may be specially adapted to function under high salinities. *Suaeda maritima*, a halophytic angiosperm takes up $Na^+$, which is required for osmotic adjustment, through a low-affinity channel resembling AKT1, a KIRC found in *A. thaliana* roots (Wang et al. 2007).

#### 1.5.1.2. Glycophytes

Glycophytes are plants that do not have the ability to tolerate long term salinity stress. They constitute most of the plant species and include the economically important agricultural crops. Though tolerance to osmotic stress is thought to be exhibited by all plants, be it halophytes or glycophytes, the threshold for tolerance varies greatly between them. While glycophytes have similar stress response mechanisms to halophytes and are able to activate them under stress like the halophytes, they are metabolically inefficient solutes under stress. This means they struggle under exposure to long term or severe stresses (Kosová et al. 2013).

An initial response to the osmotic stress imposed by salinity, is the passive accumulation of $Na^+$ and $Cl^-$ ions. The availability of these ions as a cheap osmoticum to restore the osmotic potential is exploited by glycophytes and halophytes alike. But their handling of these ions after the passive entry is what makes species either salt sensitive or salt tolerant. As discussed in the previous section, glycophytes have a lower expression of the plasma membrane $Na^+/H^+$ antiporter compared to halophytes, making them less efficient at $Na^+$ exclusion and susceptible to ion toxicity under severe or prolonged stress. Glycophytes are also found to be

less efficient at ion compartmentalization. A study on the tonoplast $Na^+/H^+$ antiporter showed that a salt-tolerant species *Plantago maritima* had much greater activity than a closely related salt-sensitive species *P. media* (Staal et al. 1991). To add to the inefficiency in compartmentalization and exclusion, glycophytes also accumulate significantly lower concentrations of compatible solutes (about 10mM) (Munns & Tester 2008). At these concentrations, they may have some use as osmoprotectants but may not contribute much as osmolytes. Among the economically important glycophytes, rice is the most salt-sensitive, whereas barley is the most tolerant (Munns & Tester 2008; Horie et al. 2012). The epidermal root cells of *Arabidopsis thaliana* have been shown to turgor regulate under hyperosmotic stress (Lew 1996; Shabala & Lew 2002). These cells respond to this stress by taking up the inorganic ions- $K^+$, $Na^+$ and $Cl^-$. This net uptake is preceded by hyperpolarization of membrane potential due to the activity of the $H^+$- ATPase, followed by a decline in conductance.

### 1.5.2. Fungi

The accumulation of organic osmolytes for turgor regulation in fungi has been well studied (Yancey 2005; Burg & Ferraris 2008). Polyols are the predominant osmolytes synthesized in many fungi under hyperosmotic stress. Some examples include *Aspergillus nidulans* (glycerol and erythriol), *Neurospora crassa* (glycerol and mannitol), *Magnaporthe grisea* (glycerol and arabitol) and many marine fungi belonging to Phycomycetes and Ascomycetes (mannitol and arabitol) (Hellebust 1976; Beever et al. 1986; Dixon et al. 1999; Zhang et al. 2002; Burg and Ferraris 2008).

The HOG (high osmolarity glycerol) pathway, a conserved mitogen-activated protein kinase (MAPK) signalling pathway was first discovered and characterized in the budding yeast *Saccharomyces cerevisiae* (Brewster et al. 1993). This pathway (described in the 'Sensing

pressure' section) is activated by high osmolarity of the external environment, in which glycerol is accumulated to restore the internal osmotic potential of the cell and thereby turgor (Lew & Levina 2007). Comparative genomic analyses have shown the possible existence of this pathway in other fungi (Krantz et al. 2006). Components of this pathway have also been identified in animals and plants (Dixon et al. 1999).

*N. crassa* is the most thoroughly studied filamentous fungus in terms of both inorganic ion transport and the accumulation of compatible solutes in response to hyperosmotic stress. Studies estimating the ion fluxes under osmotic stress have shown that the MAPK pathway regulates the ion transport process by activating the $H^+$-ATPase and triggering $K^+$ and $Cl^-$ uptake (Lew et al. 2006). Other proteins that are not part of the MAPK pathway are also involved in osmotic stress tolerance in *N. crassa*. CUT-1, a putative phosphatase encoded by the *cut-1* gene, activates glycerol production and is found to work in coordination with the MAPK pathway to regulate turgor (Lew & Levina 2007). Lew et al. (2004) demonstrated that electrical changes precede changes in net ion transport in the fungus. A hyperosmotic shock causes a hyperpolarization of membrane potential, due to activation of the proton pump and decreased conductance, followed by net uptake of $Na^+$, $K^+$ and $Cl^-$ ions leading to turgor recovery. This response is similar to that of the higher plant, *Arabidopsis thaliana* (Lew 1996; Shabala & Lew 2002).

In pathogenic fungi, turgor is vital for penetrating and infecting living tissue. For example, the rice blast fungus, *Magnaporthe grisea* penetrates the cuticles of rice using specialized structures called appressoria, which generate very high turgor pressures (Dixon et al. 1999). In the fungal hyphae, turgor is regulated by glycerol synthesis through the activation of MAPK. But turgor generation in the appressoria is mediated by another pathway that leads to arabitol production. However, this pathway is dependent on a component of the MAPK pathway, *OSM1*, suggesting regulation of turgor at multiple levels.

## 1.6. Aims of the study

Much of our knowledge of the physiological adaptations and mechanisms of osmotic adjustment in algae is limited to chlorophytan and charophycean green algae. Given this, the osmotic responses of different species of the xanthophycean alga, *Vaucheria* are addressed in this thesis. The main aims are to investigate the ability of species of *Vaucheria* from contrasting habitats to regulate turgor in response to hyperosmotic stress and elucidate the mechanisms underlying turgor regulation in the alga. The thesis is structured as follows:

Chapter 2 deals with the characterization of species of *Vaucheria* from contrasting habitats in New Zealand based on morphology of their reproductive structures and phylogenetic analyses of *rbc*L gene sequences. This chapter improves the knowledge on the diversity and distribution of *Vaucheria* in New Zealand, which is currently poorly understood.

In Chapter 3, the responses of a brackish species and a freshwater species of *Vaucheria* to a range of hyperosmotic stresses are compared and their ability to regulate turgor is investigated using a single cell pressure probe. Growth and turgor under prolonged exposure to these stresses is also compared.

Chapter 4 investigates the mechanisms of osmotic adjustment leading to turgor regulation in *Vaucheria*. The role of inorganic ion uptake in the process is studied using pharmacological inhibition of specific membrane transport proteins and measurement of ion fluxes using ion selective microelectrodes. The role of organic osmolyte accumulation is also investigated using GC-MS. A model for turgor regulation in *Vaucheria* is suggested based on results from these studies.

Chapter 5 integrates the results of this study and their implications and suggests some future directions.

Data from Chapters 2, 3 and 4 have been published (Muralidhar et al., 2013). This paper is appended at the back of the thesis. Data from Chapter 2 has been submitted for publication in New Zealand Journal of Botany and is currently under review.

## 1.7. References

Åberg H, Fries L 1976. On cultivation of the alga *Vaucheria dichotoma* (Xanthophyceae) in axenic culture. Phycologia 15: 133-141.

Ache P, Becker D, Ivashikina N, Dietrich P, Roelfsema MRG, Hedrich R 2000. GORK, a delayed outward rectifier expressed in guard cells of *Arabidopsis thaliana*, is a $K^+$-selective, $K^+$- sensing ion channel. FEBS Letters 486: 93-98.

Adams NM 1994. Seaweeds of New Zealand. Christchurch, Canterbury University Press. 360 p.

Affenzeller MJ, Darehshouri A, Andosch A, Lütz C, Lütz-Meindl U 2009. Salt stress-induced cell death in the unicellular green alga *Micrasterias denticulata*. Journal of Experimental Botany 60: 939-954.

Aharon G, Apse M, Duan S, Hua X, Blumwald E 2003. Characterization of a family of vacuolar $Na^+/H^+$ antiporters in *Arabidopsis thaliana*. Plant and Soil 253: 245-256.

Ahmad I, Hellebust JA 1984. Osmoregulation in the extremely euryhaline marine microalga *Chlorella autotrophica*. Plant Physiology 74: 1010-1015.

Al Khazaaly S, Beilby MJ 2007. Modelling ion transporters at the time of hypertonic regulation in *Lamprothamnium succinctum* (Characeae, Charophyceae). Charophytes 1: 28-47

Amtmann A, Sanders D 1999. Mechanisms of $Na^+$ uptake by plant cells. In: Callow JA ed. Advances in Botanical Research. Volume 29. Academic Press. Pp. 75-112.

Amtmann A, Jelitto TC, Sanders D 1999. $K^+$- selective inward-rectifying channels and apoplastic pH in barley roots. Plant Physiology 120: 331-338.

Andersen RA, Bailey JC 2002. Phylogenetic analysis of 32 strains of *Vaucheria* (Xanthophyceae) using the *rbc*L gene and its two flanking spacer regions. Journal of Phycology 38: 583-592.

Apse MP, Aharon GS, Snedden WA, Blumwald E 1999. Salt tolerance conferred by overexpression of a vacuolar $Na^+/H^+$ antiport in *Arabidopsis*. Science 285: 1256-1258.

Barbier-Brygoo H, De Angeli A, Filleur S, Frachisse J-M, Gambale F, Thomine S, Wege S 2011. Anion channels/transporters in plants: from molecular bases to regulatory networks. Annual Review of Plant Biology 62: 25-51.

Barkla BJ, Zingarelli L, Blumwald E, Smith JAC 1995. Tonoplast $Na^+/H^+$ antiport activity and its energization by the vacuolar $H^+$-ATPase in the halophytic plant *Mesembryanthemum crystallinum* L. Plant Physiology 109: 549-556.

Bassil E, Coku A, Blumwald E 2012. Cellular ion homeostasis: emerging roles of intracellular NHX $Na^+/H^+$ antiporters in plant growth and development. Journal of Experimental Botany.

Bassil E, Ohto M, Esumi T, Tajima H, Zhu Z, Cagnac O, Belmonte M, Peleg Z, Yamaguchi T, Blumwald E 2011. The *Arabidopsis* intracellular $Na^+/H^+$ antiporters NHX5 and NHX6 are endosome associated and necessary for plant growth and development. The Plant Cell Online 23: 224-239.

Beever RE, Laracy EP 1986. Osmotic adjustment in the filamentous fungus *Aspergillus nidulans*. Journal of Bacteriology 168: 1358-1365.

Ben-Amotz A, Avron M 1983. Accumulation of metabolites by halotolerant algae and its industrial potential. Annual Review of Microbiology 37: 95-119.

Bentrup F-W 1990. Potassium ion channels in the plasmalemma. Physiologia Plantarum 79: 705-711.

Bisson M, Gutknecht J 1975. Osmotic regulation in the marine alga, *Codium decorticatum*: I. Regulation of turgor pressure by control of ionic composition. The Journal of Membrane Biology 24: 183-200.

Bisson M, Gutknecht J 1977. Osmotic regulation in the marine alga, *Codium decorticatum*: II. Active chloride influx exerts negative feedback control on the turgor pressure. The Journal of Membrane Biology 37: 85-98.

Bisson MA, Kirst GO 1980. *Lamprothamnium*, a euryhaline charophyte: I. Osmotic relations and membrane potential at steady state. Journal of Experimental Botany 31: 1223-1235.

Bisson MA, Kirst GO 1995. Osmotic acclimation and turgor pressure regulation in algae. Naturwissenschaften 82: 461-471.

Bisson MA, Beilby MJ 2002. The transport systems of *Ventricaria ventricosa*: hypotonic and hypertonic turgor regulation. The Journal of Membrane Biology 190: 43-56.

Bisson MA, Beilby MJ, Shepherd VA 2006. Electrophysiology of turgor regulation in marine siphonous green algae. Journal of Membrane Biology 211: 1-14.

Black DR, Weeks DC 1972. Ionic relationships Of *Enteromorpha intestinalis*. New Phytologist 71: 119-127.

Blumwald E 2000. Sodium transport and salt tolerance in plants. Current Opinion in Cell Biology 12: 431-434.

Boyer JS 1969. Measurement of the water status of plants. Annual Review of Plant Physiology 20: 351-364.

Brewster JL, Valoir TD, Dwyer ND, Winter E, Gustin MC 1993. An osmosensing signal transduction pathway in yeast. Science 259: 1760-1763.

Brini F, Masmoudi K 2012. Ion transporters and abiotic stress tolerance in plants. ISRN Molecular Biology 2012: 13.

Briskin DP, Gawienowski MC 1996. Role of the plasma membrane $H^+$-ATPase in $K^+$ transport. Plant Physiology 111: 1199-1207.

Burg MB, Ferraris JD 2008. Intracellular organic osmolytes: function and regulation. Journal of Biological Chemistry 283: 7309-7313.

Chapman VJ 1956. The marine algae of New Zealand. Part 1. Myxophyceae and Chlorophyceae. Botanical Journal of the Linnean Society 55: 333–501.

Chapman VJ, Thompson RH, Segar ECM 1957. Checklist of freshwater algae of New Zealand. Transactions of the Royal Society of New Zealand 84: 695–747.

Chen L-H, Zhang B, Xu Z-Q 2008. Salt tolerance conferred by overexpression of *Arabidopsis* vacuolar Na+/H+ antiporter gene AtNHX1 in common buckwheat (*Fagopyrum esculentum*). Transgenic Research 17: 121-132.

Chen Z, Cuin TA, Zhou M, Twomey A, Naidu BP, Shabala S 2007. Compatible solute accumulation and stress-mitigating effects in barley genotypes contrasting in their salt tolerance. Journal of Experimental Botany 58: 4245-4255.

Christensen T 1988. Salinity preference of twenty species of *Vaucheria* (Tribophyceae). Journal of the Marine Biological Association of the United Kingdom 68: 531-545.

Cleland R 1967. A dual role of turgor pressure in auxin-induced cell elongation in *Avena* coleoptiles. Planta 77: 182-191.

Cosgrove D, Hedrich R 1991. Stretch-activated chloride, potassium, and calcium channels coexisting in plasma membranes of guard cells of *Vicia faba* L. Planta 186: 143-153.

Cowan AK, Rose PD, Horne LG 1992. *Dunaliella salina*: A model system for studying the response of plant cells to stress. Journal of Experimental Botany 43: 1535-1547.

Cuin TA, Shabala S 2007. Compatible solutes reduce ROS-induced potassium efflux in Arabidopsis roots. Plant, Cell and Environment 30: 875-885.

Curti G, Massardi F, Lado P 1993. Synergistic activation of plasma membrane $H^+$-ATPase in *Arabidopsis thaliana* cells by turgor decrease and by fusicoccin. Physiologia Plantarum 87: 592-600.

Cushman JC 2001. Osmoregulation in plants: implications for agriculture. American Zoologist 41: 758-769.

Davenport RJ, Tester M 2000. A weakly voltage-dependent, nonselective cation channel mediates toxic sodium influx in wheat. Plant Physiology 122: 823-834.

Delauney AJ, Verma DPS 1993. Proline biosynthesis and osmoregulation in plants. The Plant Journal 4: 215-223.

Demidchik V, Tester M 2002. Sodium fluxes through nonselective cation channels in the plasma membrane of protoplasts from *Arabidopsis* roots. Plant Physiology 128: 379-387.

Demidchik V, Maathuis FJM 2007. Physiological roles of nonselective cation channels in plants: from salt stress to signalling and development. New Phytologist 175: 387-404.

Demidchik V, Davenport RJ, Tester M 2002. Nonselective cation channels in plants. Annual Review of Plant Biology 53: 67-107.

Dietrich P, Sanders D, Hedrich R 2001. The role of ion channels in light-dependent stomatal opening. Journal of Experimental Botany 52: 1959-1967.

Dietrich P, Anschütz U, Kugler A, Becker D 2010. Physiology and biophysics of plant ligand-gated ion channels. Plant Biology 12: 80-93.

Dixon KP, Xu J-R, Smirnoff N, Talbot NJ 1999. Independent signaling pathways regulate cellular turgor during hyperosmotic stress and appressorium-mediated plant infection by *Magnaporthe grisea*. The Plant Cell Online 11: 2045-2058.

Duniway JM 1979. Water relations of water molds. Annual Review of Phytopathology 17: 431-460.

Edwards DM, Reed RH, Stewart WDP 1988. Osmoacclimation in *Enteromorpha intestinalis*: long-term effects of osmotic stress on organic solute accumulation. Marine Biology 98: 467-476.

Entwisle TJ 1988. A monograph of *Vaucheria* (Vaucheriaceae, Chrysophyta) in south-eastern mainland Australia. Australian Systematic Botany 1: 1-77.

Fernández JA, García-Sánchez MJ, Felle HH 1999. Physiological evidence for a proton pump and sodium exclusion mechanisms at the plasma membrane of the marine angiosperm Zostera marina L. Journal of Experimental Botany 50: 1763-1768.

Flowers TJ, Colmer TD 2008. Salinity tolerance in halophytes. New Phytologist 179: 945-963.

Frey N, Büchner KH, Zimmermann U 1988. Water transport parameters and regulatory processes in *Eremosphaera viridis*. The Journal of Membrane Biology 101: 151-163.

Garrill A, Tyerman SD, Findlay GP 1994. Ion channels in the plasma membrane of protoplasts from the halophytic angiosperm Zostera muelleri. The Journal of Membrane Biology 142: 381-393.

Garrill A, Findlay GP, Tyerman SD 1996. Mechanosensitive ion channels. In: Smallwood M, Knox JP & Bowles DJ, Eds., Membranes: Specialized Functions in Plants. Oxford, UK, Bios scientific publishers. Pp. 247-60.

Gassmann W, Ward JM, Schroeder JI 1993. Physiological roles of inward-rectifying $K^+$ channels. The Plant Cell Online 5: 1491-1493.

Gavrilova EE, Rudanova OV 1999. Cell architecture in the morphogenesis of coenocytic alga *Vaucheria sessilis*. I. The morphology of germination and the behaviour of nuclei. Protistology 1: 5-9.

Gimmler H 2000. Primary sodium plasma membrane ATPases in salt-tolerant algae: facts and fictions. Journal of Experimental Botany 51: 1171-1178.

Graham LE, Graham JM, Wilcox LW 2009. Algae. 2nd edition. San Francisco, Benjamin-Cummings Publishing Company. 616 p

Guiry MD, Guiry GM 2013. AlgaeBase. World-wide electronic publication, National University of Ireland, Galway. Retrieved 01 September 2013, from http://www.algaebase.org.

Hastings D, Gutknecht J 1976. Ionic relations and the regulation of turgor pressure in the marine alga,*Valonia macrophysa*. The Journal of Membrane Biology 28: 263-275.

Hara Y, Mikami Y, Shono M, Wada M 2003. $Na^+$, $K^+$-ATPase in the Marine Alga *Heterosigma akashiwo*. Annals of the New York Academy of Sciences 986: 628-629.

Hedrich R 2012. Ion channels in plants. Physiological Reviews 92: 1777-1811.

Hellebust JA 1976. Osmorfor regulation. Annual Review of Plant Physiology 27: 485-505.

Hoffmann R, Bisson MA 1988. The effect of divalent cations on $Na^+$ tolerance in charophytes. I: *Chara buckellii*. Plant, Cell & Environment 11: 461-472.

Hooker JD 1867. Handbook of New Zealand flora: a systematic description of the native plants of New Zealand and the Chatham, Kermadec's, Lord Auckland's, and Macquarrie's islands. London, Reeve and Co. 798 p.

Horie T, Karahara I, Katsuhara M 2012. Salinity tolerance mechanisms in glycophytes: An overview with the central focus on rice plants. Rice 5: 1-18.

Hulvey JP, Padgett DE, Bailey JC 2007. Species boundaries within *Saprolegnia* (Saprolegniales, Oomycota) based on morphological and DNA sequence data. Mycologia 99: 421-429.

Iwamoto K, Shiraiwa Y 2005. Salt-regulated mannitol metabolism in algae. Marine Biotechnology 7: 407-415.

Janicka-Russak M 2011. Plant plasma membrane $H^+$-ATPase in adaptation of plants to abiotic stresses. In: Shanker A, Venkateswarlu B eds. Abiotic stress response in plants- physiological, biochemical and genetic perspectives, InTech, Rijeka, Croatia. Pp. 197-218.

Johansson I, Karlsson M, Shukla VK, Chrispeels MJ, Larsson C, Kjellbom P 1998. water transport activity of the plasma membrane aquaporin PM28A is regulated by phosphorylation. The Plant Cell Online 10: 451-459.

Kader MA, Lindberg S 2005. Uptake of sodium in protoplasts of salt-sensitive and salt-tolerant cultivars of rice, *Oryza sativa* L. determined by the fluorescent dye SBFI. Journal of Experimental Botany 56: 3149-3158.

Kant S, Kant P, Raveh E, Barak S 2006. Evidence that differential gene expression between the halophyte, *Thellungiella halophila*, and *Arabidopsis thaliana* is responsible for higher levels of the compatible osmolyte proline and tight control of $Na^+$ uptake in *T. halophila*. Plant, Cell & Environment 29: 1220-1234.

Karsten U, Barrow KD, King RJ 1993. Floridoside, L-isofloridoside, and D-isofloridoside in the red alga *Porphyra columbina* (seasonal and osmotic effects). Plant Physiology 103: 485-491.

Kasamo K 1987. Reconstitution and characterization of $H^+$-translocating ATPase from the plasma membrane of *Phaseolus mungo* L. roots. Plant and Cell Physiology 28: 19-28.

Kasamo K 1990. Mechanism for the activation of plasma membrane $H^+$-ATPase from Rice (*Oryza sativa* L.) culture cells by molecular species of a phospholipid. Plant Physiology 93: 1049-1052.

Kasamo K 2003. Regulation of plasma membrane $H^+$-ATPase activity by the membrane environment. Journal of Plant Research 116: 517-523.

Kataoka H 1975. Phototropism in *Vaucheria geminata* I. The action spectrum. Plant and Cell Physiology 16: 427-437.

Katz A, Bental M, Degani H, Avron M 1991. In vivo pH Regulation by a $Na^+/H^+$ antiporter in the halotolerant alga *Dunaliella salina*. Plant Physiology 96: 110-115.

Kiegle EA, Bisson MA 1996. Plasma membrane $Na^+$ transport in a salt-tolerant charophyte (isotopic fluxes, electrophysiology, and thermodynamics in plants adapted to saltwater and freshwater). Plant Physiology 111: 1191-1197.

Kim EJ, Kwak JM, Uozumi N, Schroeder JI 1998. AtKUP1: an arabidopsis gene encoding high-affinity potassium transport activity. The Plant Cell Online 10: 51-62.

Kirst GO 1977. Ion composition of unicellular marine and fresh-water algae, with special reference to Platymonas subcordiformis cultivated in media with different osmotic strengths. Oecologia 28: 177-189.

Kirst GO 1990. Salinity tolerance of eukaryotic marine algae. Annual Review of Plant Physiology and Plant Molecular Biology 41: 21-53.

Kollist H, Jossier M, Laanemets K, Thomine S 2011. Anion channels in plant cells. FEBS Journal 278: 4277-4292.

Kosová K, Vítámvás P, Urban MO, Prášil IT 2013. Plant proteome responses to salinity stress- comparison of glycophytes and halophytes. Functional Plant Biology 40: 775-786.

Krantz M, Becit E, Hohmann S 2006. Comparative genomics of the HOG-signalling system in fungi. Current Genetics 49: 137-151.

Krol E, Trebacz K 2000. Ways of ion channel gating in plant cells. Annals of Botany 86: 449-469.

Kronzucker HJ, Britto DT 2011. Sodium transport in plants: a critical review. New Phytologist 189: 54-81.

Latijnhouwers M, de Wit PJGM, Govers F 2003. Oomycetes and fungi: similar weaponry to attack plants. Trends in Microbiology 11: 462-469.

Latorre R, Muñoz F, González C, Cosmelli D 2003. Structure and function of potassium channels in plants:some inferences about the molecular origin of inward rectication in KAT1 channels. Molecular Membrane Biology 20: 19.

Lee RE 2008. Heterokontophyta. In: Phycology. 4 ed. New York, Cambridge University Press. Pp. 409-423.

Lew RR 1996. Pressure regulation of the electrical properties of growing *Arabidopsis thaliana* L. root hairs. Plant Physiology 112: 1089-1100.

Lew RR, Levina NN 2007. Turgor regulation in the osmosensitive cut mutant of *Neurospora crassa*. Microbiology 153: 1530-1537.

Lew RR, Levina NN, Walker SK, Garrill A 2004. Turgor regulation in hyphal organisms. Fungal Genetics and Biology 41: 1007-1015.

Lew RR, Levina NN, Shabala L, Anderca MI, Shabala SN 2006. Role of a mitogen-activated protein kinase cascade in ion flux-mediated turgor regulation in fungi. Eukaryotic Cell 5: 480-487.

Liu K, Luan S 1998. Voltage-dependent $K^+$ channels as targets of osmosensing in guard cells. The Plant Cell Online 10: 1957-1970.

Maathuis FJM, Amtmann A 1999. $K^+$ nutrition and $Na^+$ toxicity: The basis of cellular $K^+/Na^+$ ratios. Annals of Botany 84: 123-133.

Massana R, Castresana J, Balagué V, Guillou L, Romari K, Groisillier A, Valentin K, Pedrós-Alió C 2004. Phylogenetic and ecological analysis of novel marine stramenopiles. Applied and Environmental Microbiology 70: 3528-3534.

Michelet B, Boutry M 1995. The plasma membrane $H^+$- ATPase: a highly regulated enzyme with multiple physiological functions. Plant Physiology 108: 1-6.

Money N, Harold F 1993. Two water molds can grow without measurable turgor pressure. Planta 190: 426-430.

Morsomme P, Boutry M 2000. The plant plasma membrane $H^+$-ATPase: structure, function and regulation. Biochimica et Biophysica Acta (BBA) - Biomembranes 1465: 1-16.

Munns R, Tester M 2008. Mechanisms Of salinity tolerance. Annual Review of Plant Biology 59: 651-681.

Muramatsu Y, Harada A, Ohwaki Y, Kasahara Y, Takagi S, Fukuhara T 2002. Salt-tolerant ATPase Activity in the plasma membrane of the marine angiosperm *Zostera marina* L. Plant and Cell Physiology 43: 1137-1145.

Murthy M, Tester M 2006. Cation currents in protoplasts from the roots of a $Na^+$ hyperaccumulating mutant of *Capsicum annuum*. Journal of Experimental Botany 57: 1171-1180.

Obermeyer G, Tyerman SD 2005. $NH_4^+$ currents across the peribacteroid membrane of soybean. macroscopic and microscopic properties, inhibition by $Mg^{2+}$, and temperature dependence indicate a SubpicoSiemens channel finely regulated by divalent cations. Plant Physiology 139: 1015-1029.

Okazaki Y 1996. Turgor regulation in a brackish water charophyte, *Lamprothamnium succinctum*. Journal of Plant Research 109: 107-112.

Okazaki Y, Shimmen T, Tazawa M 1984. Turgor regulation in a brackish charophyte, *Lamprothamnium succinctum* II. Changes in $K^+$, $Na^+$ and $Cl^-$ concentrations, membrane potential and membrane resistance during turgor regulation. Plant and Cell Physiology 25: 573-581.

Oparka KJ 1994. Plasmolysis: new insights into an old process. New Phytologist 126: 571-591.

Ott D 1992. The role of the cytoskeleton in organelle translocations in *Vaucheria longicaulis*. In: Menzel D, Ed., The cytoskeleton of the algae. Boca Raton, CRC press, Pp. 255-272.

Ott DW, Brown RM 1974. Developmental cytology of the genus *Vaucheria* I. Organisation of the vegetative filament. British Phycological Journal 9: 111-126.

Palmgren MG 1991. Regulation of plant plasma membrane $H^+$-ATPase activity. Physiologia Plantarum 83: 314-323.

Plett D, Berger B, Tester M 2010. Genetic determinants of salinity in crop plants. In: Jenks MA, Wood AJ ed. Genes for plant abiotic stress. Pp. 83-100.

Portillo F 2000. Regulation of plasma membrane $H^+$-ATPase in fungi and plants. Biochimica et Biophysica Acta (BBA) - Reviews on Biomembranes 1469: 31-42.

Quintero FJ, Blatt MR 1997. A new family of $K^+$ transporters from *Arabidopsis* that are conserved across phyla. FEBS Letters 415: 206-211.

Ray PM, Green PB, Cleland R 1972. Role of turgor in plant cell growth. Nature 239: 163-164.

Reid RJ, Jefferies RL, Pitman MG 1984. *Lamprothamnium*, a euryhaline charophyte: IV. Membrane potential, ionic fluxes and metabolic activity during turgor adjustment. Journal of Experimental Botany 35: 925-937.

Reiser V, Raitt DC, Saito H 2003. Yeast osmosensor Sln1 and plant cytokinin receptor Cre1 respond to changes in turgor pressure. The Journal of Cell Biology 161: 1035-1040.

Rep M, Reiser V, Gartner U, Thevelein JM, Hohmann S, Ammerer G, Ruis H 1999. Osmotic stress-induced gene expression in *Saccharomyces cerevisiae* requires Msn1p and the novel nuclear factor Hot1p. Molecular and Cellular Biology 19: 5474-5485.

Roberts DM, Tyerman SD 2002. Voltage-dependent cation channels permeable to $NH_4^+$, $K^+$, and $Ca^{2+}$ in the symbiosome membrane of the model legume *Lotus japonicus*. Plant Physiology 128: 370-378.

Roberts SK 2003. TOK homologue in *Neurospora crassa*: first cloning and functional characterization of an ion channel in a filamentous fungus. Eukaryotic Cell 2: 181-190.

Rodríguez-Navarro A, Rubio F 2006. High-affinity potassium and sodium transport systems in plants. Journal of Experimental Botany 57: 1149-1160.

Sanati Nezhad A, Geitmann A 2013. The cellular mechanics of an invasive lifestyle. Journal of Experimental Botany 64: 4709-4728.

Sarma P 1973. Addition to the freshwater algae of New Zealand - I. A note on the species of *Vaucheria* from Great Barrier Island. Tane 19: 167–173.

Sarma P 1974. Additions to the freshwater algae of New Zealand- II : Some *Vaucheria* from Slipper Island. Tane 20: 86–100.

Sauer G, Simonis W, Schönknecht G 1993. An inwardly rectifying cation current across the plasma membrane of the green alga *Eremosphaera viridis*. Plant and Cell Physiology 34: 1275-1282.

Schiel DR, Foster MS 2006. The population biology of large brown seaweeds: ecological consequences of multiphase life histories in dynamic coastal environments. Annual Review of Ecology, Evolution, and Systematics 37: 343-372.

Schroeder JL 1995. Anion channels as central mechanisms for signal transduction in guard cells and putative functions in roots for plant-soil interactions. Plant Molecular Biology 28: 353-361.

Schroeder JI, Allen GJ, Hugouvieux V, Kwak JM, Waner D 2001. Guard cell signal transduction. Annual Review of Plant Physiology and Plant Molecular Biology 52: 627-658.

Shabala L, McMeekin T, Shabala S 2009. Osmotic adjustment and requirement for sodium in marine protist thraustochytrid. Environmental Microbiology 11: 1835-1843.

Shabala SN, Lew RR 2002. Turgor regulation in osmotically stressed *Arabidopsis* epidermal root cells. Direct support for the role of inorganic ion uptake as revealed by concurrent flux and cell turgor measurements. Plant Physiology 129: 290–299.

Shi H, Ishitani M, Kim C, Zhu J-K 2000. The *Arabidopsis thaliana* salt tolerance gene SOS1 encodes a putative $Na^+/H^+$ antiporter. Proceedings of the National Academy of Sciences 97: 6896-6901.

Shi H, Quintero FJ, Pardo JM, Zhu J-K 2002. The putative plasma membrane $Na^+/H^+$ Antiporter SOS1 controls long-distance $Na^+$ transport in plants. The Plant Cell 14: 465-477.

Shono M, Wada M, Hara Y, Fujii T 2001. Molecular cloning of $Na^+$-ATPase cDNA from a marine alga, *Heterosigma akashiwo*. Biochimica et Biophysica Acta (BBA) - Biomembranes 1511: 193-199.

Simons J 1974. *Vaucheria compacta*: a euryhaline estuarine algal species. Acta Botanica Neerlandica 23: 613-626.

Skerrett M, Tyerman SD 1994. A channel that allows inwardly directed fluxes of anions in protoplasts derived from wheat roots. Planta 192: 295-305.

Somero GN, Yancey PH 2010. Osmolytes and cell-volume regulation: physiological and evolutionary principles. Comprehensive Physiology, John Wiley & Sons, Inc.

Staal M, Maathuis FJM, Elzenga JTM, Overbeek JHM, Prins HBA 1991. $Na^+/H^+$ antiport activity in tonoplast vesicles from roots of the salt-tolerant *Plantago maritima* and the salt-sensitive *Plantago media*. Physiologia Plantarum 82: 179-184.

Stento NA, Ryba NG, Kiegle EA, Bisson MA 2000. Turgor regulation in the salt-tolerant alga *Chara longifolia*. Plant, Cell & Environment 23: 629-637.

Stoelzle S, Kagawa T, Wada M, Hedrich R, Dietrich P 2003. Blue light activates calcium-permeable channels in *Arabidopsis* mesophyll cells via the phototropin signaling pathway. Proceedings of the National Academy of Sciences 100: 1456-1461.

Taiz L 1984. Plant cell expansion: regulation of cell wall mechanical properties. Annual Review of Plant Physiology 35: 585-657.

Tarczynski MC, Jensen RG, Bohnert HJ 1993. stress protection of transgenic tobacco by production of the osmolyte mannitol. Science 259: 508-510.

Taylor E, Taylor T, Krings M 2008. Algae. In: Paleobotany: The biology and evolution of fossil plants. 2nd Edition. Elsevier Academic Press, USA. Pp.121–160

Teodoro AE, Zingarelli L, Lado P 1998. Early changes of $Cl^-$ efflux and $H^+$ extrusion induced by osmotic stress in *Arabidopsis thaliana* cells. Physiologia Plantarum 102: 29-37.

Tester M 1990. Plant ion channels: whole-cell and single channel studies. New Phytologist 114: 305-340.

Tester M 1996. Functions of ion channels in plant cells. In: Smallwood M, Knox, JP & Bowles, DJ eds. Membranes: Specialized Functions in Plants. Oxford, UK, Bios scientific publishers. Pp. 231-245.

Tester M, Davenport R 2003. $Na^+$ tolerance and $Na^+$ transport in higher plants. Annals of Botany 91: 503-527.

Tufariello JAM, Hoffmann R, Bisson MA 1988. The effect of divalent cations on $Na^+$ tolerance in Charophytes. II: *Chara corallina*. Plant, Cell & Environment 11: 473-479.

Tyerman SD 1992. Anion channels in plants. Annual Review of Plant Physiology and Plant Molecular Biology 43: 351-373.

Tyerman SD, Skerrett IM 1999. Root ion channels and salinity. Scientia Horticulturae 78: 175-235.

Tyerman SD, Niemietz CM, Bramley H 2002. Plant aquaporins: multifunctional water and solute channels with expanding roles. Plant, Cell and Environment 25: 173-194.

Tyerman SD, Skerrett M, Garrill A, Findlay GP, Leigh RA 1997. Pathways for the permeation of $Na^+$ and $Cl^-$ into protoplasts derived from the cortex of wheat roots. Journal of Experimental Botany 48: 459-480.

Tyerman SD, Bohnert HJ, Maurel C, Steudle E, Smith JAC 1999. Plant aquaporins: their molecular biology, biophysics and significance for plant water relations. Journal of Experimental Botany 50: 1055-1071.

Uji T, Monma R, Mizuta H, Saga N 2012. Molecular characterization and expression analysis of two $Na^+/H^+$ antiporter genes in the marine red alga *Porphyra yezoensis*. Fisheries Science 78: 985-991.

Wada M, Satoh S, Kasamo K, Fujii T 1989. Presence of a $Na^+$-activated ATPase in the plasma membrane of the marine raphidophycean *Heterosigma akashiwo*. Plant and Cell Physiology 30: 923-928.

Walker SK, Chitcholtan K, Yu Y, Christenhusz GM, Garrill A 2006. Invasive hyphal growth: An F-actin depleted zone is associated with invasive hyphae of the oomycetes *Achlya bisexualis* and *Phytophthora cinnamomi*. Fungal Genetics and Biology 43: 357-365.

Wang S-M, Zhang J-L, Flowers TJ 2007. Low-affinity $Na^+$ uptake in the halophyte *Suaeda maritima*. Plant Physiology 145: 559-571.

Wegmann K 1986. Osmoregulation in eukaryotic algae. FEMS Microbiology Letters 39: 37-43.

Wilkinson M, Telfer T, Grundy S 1995. Geographical variation in the distributions of macroalgae in estuaries. Netherland Journal of Aquatic Ecology 29: 359-368.

Wilcox MD 2011. Occurence of marine yellow-green algae *Vaucheria velutina* C. Agardh and *Vaucheria longicaulis* Hoppaugh (Xanthophyceae: Vaucheriaceae) in Auckland, New Zealand. New Zealand Journal of Marine and Freshwater Research 46: 285–290.

Whittington J, Bisson MA 1994. $Na^+$ fluxes in *Chara* under salt stress. Journal of Experimental Botany 45: 657-665.

Yancey PH 2001. Water stress, osmolytes and proteins. American Zoologist 41: 699-709.

Yancey PH 2005. Organic osmolytes as compatible, metabolic and counteracting cytoprotectants in high osmolarity and other stresses. Journal of Experimental Biology 208: 2819-2830.

Yancey P, Clark M, Hand S, Bowlus R, Somero G 1982. Living with water stress: evolution of osmolyte systems. Science 217: 1214-1222.

Ye Q, Wiera B, Steudle E 2004. A cohesion/tension mechanism explains the gating of water channels (aquaporins) in *Chara* internodes by high concentration. Journal of Experimental Botany 55: 449-461.

Young AJ, Collins JC, Russell G 1987a. Solute regulation in the euryhaline marine alga *Enteromorpha prolifera* (O. F. Müll) J. Ag. Journal of Experimental Botany 38: 1298-1308.

Young AJ, Collins JC, Russell G 1987b. Ecotypic variation in the osmotic responses of *Enteromorpha intestinalis* (L.) Link. Journal of Experimental Botany 38: 1309-1324.

Zhang W, Fan L-M, Wu W-H 2007. Osmo-sensitive and stretch-activated calcium-permeable channels in *Vicia faba* guard cells are regulated by actin dynamics. Plant Physiology 143: 1140-1151.

Zhang X, Wang H, Takemiya A, Song C-P, Kinoshita T, Shimazaki K-I 2004. Inhibition of blue light-dependent $H^+$ pumping by abscisic acid through hydrogen peroxide-induced dephosphorylation of the plasma membrane $H^+$-ATPase in guard cell protoplasts. Plant Physiology 136: 4150-4158.

Zhang Y, Lamm R, Pillonel C, Lam S, Xu J-R 2002. Osmoregulation and fungicide resistance: the *Neurospora crassa* os-2 gene encodes a HOG1 mitogen-activated protein kinase homologue. Applied and Environmental Microbiology 68: 532-538.

Zhu J-K 2003a. Regulation of ion homeostasis under salt stress. Current Opinion in Plant Biology 6: 441-445.

Zhu J-K 2003b. Salt and drought stress signal transduction in plants. Annual Review of Plant Biology 53: 247-273.

Zimmermann S, Talke I, Ehrhardt T, Nast G, Müller-Röber B 1998. Characterization of SKT1, an inwardly rectifying potassium channel from potato, by heterologous expression in insect cells. Plant Physiology 116: 879-890.

Zimmermann U 1978. Physics of turgor and osmoregulation. Annual Review of Plant Physiology 29: 121-148.

Zingarelli L, Teresa Marrè M, Massardi F, Lado P 1999. Effects of hyper-osmotic stress on $K^+$ fluxes, $H^+$ extrusion, transmembrane electric potential difference and comparison with the effects of fusicoccin. Physiologia Plantarum 106: 287-295.

## Chapter 2

## Morphological and phylogenetic characterization of seven species of *Vaucheria*, including two new species, from contrasting habitats in New Zealand

### 2.1. Introduction

*Vaucheria* De Candolle is a genus of yellow-green algae (Xanthophyceae) characterized by siphons with apical growth. It has a cosmopolitan distribution with over 75 accepted species worldwide (Guiry and Guiry 2013). Taxonomy of the genus is based on a morphospecies concept, where species are characterized on morphology, especially the shape, size and arrangement of antheridia and oogonia. Identification of closely related species is a challenge because of overlapping characteristics (Entwisle 1988a, 1988b) and due to paucity of fertile material in field specimens (Rieth 1980). Cryptic species that are morphologically indistinguishable are known to exist, but there is no current consensus on what to do with such entities (Andersen and Bailey 2002).

The distribution of *Vaucheria* in New Zealand is poorly known, with most records from the North Island. There are reports of seven freshwater species - *V. geminata* (Vaucher) De Candolle (Chapman et al. 1957), *V. dillwynii* (Weber and Mohr) Agardh (=*V. pachyderma* Walz) (Hooker 1867; Sarma 1974), *V. hamata* (Vaucher) De Candolle, *V. jaoi* Ley (Sarma 1973), *V. aversa* Hassall, *V. sessilis* (Vaucher) De Candolle f. *repens* (Hassall) Hansgirg and *V. undulata* Jao (Sarma 1974), and four marine species – *V. velutina* Agardh , *V. synandra* Woronin , *V. pseudosessilis* Chapman (Chapman 1956) and *V. longicaulis* Hoppaugh (Wilcox 2011). Two additional marine species were listed by Adams (1994) as *Vaucheria* sp. from mudflats in the North Island and *Vaucheria* sp. 'Chathams' from the Chatham Islands. There are no reports of soil-dwelling species in New Zealand.

Here, seven species of *Vaucheria*, including new species, are identified based on the morphology of reproductive structures. Also, *rbc*L sequences were used to assess genetic variation among our strains and to determine relationships with other strains using phylogenetic analysis.

## 2.2. Materials and methods

### 2.2.1. Sample collection and culturing

Specimens of *Vaucheria* were collected from freshwater, soil, brackish / intertidal and marine sources. All were collected from different locations in Canterbury, New Zealand except for the marine specimen that was sourced from Whangateau Harbour, Auckland, New Zealand (Fig. 2.1). Details of sample locations are given in the results section.

All samples were collected in sterile polycarbonate bottles and transported to the laboratory on the same day. Clonal cultures were established for all the isolates using the methods described below. No attempt was made to free strains from bacterial contaminants.

For the freshwater isolates, dense mats of siphons were vigorously washed with filtered habitat water and excised lengths of about 1 cm were inoculated onto agarised (1% w/v) Bold's Basal Medium (BBM, Bischoff and Bold 1963) amended with vitamin solution (0.5 ml $l^{-1}$) from a stock of thiamine HCl (200 mg $l^{-1}$), biotin (244.31 mg $l^{-1}$) and cyanocobalamin (1355.4 mg $l^{-1}$). Petri dishes with agarised media (1% w/v) were incubated under standard conditions (16:8 h light:dark regime at 14 °C and ~50 µmol $m^{-2}$ $s^{-1}$ light intensity).

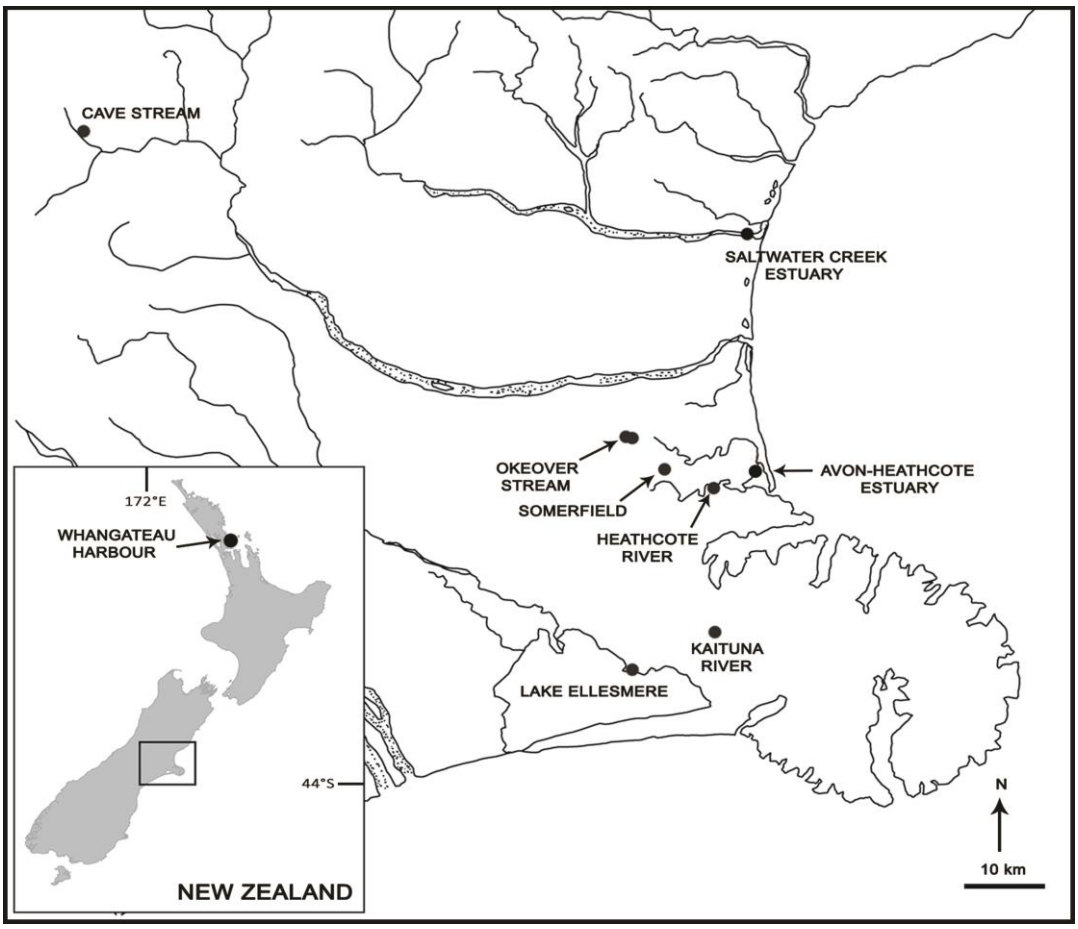


**Figure 2.1.** Map of the collection sites in Canterbury (black dots). Inset map shows collection site of marine sample, Whangateau Harbour (black dot), Auckland and also the location of the main collection area in Canterbury, New Zealand.

Because specimens from brackish habitats did not form dense mats, growth was initially enriched in Petri dishes by moistening with habitat water filtered through a 0.2 µm pore filter, followed by incubation under standard conditions. Siphons growing upwards towards the light were excised and inoculated onto modified agarised f/2 medium (Guillard and Ryther 1962) in 90 mm Petri dishes. Natural seawater in the original recipe for f/2 medium was diluted with distilled water to obtain media with salinities ranging from 2.5–35 ppt (parts per thousand by weight) to test for optimal growth. Reproductive structures were absent both in field material and in solid agarised culture media for specimens from brackish habitats. In order to generate reproductive structures, siphons were stressed by placing them in small amounts of liquid medium (10-15 ml) in uncapped polycarbonate bottles and allowing the medium to evaporate for a week.

For the specimen from soil, habitat soil was enriched with sterile liquid BBM enriched with vitamins in the base of a Petri dish. Siphons growing upwards towards the light were excised and inoculated onto agarised BBM. The tips of siphons that developed in these cultures were excised and transferred to fresh culture medium.

For the marine specimen, sterile natural seawater was used to enrich habitat sediment in the base of a Petri dish. Siphons growing upwards towards the light were excised and inoculated onto natural seawater enriched with mineral and trace metal solutions as used for f/2 medium.

### 2.2.2. Microscopy

Photomicrographs of reproductive structures were obtained using a Nikon E5400 camera (Nikon Corporation, Chiyoda-ku, Tokyo, Japan) mounted on a Zeiss IM 35 inverted microscope (Carl Zeiss, Jena, Germany) using brightfield settings. Images were obtained straight from agar surfaces for freshwater and terrestrial strains and from liquid media cultures for other strains. Descriptions of morphological characters of each species were

based on 30–50 observations and a minimum of 20 measurements. Voucher specimens were deposited in the Allan Herbarium, Landcare Research, Lincoln, New Zealand (Table 2.1).

**Table 2.1**. *Vaucheria* species used in the phylogenetic analysis, their habitats, strain numbers and accession numbers listed in the order in which they appear in Fig. 2.2.

| Species | Habitat | Collector | Voucher no. | Genbank acc no. |
|---|---|---|---|---|
| *Vaucheria medusa* | Brackish | Christensen, T. | K362 | AF476936 |
| ***Vaucheria aestuarii*** | **Brackish** | **MacIntyre, D.** | **CHR631518** | KF791051 |
| *Vaucheria compacta* | Terrestrial, brackish | Lane, CE. | CL001901 | AF476928 |
| *Vaucheria litorea* | Marine | Faux, L. | - | AF207527 |
| *Vaucheria litorea* | Brackish | Christensen, T. | K379 | AF476935 |
| ***Vaucheria litorea*** | **Brackish** | **Broady, PA & Macintyre,D.** | **CHR631519** | KF791053 |
| *Vaucheria terrestris* | Freshwater | Christensen, T. | UTEX2065 | AF476946 |
| *Vaucheria terrestris* | Freshwater | Christensen, T. | CCAP745/6 | AF476947 |
| *Vaucheria terrestris* | Freshwater | Christensen, T. | CCAP745/6 | AJ874702 |
| *Vaucheria frigida* | Freshwater | Christensen, T. | K461 | AF476948 |
| *Vaucheria frigida* | Freshwater | - | - | AB266740 |
| *Vaucheria frigida* | Terrestrial | Christensen, T. | - | AF476945 |
| *Vaucheria prona* | Terrestrial | Christensen, T. | K568 | AF476956 |
| *Vaucheria prona* | Terrestrial, freshwater | Schneider, CW. | HML1 | AF476957 |
| *Vaucheria prona* | Terrestrial, freshwater | Norland, A & Lane, CE. | QP1A | AF476958 |
| *Vaucheria prona* | Terrestrial | Christensen, T. | K462 | AF476955 |
| *Vaucheria hamata* | Terrestrial | Linne von Berg, KH. | SAG48.81 | AF476954 |
| *Vaucheria geminata* | Terrestrial, freshwater | Bold, H. | TEX1035 | AF476952 |
| *Vaucheria geminata* | Terrestrial, freshwater | Fawley, M. | CCMP2055 | AF476953 |
| *Vaucheria pseudogeminata* | Terrestrial, freshwater | Christensen, T. | K460 | AF476949 |
| *Vaucheria erythrospora* | Brackish | Christensen, T. | K387 | AF476951 |
| ***Vaucheria erythrospora*** | **Brackish** | **Muralidhar, A.** | **CHR631517** | KF791051 |
| *Vaucheria walzii* | Terrestrial | Linne von Berg, KH. | SAG51.81 | AF476950 |
| ***Vaucheria edaphica*** | **Terrestrial** | **Broady, PA.** | **CHR631520** | KF791054 |
| *Vaucheria canalicularis* | Freshwater | Christensen, T. | K385 | AF476944 |
| ***Vaucheria bursata*** | **Freshwater** | **Muralidhar, A.** | **CHR631512** | KF791046 |
| ***Vaucheria bursata*** | **Freshwater** | **Muralidhar, A.** | **CHR631514** | KF791048 |
| ***Vaucheria bursata*** | **Freshwater** | **Broady, PA.** | **CHR631515** | KF791049 |
| ***Vaucheria bursata*** | **Freshwater** | **Muralidhar, A.** | **CHR631511** | KF791045 |
| ***Vaucheria bursata*** | **Freshwater** | **Muralidhar, A.** | **CHR631513** | KF791047 |
| ***Vaucheria* cf. *borealis*** | **Freshwater** | **Muralidhar, A.** | **CHR631516** | KF791050 |
| *Vaucheria repens* | Freshwater | Christensen, T. | K583 | AF476942 |
| *Vaucheria bursata* | Freshwater | Christensen, T. | K402 | AF476937 |
| *Vaucheria dillwynii* | Freshwater | Christensen, T. | K464 | AF476941 |
| *Vaucheria bursata* | Freshwater | Biebel, P. | TEX761 | AF476940 |
| *Vaucheria bursata* | Freshwater | Christensen, T. | CCMP1084 | AF476938 |
| *Vaucheria bursata* | Freshwater | Christensen, T. | CCMP1084 | AF015589 |
| *Vaucheria bursata* | Freshwater | Christensen, T. | UTEX2067 | AF476939 |
| *Vaucheria conifera* | Marine | Christensen, T. | K366 | AF476930 |
| ***Vaucheria* cf. *conifera*** | **Marine** | **Wilcox, MD.** | **AK328489** | KF791055 |
| *Vaucheria dichotoma* | Freshwater | Christensen, T. | K314 | AF476932 |
| *Vaucheria dichotoma* | Freshwater | Christensen, T. | K312 | AF476931 |
| *Vaucheria schleicheri* | Freshwater | Christensen, T. | K386 | AF476933 |
| *Vaucheria synandra* | Brackish | Nielsen, R. | K388 | AF476929 |
| *Vaucheria coronata* | Marine | Christensen, T. | K364 | AF476928 |
| *Vaucheria aversa* | Freshwater | Christensen, T. | K384 | AF476943 |

* Strains investigated in this study are shown in bold

### 2.2.3. DNA extraction, PCR and sequencing

Manual DNA extraction was performed for 8 isolates (*Muralidhar UCVFW1-4*, *Broady UCVFW5*, *Muralidhar UCVFW6*, *Muralidhar UCVBW1* and *Wilcox 4431b* ) in which siphons were ground up using a pre-heated mortar and pestle at 65°C in CTAB (cetyl trimethyl ammonium bromide) extraction buffer (3 ml 5M NaCl, 2 ml 10% CTAB, 1ml 1M TRIS-HCl (pH 8), 0.4 ml 0.5 M EDTA made up to 10 ml with PCR grade water) and incubated at 65°C for 30 min. DNA was extracted from the CTAB using phenol chloroform extractions (24 : 1 chloroform : isoamyl alcohol extraction, followed by a 25 : 24 : 1 phenol : chloroform : isoamyl alcohol extraction, followed by another 24 : 1 chloroform : isoamyl alcohol extraction) and concentrated using a Zymo DNA Clean and Concentrator kit (Zymo Research Corporation, Irvine, CA, USA). For three isolates (*Macintyre G7*, *Broady and Macintyre E5A*, *Broady UCVT1*), the Maxwell 16 tissue DNA purification kit run in a Maxwell automated DNA extractor (Promega Corporation, Fitchburg, WI, USA) was used for DNA extraction from ground up *Vaucheria* siphons. The product from the machine was subjected to a round of phenol chloroform extractions followed by DNA concentration as mentioned above. It should be noted that the DNA for the marine specimen was obtained from cleaned field material.

Two overlapping fragments of the *rbc*L gene were amplified using the primers X7F (forward) and RS3 (reverse) and XanRF1 (forward) and 9R (reverse) (Table 2.2) (Andersen and Bailey 2002) using the program 96°C for 4 min, followed by 35 cycles of 96°C for 45 s, 46°C for 30 s, and 72°C for 90 s. Sequencing and capillary separation of Big Dye Terminator 3.1 reactions were carried out at Landcare Research, Auckland, New Zealand. The XanRF1 primer was newly developed for this study (sequence given in Table 2.1). Electropherograms were checked using Sequencher 4.5 (Gene Codes Corporation, Michigan, USA). The start of XanRF1 corresponds to position 1165, X7F to position 1617 and 9R to position 1622 in

*V. prona* in Genbank sequence AF476958 as reported by Andersen and Bailey (2002). The X7F-RS3 fragment includes the 3' end of the *rbc*L gene and the *rbc*L-*rbc*S intergenic spacer.

**Table 2.2**. Primers used for amplification and sequencing according to their position in *Vaucheria prona* (Genbank accession AF476958).

| Primers | Sequences | Positions |
|---|---|---|
| Forward primers (5'-3') | | |
| Primer XanRF1 | AAGAAATGTATGAACGTGC | 1165-1183 |
| Primer X7F | CTTCAATTTGGTGGTGG | 1617-1633 |
| Reverse primers (3'-5') | | |
| Primer 9R | ATTTGGTGGTGGTACGATTGG | 1622-1642 |
| Primer RS3 | GAATGGACAGATGATC | 1913-1928 |

### 2.2.4. Phylogenetic analysis

Multiple sequence alignments of *Vaucheria* taxa were constructed in Clustal X 1.8 (Thompson et al. 1997) with default parameters and edited by eye. Sequences from 51 strains including 46 *Vaucheria* strains and 5 closely related xanthophyceans (Andersen and Bailey 2002) which formed the outgroup (*Botrydium stoloniferum* Mitra 1950, B. *becharianum* Vischer 1938, *B. cytosum* Vischer 1938, *Tribonema intermixum* Pascher 1923 and *Asterosiphon dichotomus* (Kützing) Rieth 1963), were used for the analysis (Fig. 2.2). The uncorrected p-distance was measured using MEGA 5, as a measure of variation between sequences (Tamura et al. 2011). Details of *Vaucheria* sequences used in the analysis including their accession numbers, voucher numbers and collection details are given in Table 2.2. Regions of ambiguous alignment were deleted back to the nearest conserved base position on either side. The complete dataset was 1533 bp long with 1011 conserved sites, 522 variable sites and 414 parsimony informative sites. The sequence lengths of our strains

ranged from 761 bp in AK 328489 to 417 bp in CHR 631520. In the phylogenetic analyses, the lengths of other sequences obtained from Genbank were longer than our sequences. Positions 772–1533 which represented the coverage range of our sequences, had 488 conserved sites, 273 variable sites and 214 parsimony informative sites. Two methods were used for the analyses. 1) Maximum parsimony (MP) implemented in PAUP*4.0b10 (Swofford 2002) with the following settings: branches collapsed if maximum length = 0, maximum number of trees = 100000, 10 random sequence additions, non-parametric bootstrap values calculated for 1000 replicates. 2) Bayesian Inference (BI) implemented in MrBayes v3.0B4 (Ronquist and Huelsenbeck 2003). The evolutionary model GTR+G+I was chosen using default parameter settings in the MEGA 5 model testing function. Two simultaneous runs were performed, each with 16 chains, for 2500000 generations with sampling frequency = 1000 and a random starting tree on the SCENZ-Grid cluster at Landcare Research, Palmerston North, New Zealand. Trees were summarized using up to 500000 generations as burnin, as judged from log-likelihood plots. Variation around parameter estimates was examined to check for over-parameterisation.

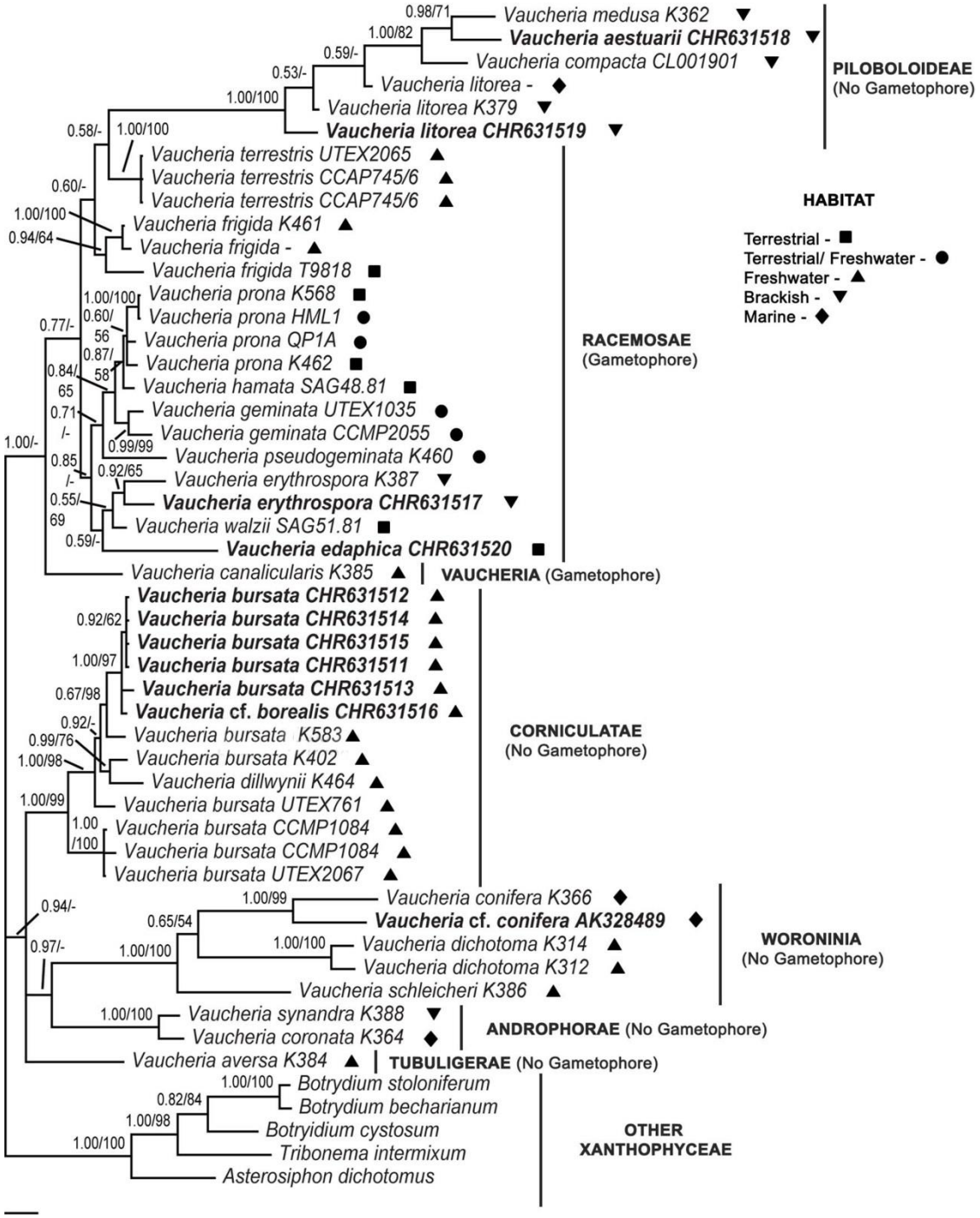


**Figure 2.2**. 50% majority rule consensus tree showing Bayesian phylogenies of *Vaucheria* strains from different habitats in New Zealand (indicated in bold) based on the phylogenetic analysis of the *rbc*L gene and partial *rbc*L-*rbc*S spacer region. Support numbers and branches are Bayesian posterior probabilities/ Maximum Parsimony bootstrap values. The different taxonomic sections of the strains as in Andersen and Bailey (2002) and the presence and absence of a gametophore bearing antheridia and oogonia are indicated beside the tree. Scale bar = 0.1 substitutions/site. Substitution model and data sets described in text.

## 2.3. Taxonomy

**2.3.1.** ***Vaucheria bursata*** (Müller) Agardh 1811: p. 21. Christensen 1969, p. 26, fig. 15; 1973:

p.513, fig. 1A–G. Heering 1907: 181.

BASIONYM**:** *Conferva bursata* Müller 1788, p. 96, pl. 2, fig. 10.

HETEROTYPIC SYNONYMS:

*Vaucheria sessilis* (Vaucher) De Candolle in Lamarck and de Candolle 1805 : Hoppaugh 1930, p. 335 pl. 24, fig. 1.; Venkataraman 1961, p. 68, fig. 46a; Blum 1972, p. 16, fig. 23 and 35; Rieth 1980, p. 59, fig. 21, p.61, fig. 22.

*Vaucheria sessilis* f. *clavata* Heering 1907: Hoppaugh 1930, p. 336, pl. 24, fig. 3-4; Venkataraman 1961, p. 69; Rieth 1980, p. 60.

*Vaucheria sessilis* f. *repens* (Hassall) Hansgirg 1886: Hassall 1845, p. 52, pl. 6, fig. 7; Hoppaugh 1930, p. 336, pl. 24, fig. 2.; Venkataraman 1961, p.70; Blum 1972: 15, fig. 24, 36-37; Sarma 1974, p. 87, figs. 2, 4, 5, 15, 16; Rieth 1980, p. 60.

REPRESENTATIVE SPECIMENS: Okeover Stream, Christchurch, Canterbury (lat. 43.522546°S, long. 172.584832°E), *Muralidhar UCVFW1* (CHR 631511); Okeover Stream, Christchurch, Canterbury (lat. 43.523075°S, long. 172.587363°E), *Muralidhar UCVFW2* (CHR 631512); Heathcote River, Christchurch, Canterbury (lat 43.551215°S, long. 172.671878°E), *Muralidhar UCVFW3* (CHR 631513); Kaituna River, Canterbury (lat. 43.725468°S, long. 172.693239°E), *Muralidhar UCVFW4* (CHR 631514); Knights Stream, Canterbury (lat. 43.592133°S, long. 172.559791°E), *Broady UCVFW5* (CHR 631515).

REFERENCES: Entwisle 1987, p. 309, fig. 12–13; Entwisle 1988a, p. 17, fig. 8–9, 12.

DESCRIPTION: Siphons 35–110 µm diam., light to dark green, texture velvety to coarse; branches occasional to frequent. Alga monoecious; antheridia and oogonia adjacent; occasional to frequent, sometimes with two oogonia per antheridium (Fig. 2.3). Antheridia circinate-cylindrical, 35–110 µm long, 25–35 µm diam., turning through less than a full circle. Antheridial pedicel straight or curved distally. Oogonia sessile, ovoid-reniform, 30–120 µm diam, 35–155 µm long; long axes parallel or oblique to the length of siphons. Oospores and oogonia similar in size and shape.

MOLECULAR DATA: Our five *V. bursata* strains grouped together in a robust clade making up section *Corniculatae* in both MPB (maximum parsimony bootstrap) and Bayesian analyses (Fig. 2.2). This clade also included sequences of strains designated as *V. bursata*, *V. repens* and *V. dilwynii* from Genbank in addition to *V.* cf. *borealis* from this study. All five *V. bursata* strains in this study were very closely related with a maximum p-distance of 0.005 between them. It should be noted that *V. bursata* is not monophyletic.

NOTES: All five strains conformed closely to the published descriptions of *Vaucheria bursata* (Müller) Agardh (Entwisle 1987, 1988a). *V. bursata* has been recorded previously in New Zealand as the synonym *Vaucheria sessilis* f. *repens* (Sarma 1974). This is a common species found in freshwater habitats worldwide.

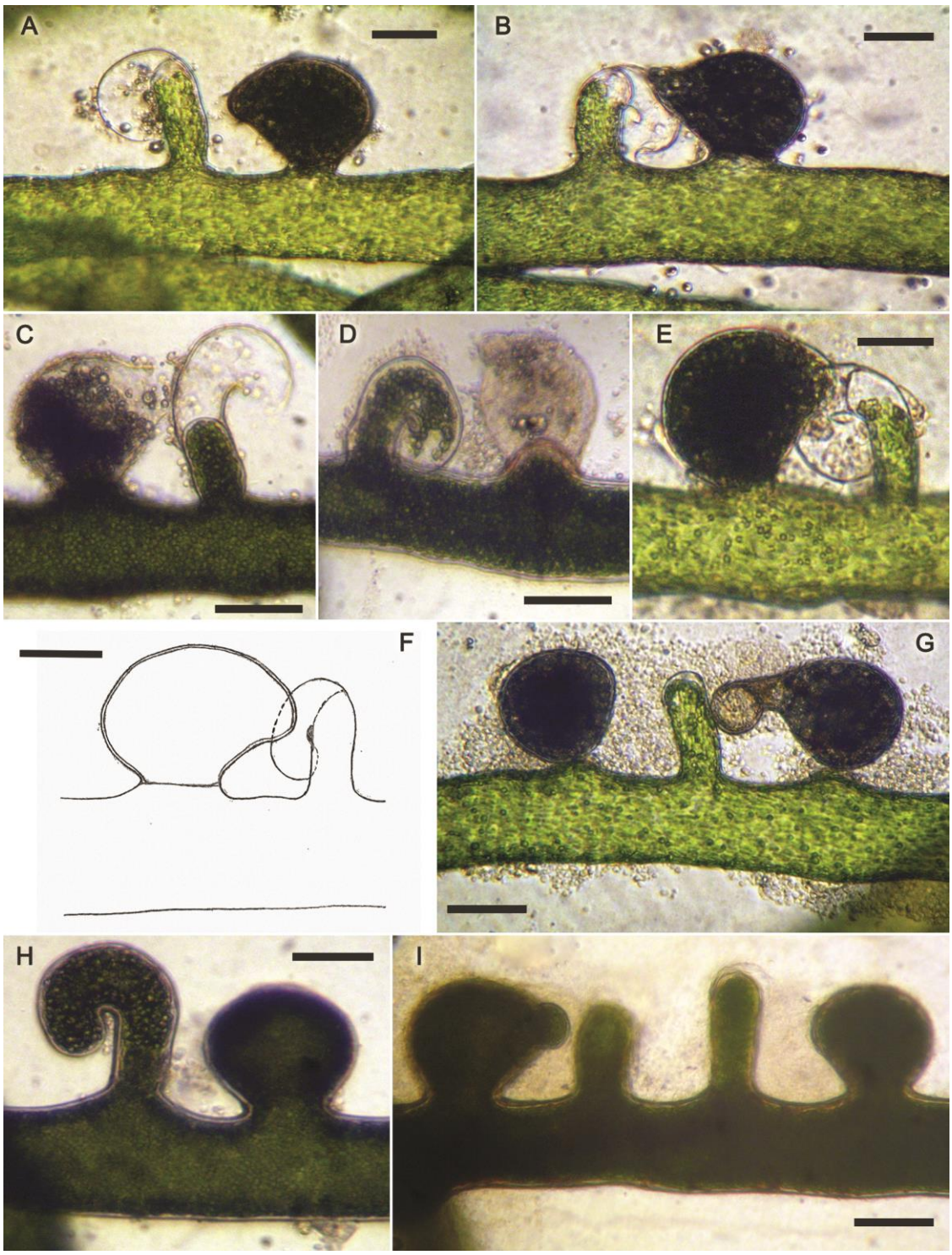


**Figure 2.3.** Light micrographs and illustration of *Vaucheria bursata* reproductive structures. A and E- CHR631511; G- CHR631512; C and D- CHR631513; B- CHR631514; H and I- CHR631515. A, F and H - Circinate, cylindrical antheridia turning less than a full circle and an ovoid- reniform oogonia. G- Two oogonia either side of a developing antheridium. I- Two sets of antheridia and oogonia side by side. Bars= 50 µm.

**2.3.2. *Vaucheria* cf. *borealis*** Hirn 1900, p. 87, Fig. 2

REPRESENTATIVE SPECIMEN: Cave Stream, Canterbury (lat. 43.194954°S, long. 171.743010°E), *Muralidhar UCVFW6* (CHR 631516).

REFERENCES: Brown 1929, p. 94, pl. 16, fig. 11; Hoppaugh 1930, p. 337, pl. 24, fig. 5; Venkataraman 1961, p. 71, fig. 47; Reith 1980, p. 57, fig. 20; Entwisle 1987, p. 316, fig. 34; Johnson 2002, p. 267, pl. 72A

DESCRIPTION: Siphons 35–50 µm diam.; branches frequent. Alga monoecious; antheridia and oogonia adjacent, rarely observed (Fig. 2.4). Antheridia circinate-cylindrical, 50–55 µm long, 20–35 µm diam. Oogonia ovoid, 55–70 µm diam., 60–80 µm long; long axes parallel to length of siphons; scarcely stalked with a beak, parallel to length of siphon; oogonial wall evenly textured, smooth. Mature oospores similar in shape but smaller in size to oogonia, a portion of oogonium left vacant by mature oospore.

MOLECULAR DATA: This strain was found to be very closely related to the *V. bursata* strains in our study (maximum p-distance = 0.005). The next closest match was a strain designated as *V. repens* (p-distance = 0.019).

NOTES: We had difficulty in unequivocally placing this strain under any species in section *Corniculatae*. The presence of just one oogonium per antheridium as opposed to two in *V. bursata* and the fact that the long axes of the oogonia were always parallel to the length of the siphons rather than oblique, separated it from *V. bursata* (Hoppaugh 1930; Venkataraman 1961; Reith 1980). Oogonial orientation also separated another species from our strain- *V. repens* Hassall (= *V. sessilis* f. *repens* (Hassall) Hansgirg), considered a heterotypic synonym of *V. bursata* in this study and by most authors (Venkataraman 1961; Christensen 1969; Entwisle 1987, 1988). In this species, the long axes of the oogonia are at an angle to

the siphons (Hassall 1845; Hoppaugh 1930, Sarma 1974). We found that this strain conformed most closely to published descriptions of *V. borealis* Hirn (Hoppaugh 1930; Venkataraman 1961; Reith 1980; Entwisle 1987; Johnson 2002). The characters which matched it to *V. borealis* were- the ovoid-reniform shape of the oogonia, the long axes of the oogonia always parallel to siphons, mature oospores smaller than the oogonia, smooth texture of oogonial walls. The smaller size of the siphons and smaller length and diameter of the oogonia were the only characters which did not conform with this species. Hoppaugh (1930) also reported two strains, which conformed closely to the original description of *V. borealis* Hirn, except for the smaller size of siphons and oogonia. This strain was found to be genetically more closely related to our *V. bursata* strains than a strain designated as *V. repens* (see above and Fig. 2.2). It should be noted that Entwisle (1987) found the orientation of the oognonial long axes too variable as a character to distinguish between species in the section. But, after extensive scrutiny of other species descriptions of section *Corniculatae* and considering the unavailability of representative gene sequences for *V. borealis*, this strain has been named *Vaucheria* cf. *borealis*, pending further analysis. Oospores in this strain were brown when mature with a prominent reddish colouration towards the center. The base of the oogonial pedicel was also found to be reddish-brown. These characters were obvious in all oogonia. There is no mention of these characters in reports of *V. borealis*. A comparison of characters of some closely related morphospecies in the section *Corniculatae* is given in Table 2.3.

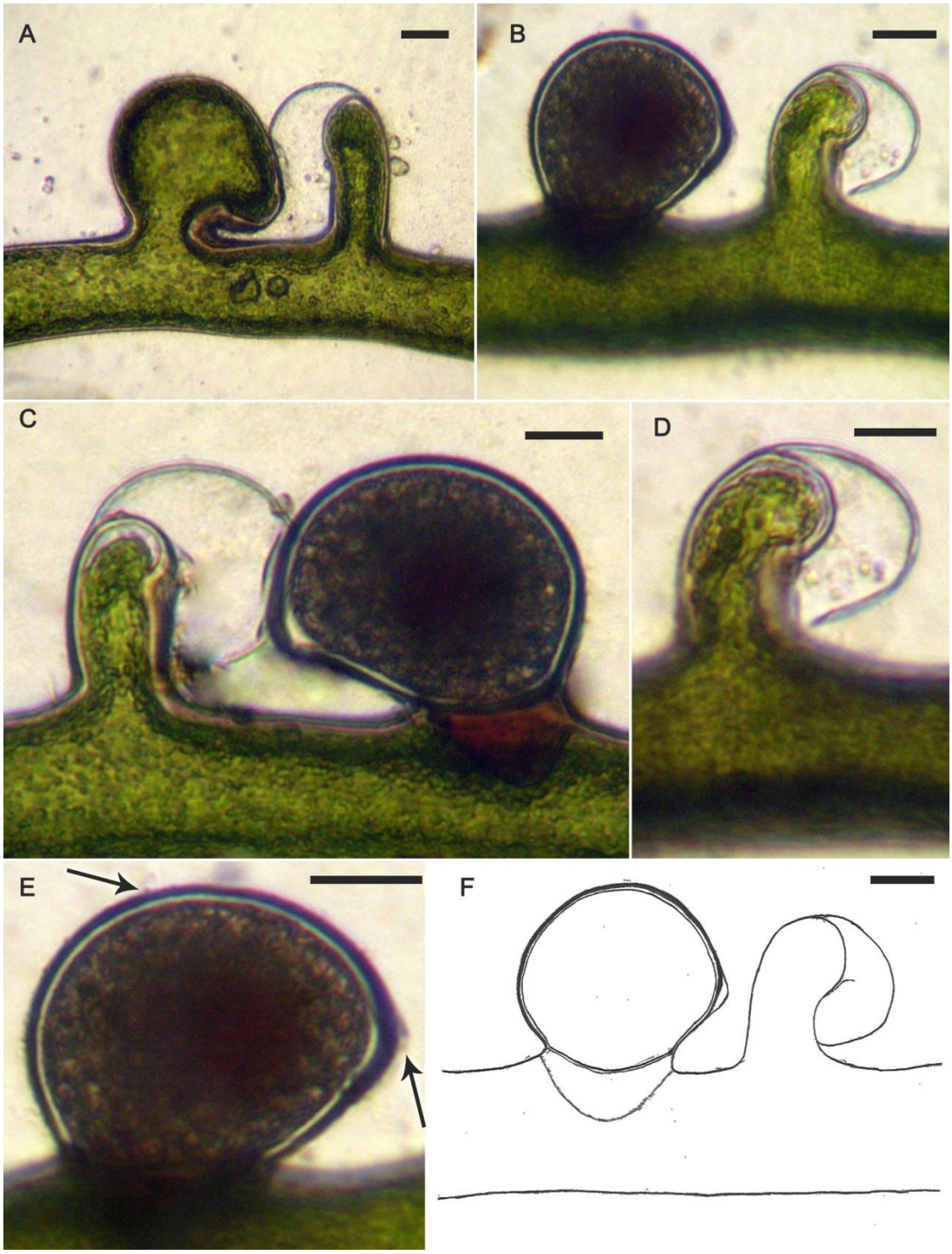


**Figure 2.4**. Light micrographs and illustration of *Vaucheria borealis* reproductive structures (CHR631516). A- Antheridium with developing oogonia. B, C and F- Single ovoid oogonia with an evenly textured, smooth wall, a horizontal beak, long axis parallel to length of siphon and a circinate antheridium C. D- Mature antheridium. E- Mature oogonium with smooth wall, horizontal beak, long axis parallel to length of the siphon (arrows). Bars= 20 µm.

**Table 2.3.** A comparison of diagnostic features of *V.* cf. *borealis* with other species in section *Corniculatae* (Hoppaugh 1930; Blum & Womersley 1955; Venkataraman 1961; Blum 1972; Johnson 2002; Entwisle 1987).

| Species | Oogonia | | | | | Siphon diameter (µm) |
|---|---|---|---|---|---|---|
| | Number | Shape | Length (µm) | Diameter (µm) | Orientation of long axes in relation to length of siphon | |
| *V. borealis* | 1 | Ovoid-reniform | >135 | 101-132 | Parallel | 58-91 |
| ***V.* cf. *borealis*** | **1** | **Ovoid** | **60-80** | **55-75** | **Parallel** | **35-50** |
| *V. bursata* | 1-2 | Ovoid-reniform | <135 | 53-103 | Oblique or erect | 29-115 |
| *V. dillwynii* | 1 | Truncate-napiform | 101-150 | 79-120 | Parallel | 36-72 |
| *V. repens* | 1 | Ovoid-reniform | 60-70 | 50-70 | Oblique | 33-65 |

This strain grew in Cave Stream, close to the bank, by the entrance to a limestone cave, attached to aquatic plants and other filamentous algae. The field material was fertile. *V. borealis* is a rare species which grows on damp soils, in peat bogs and freshwater habitats (Entwisle 1988a; Johnson 2002; Nemjová and Kaufnerová 2009). There are no published records of *V. borealis* from New Zealand. It has been reported previously from China, USA, Canada, Spain, Czech Republic and the British Isles.

### 2.3.3. ***Vaucheria erythrospora*** Christensen 1956, p. 275, fig. l a-d and 2

HOMOTYPIC SYNONYM: *Vaucheria hamata* f. *salina* Rieth: Rieth 1956, p. 135, pl. 1, fig. 7 and 8.

REPRESENTATIVE SPECIMEN: Saltwater Creek, Canterbury (lat. 43.277782°S, long. 172.696999°E), *Muralidhar and Broady UCVBW1* (CHR 631517).

REFERENCES: Christensen 1956, pp 277-279, fig. 1–2; Entwisle 1988a, p. 34, fig. 47–50.

DESCRIPTION: Siphons 45–65 µm diam., pale green; branches frequent. Alga monoecious; antheridia lateral to two oogonia borne on a gametophore, more than one gametophore can occur on a single peduncle; gametophores frequent (Fig. 2.5). Antheridia circinate, 75-80 µm long, 15–25 µm diam. Oogonia ovoid-reniform, pendent, 50–75 µm diam., 80–100µm long. Oospores same shape as oogonia. Mature oospores reddish- brown, break off easily, leave conical distal cavity in oogonia.

MOLECULAR DATA: The closest match to our *V. erythrospora* strain belonging to section *Racemosae*, was a strain of the same species collected from a brackish salt marsh in Amager, Denmark (p-distance = 0.031). It clustered with strains of other species in the section *Racemosae* (*V. geminata*, *V. pseudogeminata*, *V. prona*, *V. frigida* and *V. terrestris*, Fig. 2.2).

NOTES: This strain was identified as *Vaucheria erythrospora* Christensen, based on descriptions by Christensen (1956) and Entwisle (1988a). The field material was fertile. It grew on intertidal sediments of a creek. These were submerged during high tide and exposed during low tide. Salinity of the creek ranged from 2 ppt during low tide up to 35 ppt during high tide (Muralidhar et. al. 2013). This is the first record of *V. erythrospora* from New Zealand. It is common in terrestrial to semi-aquatic habitats of salt marshes and estuaries worldwide.

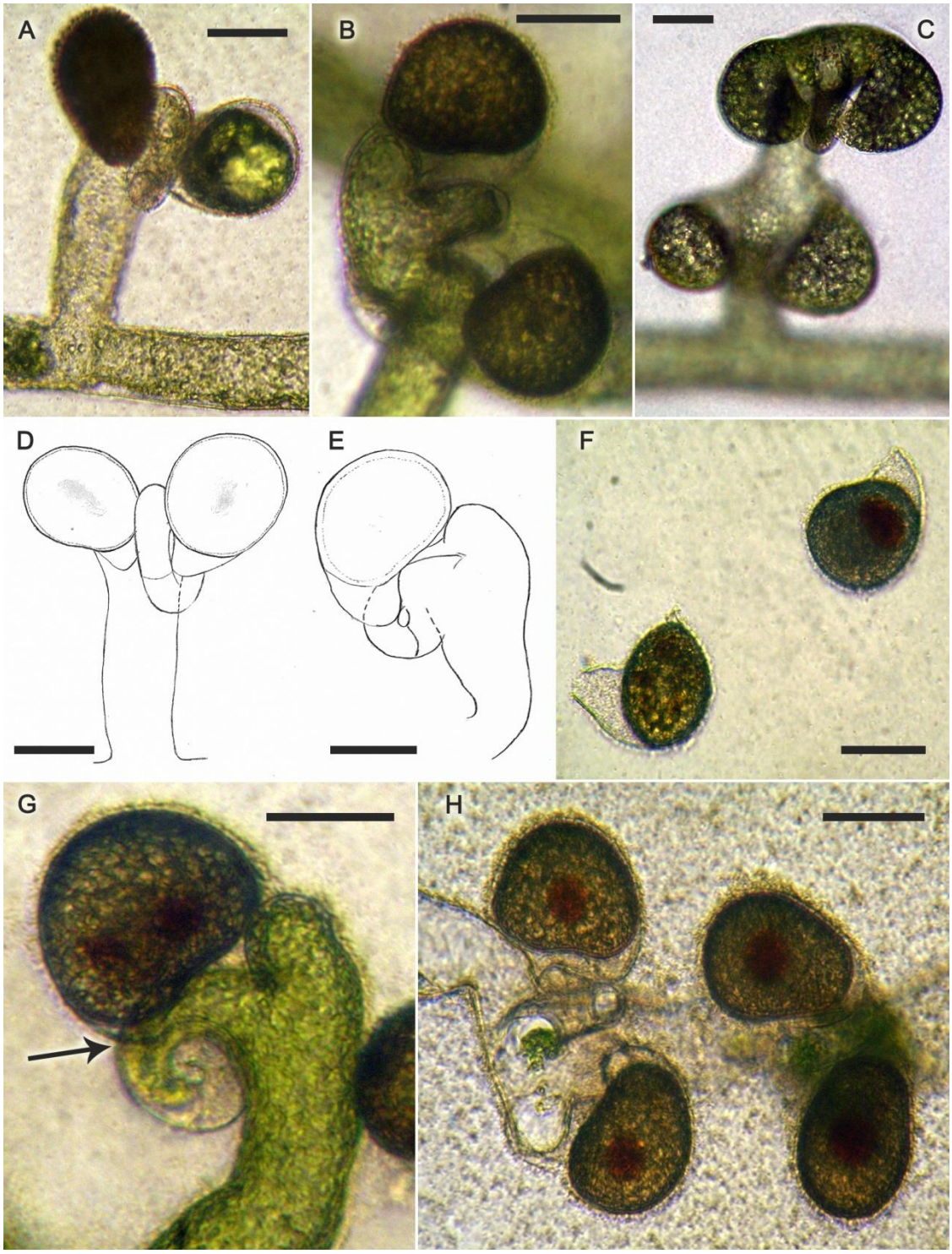


**Figure 2.5**. Light micrographs and illustrations of *Vaucheria erythrospora* reproductive structures (CHR631517). A-D and H- Two pendant oogonia borne laterally on pedicels to 1 circinate antheridium. E and G- Gametophore with a single oogonia; note distal oogonial cavity (arrow). F- Mature oogonia broken off from gametophore; note characteristic red colouration of the oospore and distal oogonial cavity. Bars= 50 µm.

**2.3.4. *Vaucheria aestuarii* sp. nov.** Muralidhar, Novis and Broady (Fig. 2.6)

HOLOTYPE: Avon Heathcote Estuary, Christchurch, Canterbury (lat. 43.525723°S, long. 172.724087°E), *Macintyre G7* (CHR 631518).

DESCRIPTION: Siphons 45–65 µm diam.; branches frequent. Alga dioecious (sensu Entwisle 1998a); antheridia and oogonia borne terminally on separate, long siphons; distribution frequent (Fig. 2.6). Antheridia cylindrical-acuminate; 180–400 µm long; in monopodial clusters of three and subtended by 1–2 wall bound cavities; with short cylindrical papillae (one-three lateral and one terminal), 10–14 µm long. Oogonia clavate, 110–130 µm diam., not subtended by wall-bound cavity, irregular mass of protoplasm subtending oogonium. Oospores ellipsoid, thin-walled, covering entire terminal portion of oogonium, never free from the oogonial wall.

MOLECULAR DATA: This strain grouped together with other species from section *Piloboloideae* (*V. litorea*, *V. medusa* and *V. compacta*, Fig. 2.2). The closest relative to the *V. aestuarii* strain was a *Vaucheria medusa* strain (p-distance = 0.045) collected from an estuary at Frogmore, South Devon, England.

NOTES: The diagnostic characters which set this strain apart from the other species in section *Piloboloideae* (Entwisle 1988a and Blum 1972) are: the ellipsoidal shape of the oospore which occupies the entire portion of the terminal oogonium, the absence of a wall bound cavity subtending the oospore, the presence of an irregular mass of protoplasm left behind by the mature oospore and long terminal antheridia in monopodial clusters of three with short cylindrical papillae. *Vaucheria litorea* and *V. glomerata* are the closest morphologically to *V. aestuarii*. They both have spherical masses of protoplasm left behind by the mature oogonia, in contrast to an irregular mass of protoplasm seen in *V. aestuarii*. Both have a wall bound cavity subtending the oogonia, which is lacking in *V. aestuarii*. The

length of the antheridia is slightly greater in *V. glomerata* than in *V. aestuarii* whilst both exhibit similar cylindrical protuberances. Other antheridial characters that differ between *V. aestuarii* and *V. glomerata* are the presence of up to three lateral protuberances (up to two in *V. glomerata*) and sometimes two wall-bound cavities in a single antheridium (mostly one in *V. glomerata*). These antheridial characters have not been used previously as characters with which to define species in this section. Striking differences in oogonial morphology and to a lesser extent, antheridial morphology, warranted recognition of this strain as a new species. A comparison of characters of some closely related morphospecies in the section *Piloboloideae* is given in Table 2.4.

This strain grew as pale green mats on intertidal mud flats of the Avon-Heathcote Estuary. Field material was sterile but developed reproductive structures when stressed (see Methods).

**Table 2.4.** A comparison of diagnostic features of *V. aestuarii* sp. nov. with *Vaucheria* species with similar morphological characteristics in section *Piloboloideae* (Hoppaugh 1930; Blum 1972; Rieth 1980).

| Species | Gametangial arrangement | Oogonia | | | Antheridia | | | | |
|---|---|---|---|---|---|---|---|---|---|
| | | Wall bound cavity | Proximal mass of protoplasm | Oospore shape | Shape | Length (µm) | Protuberances | | |
| | | | | | | | Shape | Number | Length (µm) |
| ***V. aestuarii*** | **Terminal; dioecious** | **No** | **Yes; irregular mass** | **Ellipsoid** | **Cylindrical-fusiform-acuminate** | **180-400** | **Cylindrical** | **1 terminal, 1-3 lateral** | **10-14** |
| *V. compacta* | Lateral; dioecious | No | No | Spherical-ovoid | Acuminate | 85-225 | Conical | 2- 4 lateral | 16-50 |
| *V. glomerata* | Terminal; dioecious | Yes | Yes; spherical mass | Globose-ellipsoid | Cylindrical-fusiform | < 500 | Cylindrical | 1 terminal, 1-2 lateral | 10-25 |
| *V. litorea* | Terminal; dioecious | Yes | Yes; spherical mass | Globose | Cylindrical-fusiform | > 500 | Conical | 1 terminal, 1-6 lateral | 12-48 |
| *V. longicaulis* | Terminal; dioecious | No | No | Globose-ellipsoid | Cylindrical-fusiform | 330-730 | Conical | 1 terminal, 1-4 lateral | Up to 190 |
| *V. piloboloides* | Terminal; monoecious | No | No | Ellipsoid-lenticular | Cylindrical-fusiform-bifurcate | 212-300 | Cylindrical-conical | 1 terminal, 1-4 lateral | 16-108 |

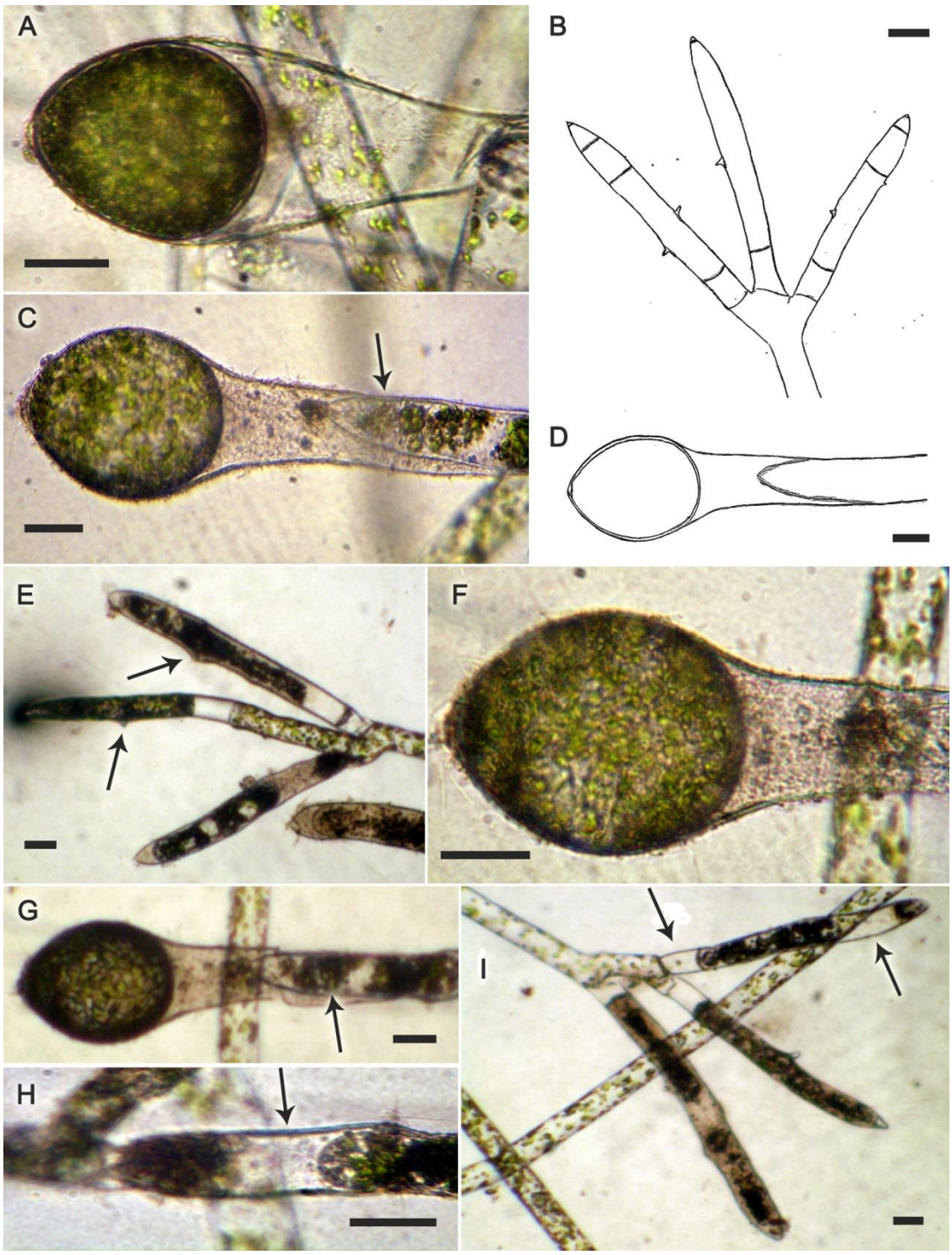


**Figure 2.6**. Light micrographs and illustrations of *Vaucheria aestuarii* reproductive structures (CHR631518). A, C, D, F and G- Clavate oogonia with mass of protoplasm left behind by mature oospore (arrows); note there is no wall bound cavity subtending the oogonia. E- Long cylindrical antheridia with short cylindrical- conical papillae (arrows) in a monopodial cluster, subtended by a wall bound cavity. H- Antheridium with a wall bound cavity (arrow). I- Antheridia in a monopodial cluster; note 2 wall bound cavities (arrows) in a single antheridium separated by a mass of sperm. Bars= 50 µm.

**2.3.5. *Vaucheria litorea*** Agardh 1823, p. 463.

REPRESENTATIVE SPECIMEN: Lake Ellesmere (Te Waihora), Canterbury (lat. 43.763501°S, long. 172.550004°E), *Broady and MacIntyre E5A* (CHR 631519).

REFERENCES: Blum and Womersley 1955, p. 714, fig. 15–17; Christensen 1987, p. 18, fig. 4H and I; Entwisle 1988a, p. 27 and 30, fig. 36 and 40.

DESCRIPTION: Siphons 90–150 µm diam.; branches sparse. Alga dioecious. Antheridia cylindrical-acuminate, terminal on siphons, 400–650 µm long; distribution frequent; borne in sympodial clusters of 3 or more (Fig. 2.7). Antheridia have 1–2 lateral conical papillae 20–30 µm long; terminal pore, 8–10 µm long. Antheridia subtended by wall bound cavity. Oogonia not observed.

MOLECULAR DATA: This strain grouped together with other species from section *Piloboloideae* (*V. aestuarii*, *V. medusa* and *V. compacta*, Fig. 2.2). In terms of p-distance, our strain of *V. litorea* was closest to another strain of the same species collected from a salt pan in North Jutland, Denmark (p-distance = 0.028). But phylogenetic analyses failed to resolve the relationships between the three strains of *V. litorea* in our study.

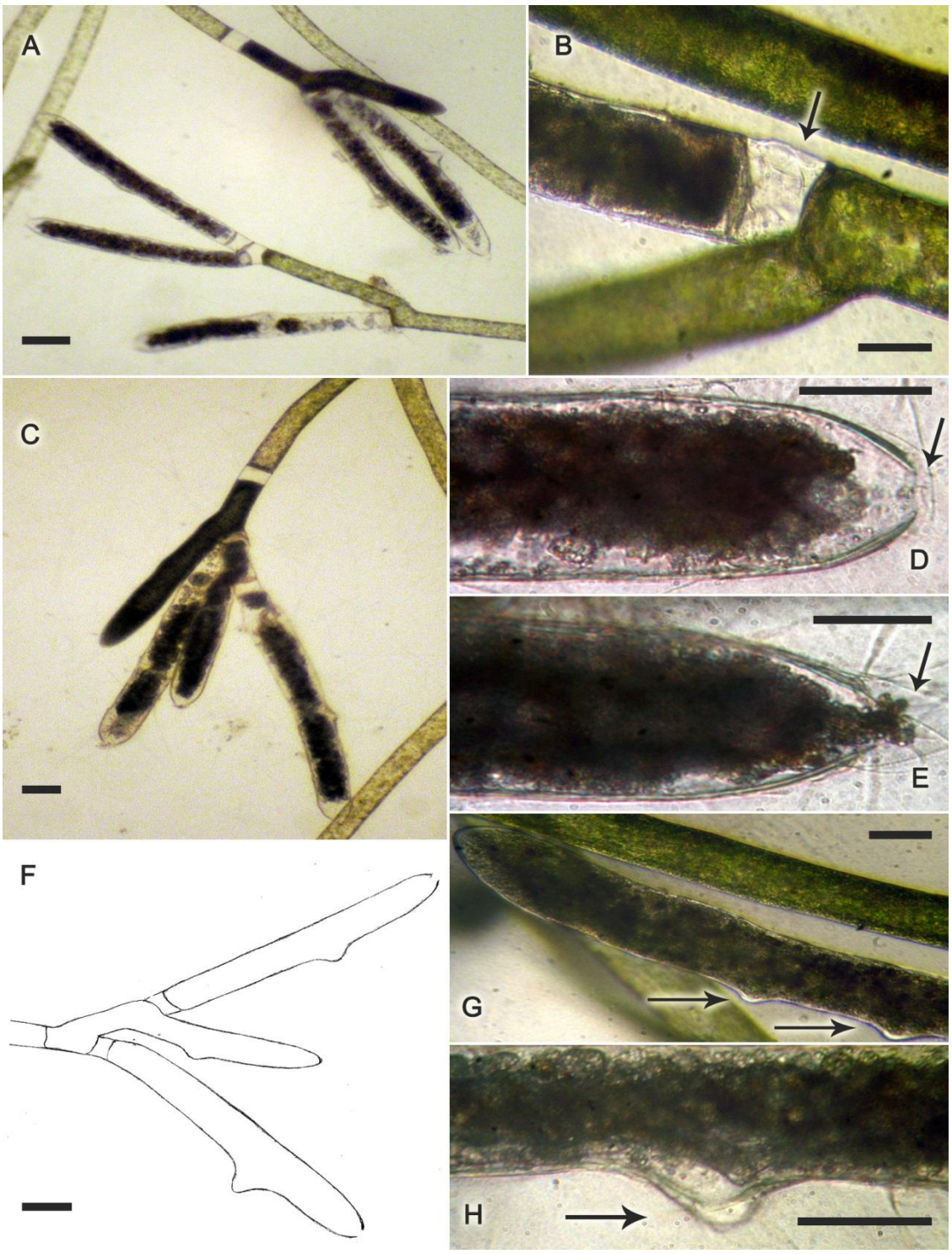


**Figure 2.7**. Light micrographs and illustration of *Vaucheria litorea* antheridia (CHR631519). A, C and F- Long cylindrical antheridia with short conical papillae and subtended by a wall bound cavity in a sympodial cluster. B- Wall bound cavity subtending an antheridium (arrow). D and E- Large terminal pore of an antheridium (arrow); E- sperm material being ejected from pore; G and H- Lateral conical papillae in antheridium (arrows). A, C and F- Bars= 200 µm; B, D, E, G - F- Bars= 100 µm.

NOTES: This strain was identified as *Vaucheria litorea* Agardh based on the morphology and arrangement of the antheridia which exhibited characteristic conical protuberances (1 terminal and 1-4 lateral protuberances). *V. compacta* and *V. longicaulis* of section *Piloboloideae* also exhibit conical protuberances. The lateral protuberances in *V. longicaulis* reach 190 µm long (Entwisle 1988a). In this strain they were up to 20-30 µm long, clearly separating it from *V. longicaulis*. In *V. compacta,* antheridia are on lateral branches whereas in *V. litorea* they are terminal. All strains of *V. litorea* were separated from *V. compacta* by a robust branch in our phylogenetic analyses, but the relationships between these strains were not resolved; it is possible that *V. litorea* represents a grade.

This strain grew sheltered under plants in moist soil on the mudflats of Lake Ellesmere / Te Waihora, a brackish lake. Field material was sterile but developed reproductive structures when stressed (see Methods). This is the first record of *V. litorea* from New Zealand. It is common in intertidal saltmarshes and estuarine habitats worldwide.

**2.3.6. *Vaucheria edaphica* sp. nov.** Muralidhar, Novis and Broady **(**Fig. 2.8)

HOLOTYPE**:** Christchurch, Canterbury (lat. 43.554800°S, long. 172.628833°E), *Broady UCVT1* (CHR 631520).

DESCRIPTION: Siphons 25–40 µm diam.; branches frequent. Alga monoecious; antheridia lateral to 1–2 oogonia borne on a gametophore; gametophores frequent (Fig. 8). Antheridia circinate, 70–90 µm long, 20–35 µm diam. Oogonia 1–2, reniform, pendent, 25–35 µm diam., 75–100 µm long, usually sessile, rarely with short pedicels (always < 10 µm long); distal prominence towards peduncle; wall thin. Oospores same size as oogonia, no oogonial cavity left behind by mature oospores.

MOLECULAR DATA: In terms of p-distance, our *V. edaphica* strain was closest to a *V. walzii* strain (p-distance= 0.063) from Botanical Garden, University of Düsseldorf, Germany.

NOTES: Although *V. edaphica* shared some common traits with other species in section *Racemosae,* it was difficult to place it unequivocally under any of these species. It most closely resembled *V. prona* Christensen as recorded by Entwisle (1988a, 1988b) but his strains showed up to four oogonia on a gametophore which were in different orientations and had pedicels always >10 µm long (Entwisle 1988a, b). Our strain was distinct as it never had more than two oogonia which were usually sessile and rarely possessed very short pedicels always < 10 µm long. The number of oogonia and length of the oogonial pedicels have been used as delineating characters in this section and we based our decision to erect this strain as a new species based on these characters. We suggest that populations with one to two oogonia, mostly sessile or sometimes with a short oogonial pedicel (<10 µm) and with no oogonial cavity left behind by the mature oospore, should be referred to as *Vaucheria edaphica*. A comparison of characters of some closely related morphospecies in the section *Racemosae* is given in Table 2.5.

While we erected the species solely based on the morphological differences mentioned above, our strain was found to be genetically distinct from all other species in section *Racemosae* including all *V. prona* sequences in Genbank.

This strain grew as light green mats on moist soil surfaces. Field material was fertile.

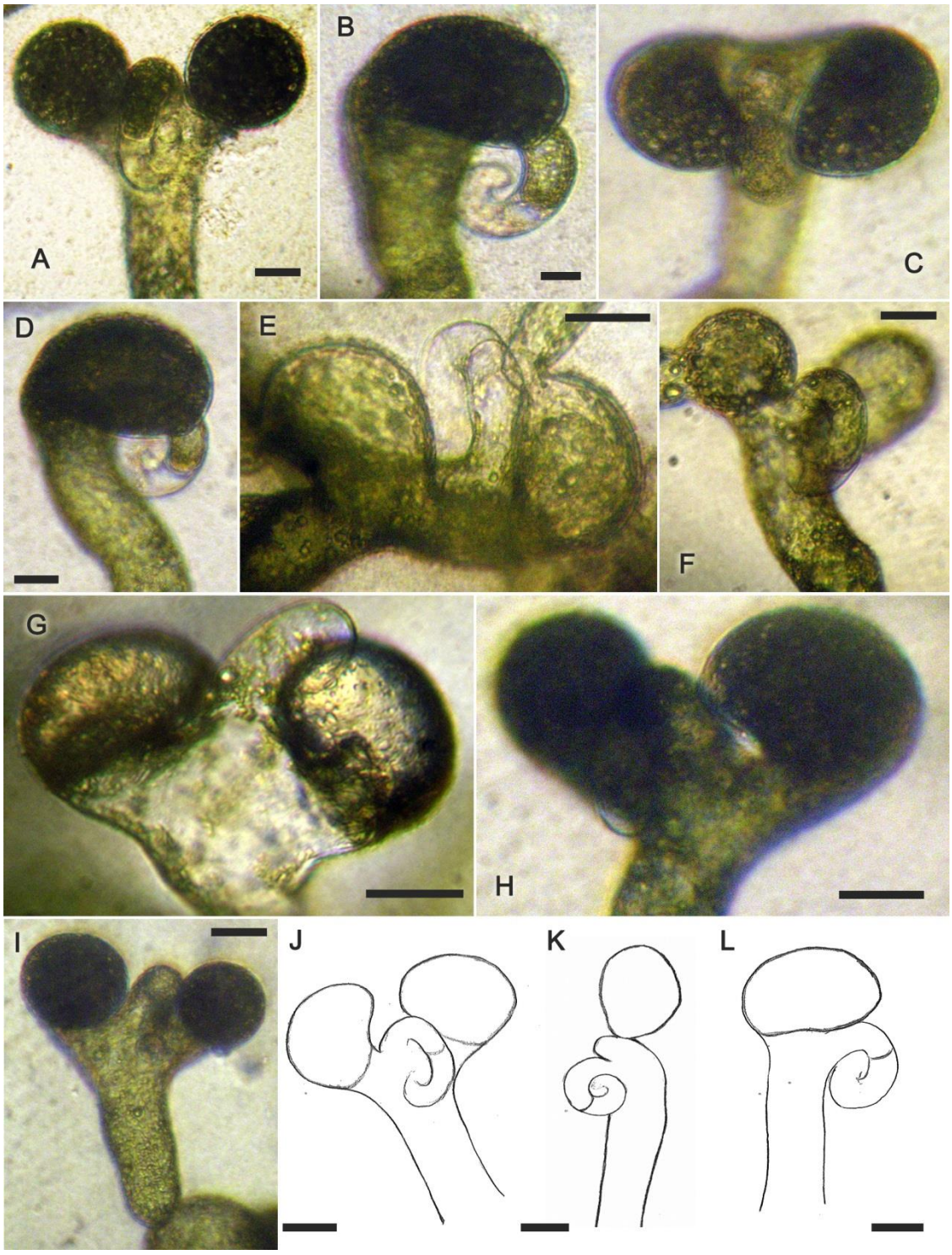


**Figure 2.8**. Light micrographs and illustrations of *Vaucheria edaphica* reproductive structures (CHR631520). A, C, G-I- Gametophore bearing pendent, mostly sessile oogonia with distal prominence and a circinate antheridium; note oospores covering entire portion of oogonium. B and D- Single reniform oogonium with circinate antheridium. E & F- Developing oogonia; note green colouration. J, K and L- Variations of gametophore arrangement. Bars= 20 µm.

**Table 2.5.** A comparison of diagnostic features of *V. edaphica* sp. nov. with *Vaucheria* species with similar morphological characteristics (Hoppaugh 1930; Christensen 1987; Entwisle 1988a, 1988b).

| Species | Oogonia | | | | | |
|---|---|---|---|---|---|---|
| | Number | Orientation | Shape | Lamellate wall | Oogonial cavity | Pedicel length (µm) |
| ***V. edaphica*** | **1-2** | **Pendent** | **Reniform** | **No** | **No** | **Sessile; if present, < 10 µm long** |
| *V. erythrospora* | 1-2 | Pendent | Ovoid-reniform | No | Yes; conical | 10-24 |
| *V. frigida* | 1 | Erect | Globose | Yes | No | Sessile-12-48 |
| *V. geminata* | 2 | Erect | Ellipsoid-ovoid | No | No | 28-86 |
| *V. mulleola* | 1-2 | Erect | Reniform | Yes | Yes; conical | - |
| *V. prona* | 1-4 | Pendent; variously directed | Ovoid-reniform | No | No | 10-90 |
| *V. pseudogeminata* | 2 | Erect | Reniform | No | Yes; conical | 24-65 |

### 2.3.7. *Vaucheria* cf. *conifera* Christensen 1987, p. 620, fig. 9–19

REPRESENTATIVE SPECIMEN: Whangateau Harbour, Auckland, New Zealand (lat. 36.335604°S, long. 174.765502°E), *Wilcox 4431b* (AK 328489).

DESCRIPTION: Siphons 35–50 µm diam., branches sparse.

MOLECULAR DATA: This strain (sequenced length of 761 bp) was grouped in a robust clade making up species of the section *Woroninia* (*V. dichotoma*, *V. schleicheri* and *V. conifera*, Fig. 2).The closest relative to our strain was a *V. conifera* strain from a mangrove on Garden Island, Adelaide, Australia (p-distance = 0.060).

NOTES: We have named this strain *Vaucheria* cf. *conifera* based on molecular analyses, pending observation of fertile material. Growths were short turfs on shaded decaying rock in Whangateau Harbour, at the mouth of the Omaha Estuary. Although the location is estuarine, salinity is close to that of seawater as river flows are small relative to the total volume of the estuary (Kelly 2009). There are no reports of *V. conifera* from New Zealand. It has been recorded previously from coastal south-eastern Australia (Christensen 1987b; Entwisle 1988a).

## 2.4. Discussion

Seven species of *Vaucheria* collected from contrasting habitats in New Zealand were characterized based on the morphology of their reproductive structures. Genetic variation among these species and their genetic grouping in relation to other *Vaucheria* sequences was studied using phylogenetic analyses of *rbc*L gene sequences. Two strains were described as new species- *V. aestuarii* (section *Piloboloideae*) and *V. edaphica* (section *Racemosae*). Apart from being morphologically distinct, they were both also found to be genetically distinct from other species in their respective sections. Two species (*V. erythrospora* and *V. litorea*) were reported for the first time from New Zealand. Two other species were not conclusively identified based on available evidence and were tentatively named *Vaucheria* cf. *borealis* and *Vaucheria* cf. *conifera*, pending further analyses. Of the species previously reported from New Zealand only *V. bursata* (=*V. sessilis* f. *repens*) was found in our study. Sparse sampling may be the reason for absence of the remaining species that were previously reported from New Zealand.

The two new species were described based on morphological characters which have been used previously to delineate species. In section *Piloboloideae*, these characters are monoecious/dioecious arrangement of the gametangia, presence / absence of a wall-bound

cavity subtending oogonia and antheridia, presence / absence of a proximal mass of protoplasm subtending the oogonia, length of the antheridia and shape and length of antheridial protuberances (Blum and Womersley 1955; Blum 1972; Entwisle 1988a). For example, Blum and Womersley (1955) used the presence of a proximal spherical mass of protoplasm and a wall bound cavity subtending the oogonia, to distinguish *V. glomerata* from the other species in section *Piloboloideae*, with the exception of *V. litorea* which also exhibited these characters. They used the length of the antheridia and shape of the antheridial protuberances to separate *V. glomerata* from *V. litorea* (Table 2.4). Species with oogonia lacking a wall bound cavity and proximal mass of protoplasm have also been separated based on length and shape of the antheridial protuberances, for example *V. longicaulis* and *V. piloboloides* (Hoppaugh 1930; Blum 1972; Table 2.4). We erected *V. aestuarii* as a new species based on the absence of a wall bound cavity subtending the oospore, which distinguished it from *V. litorea* and *V. glomerata*, and presence of a non-spherical mass of protoplasm, which separated it from the rest of the species in *Piloboloideae*. We also used the shape and length of the antheridial protuberances to further separate it from the other species in the section (see Table 2.4 and notes section).

In section *Racemosae*, the main characters used to delineate species are number, shape and orientation of oogonia, presence/ absence of an oogonial cavity, presence/ absence of a lamellate wall and shape and length of the antheridial pedicel (Hoppaugh 1930; Entwisle 1988a, 1988b). For example, Hoppaugh (1930) distinguished *V. frigida* (= *V. terrestris* (Vaucher) De Condolle) from *V. prona* (= *V. hamata* (Vaucher) De Condolle) based on the length of the oogonial pedicel, number of oogonia and the presence of a lamellate oogonial wall. *V. frigida* always has a single oogonium which is almost sessile or has a short pedicel, while *V. prona* usually has 2–4 (rarely 1) oogonia variously directed with long pedicels (always > 10μm) (Hoppaugh 1930; Entwisle 1988b; Johnson 2002). We erected *V. edaphica*

as a new species by distinguishing it from *V. prona* based on the length of the oogonial pedicel (oogonia mostly sessile or < 10 μm if present) and the number of oogonia which was never more than two. The lack of a lamellate oogonial wall separated it from *V. frigida* (Table 2.5).

Our phylogenetic analyses used a smaller region of the *rbc*L gene compared to the study by Andersen and Bailey (2002) but employed more *Vaucheria* sequences, 46 compared to 32 in their study. These differences may have contributed to the different topology and arrangement of the sections in our study (Fig. 2.2)

The existence of cryptic species complexes in *Vaucheria* has been well-documented. Andersen and Bailey (2002) found some *V. bursata* strains to be genetically more closely related to *V. dillwynii* than to other *V. bursata* strains. This was also apparent in our study (Fig. 2.2). Although all our *V. bursata* strains grouped together in both MPB and Bayesian analyses, there was more sequence variability between our strains and other *V. bursata* strains from Genbank (p-distance = 0.028) than between our *V. bursata* strains and our morphologically distinct strain *Vaucheria* cf. *borealis* (p-distance = 0.005), which formed a well-supported clade with our *V. bursata* strains to the exclusion of all others. These results compromise a morphology-based species classification in section *Corniculatae*. Cryptic species complexes may also exist in other sections but whether this is the case requires further investigation.

There has been considerable disagreement about the classification and naming of species in *Vaucheria*. This is especially true for section *Corniculatae* and in particular the *V. bursata* complex. The synonymy of *V. bursata* and *V. sessilis* is well-accepted (Rieth 1963; Christensen 1969; Rieth 1980; Entwisle 1987; Entwisle 1988a; Johnson 2002) but there is conflict about which name has priority. Johnson (2002) used the name *V. sessilis* (Vaucher)

De Candolle (1805), while Entwisle (1988a) used the name *V. bursata* (Müller) Agardh (1811). Because *Conferva bursata* Müller (1788), the basionym from which *V. bursata* originates, clearly predates *Ectosperma sessilis* Vaucher (1803), we follow Entwisle (1988a) in naming our strains *V. bursata*. Entwisle placed two other species with slightly different morphologies, *V. repens* and *V. clavata*, in synonymy with *V. bursata* but Blum (1972) considered *V. repens* as a unique species while Johnson (2002) listed it as a doubtful species.

This is the first study involving morphological and molecular phylogenetic characterization of *Vaucheria* strains from New Zealand. Andersen and Bailey (2002) suggested a phylogenetic classification scheme at the sectional level, but further studies which include representative sequences from other sections of *Vaucheria* are required in order to confirm this. Difficulty in distinguishing closely related species that are currently recognized, and genetic variation amongst morphologically identical strains (especially in *Racemosae* and *Corniculatae*) suggest that the morphology-based classification may need revision.

## 2.5. References

Adams NM 1994. Seaweeds of New Zealand. Christchurch, Canterbury University Press. 360 p.

Agardh CA 1811. Dispositio Algarum Sueciae. Part 2. Berling's Printing Office, Lund. Pp. 17–26.

Agardh CA 1823. Species Algarum. Vol. 1, Part 2. Berling's Printing Office, Lund. Pp. 399–531.

Andersen RA, Bailey JC 2002. Phylogenetic analysis of 32 strains of *Vaucheria* (Xanthophyceae) using the *rbc*L gene and its two flanking spacer regions. Journal of Phycology 38: 583–592.

Bischoff HW, Bold HC 1963. Phycological studies IV. Some soil algae from Enchanted Rock and related algal species. University of Texas Publication 6318: 1–95.

Blum JL 1972. Vaucheriaceae. North American Flora Series II, Part 8. New York, New York Botanical Garden. Pp 1–64.

Blum JL, Womersley HBS 1955. A new marine *Vaucheria* from Australia. American Journal of Botany 42: 713–717.

Brown HJ 1929. The algal family Vaucheriaceae. Transactions of the American Microscopical Society. 48: 86-117

Chapman VJ 1956. The marine algae of New Zealand. Part 1. Myxophyceae and Chlorophyceae. Botanical Journal of the Linnean Society 55: 333–501.

Chapman VJ, Thompson RH, Segar ECM 1957. Checklist of freshwater algae of New Zealand. Transactions of the Royal Society of New Zealand 84: 695–747.

Christensen T 1956. Studies on the genus *Vaucheria*. III. Remarks on some species from brackish water. Botaniska Notiser 109: 275–280.

Christensen T 1969. *Vaucheria* collections from Vaucher's region. Det Kongelige Danske Videnskabernes Selskab. Biologiske Skrifter 16: 1–36.

Christensen T 1973. Some early *Vaucheria* descriptions. Botaniska Notiser. 126: 513–18

Christensen T 1987. Some collections of *Vaucheria* (Tribophyceae) from Southeastern Australia. Australian Journal of Botany 35: 617–629.

Entwisle TJ 1987. An evaluation of taxonomic characters in the subsection Sessiles, section *Corniculatae*, of *Vaucheria* (Vaucheriaceae, Chrysophyta). Phycologia 26: 297–231.

Entwisle TJ 1988a. A monograph of *Vaucheria* (Vaucheriaceae, Chrysophyta) in south-eastern mainland Australia. Australian Systematic Botany 1: 1–77.

Entwisle TJ 1988b. An evaluation of taxonomic characters in the *Vaucheria prona* complex (Vaucheriaceae, Chrysophyta). Phycologia 27: 183–200.

Guillard RRL, Ryther JH 1962. Studies on the marine planktonic diatoms: I. *Cyclotella nana* Hustedt, and *Detonula confervaceae* (Cleve) Gran. Canadian Journal of Microbiology 8: 229–239.

Guiry MD, Guiry GM 2013. AlgaeBase. World-wide electronic publication, National University of Ireland, Galway. Retrieved 01 September 2013, from http://www.algaebase.org.

Hansgirg A 1886. *Vaucheria*. In: Prodromus der Algenflora von Böhmen. Vol. I. Cramer J, Vaduz, Germany. Pp 93–96

Hassall AH 1843. Descriptions of British freshwater Confervae, mostly new, with observations on some of the genera. Annals and Magazine of Natural History. 11: 428–437.

Hassall AH 1845. A history of the British freshwater algae. Volume 2. London, Highley, S and Bailliere, H. p 52.

Heering W 1907. Die Susswasseralgen Schleswig-Holsteins. Part 2. Chlorophyceae (Allgemeines-

Siphonales). Jahrbuch der Hamburgischen Wissenschaftlichen Anstalten. 24: 105–235.

Hirn KE 1900. Finnländische Vaucheriaceen. Meddelanden af Societatis pro Fauna et Flora Fennica. 26: 85–90

Hooker JD 1867. Handbook of New Zealand flora: a systematic description of the native plants of New Zealand and the Chatham, Kermadec's, Lord Auckland's, and Macquarrie's islands. London, Reeve and Co. 798 p.

Hoppaugh KW 1930. A taxonomic study of species of the genus *Vaucheria* collected in California. American Journal of Botany 17: 329-347

Johnson LR 2002. Phylum Xanthophyta (Yellow-Green Algae). In: John DM, Whitton BA and Brook AJ eds. The freshwater algal flora of the British Isles: an identification

guide to freshwater and terrestrial algae. 2nd edition. Cambridge, Cambridge University Press. Pp. 245–270.

Kelly S 2009. Whangateau catchment and harbour study: Review of marine environment information. Prepared for Auckland Regional Council. Auckland Regional Council technical report 2009/003.

Lamarck JB, De Candolle AP 1805. Flore Francaise. 3rd edition. Vol. 2. Desray,Paris.

Müller OF 1788. Histoire de Confervis palustribus oculo nudo invisibilibus. Nova Acta Academiae Scientiarum Imperialis Petropolitanae 3: 89–98.

Muralidhar A, Novis PM, Broady PA, Collings DA, Garrill A 2013. An estuarine species of the alga *Vaucheria* (Xanthophyceae) displays an increased capacity for turgor regulation when compared to a freshwater species. Journal of Phycology 49: 967–978

Nemjová K, Kaufnerová V 2009. New reports of *Vaucheria* species (Vaucheriales, Xanthophyceae, Heterokontophyta) from the Czech Republic. Fottea 9: 53–57.

Rieth A 1956. Zur Kenntnis halophiler Vaucherien. Flora 143: 127-160

Rieth A 1963. Die Algen der chinesisch-deutschen biologischen- Sammelreise durch Nord- und Nordostchina 1956. I. Die Vaucheriaceen. Part 1. Limnologica 1: 287–313.

Rieth A 1980. Xanthophyceae, Part 2. In: Ettl H, Gerloff J and Heynig Heds. Süsswasserflora von Mitteleuropa. Volume 4. Gustav Fischer Verlag, Stuttgart. 147 p.

Ronquist F, Huelsenbeck JP 2003. MRBAYES 3: Bayesian phylogenetic inference under mixed models. Bioinformatics 19: 1572–1574.

Sarma P 1973. Addition to the freshwater algae of New Zealand - I. A note on the species of *Vaucheria* from Great Barrier Island. Tane 19: 167–173.

Sarma P 1974. Additions to the freshwater algae of New Zealand- II : Some *Vaucheria* from Slipper Island. Tane 20: 86–100.

Swofford DL 2002. PAUP*: phylogenetic analysis using parsimony (*and other methods), version 4.0b10. Sinauer Associates, Sunderland, Massachusetts.

Tamura K, Peterson D, Peterson N, Stecher G, Nei M, and Kumar S 2011. MEGA5: Molecular evolutionary genetics analysis using maximum likelihood, evolutionary distance, and maximum parsimony methods. Molecular Biology and Evolution 28: 2731-2739.

Thompson JD, Gibson TJ, Plewniak F, Jeanmougin F, Higgins DG 1997. The ClustalX windows interface: flexible strategies for multiple sequence alignment aided by quality analysis tools. Nucleic Acids Research 25: 4876–4882.

Vaucher JPE 1803. Histoire des Conferves d'Eau Douce. Geneva, Paschoud J. J.

Venkataraman GS 1961. Vaucheriaceae. New Delhi, Indian Council of Agricultural Research. 112 p

Wilcox MD 2011. Occurence of marine yellow-green algae *Vaucheria velutina* C. Agardh and *Vaucheria longicaulis* Hoppaugh (Xanthophyceae: Vaucheriaceae) in Auckland, New Zealand. New Zealand Journal of Marine and Freshwater Research 46: 285–290.

# Chapter 3

## A comparison of the abilities of an estuarine and a freshwater species of *Vaucheria* to regulate turgor after hyperosmotic shock

### 3.1. Introduction

Maintaining turgor is particularly challenging in environments with constantly changing external osmotic potential (Young et al. 1987a, b, Kirst 1990, Karsten et al. 1991). The ability to maintain turgor may determine survival of walled organisms in these environments as it is thought to be the driving force for growth as the cell wall yields to the turgid protoplast (Ray et al. 1972, Money 1997). In hypoosmotic conditions, organisms have to release ions and osmolytes to prevent cell swelling and potential rupture of cells. In hyperosmotic conditions, they have to adjust their internal osmotic potential by accumulating ions and osmolytes in order to prevent plasmolysis (Lew et al. 2004, Chitcholtan et al. 2012).

Freshwater habitats provide organisms with a stable environment with little osmotic variation. In contrast, osmotic variation is a significant factor in terrestrial and brackish water habitats. In intertidal zones, estuaries and lagoons, salinity and osmotic potential varies constantly due to the different mixing of freshwater and seawater governed by the tidal cycle (Karsten et al. 1991, Bisson and Kirst 1995). Organisms living in the intertidal zone are subjected to further stress, where evaporation and precipitation may, respectively, cause increases or decreases in salinity (Wegmann 1986, Wichmann and Kirst 1989, Bisson and Kirst 1995).

Some organisms are able to alter their internal osmotic potential in response to changes in external osmotic pressure. This ensures that osmotic gradient remains unchanged between the

inside and outside of the cell and turgor remains constant, despite changes in external osmotic potential. This process, referred to as turgor regulation, is thought to be brought about by a manipulation of intracellular concentration of inorganic ions and organic osmolytes (Bisson and Kirst 1995). Many higher plants, e.g., *Arabidopsis thaliana*, fungi, e.g., *Neurospora crassa* and euryhaline species of green algae, e.g., *Chara longifolia*, *Lamprothamnium succinctum* are known to turgor regulate (Bisson and Gutknecht 1975, Beilby and Shepherd 1996, Money 1997, Stento et al. 2000, Shabala and Lew 2002, Lew and Levina 2007). However, some oomycetes, e.g. *Achlya bisexualis* and freshwater species of green algae, e.g. *Chara corallina* have been shown to lack a turgor regulation mechanism when subjected to hyperosmotic stress (Lew et al. 2004; Bisson and Bartholomew 1984).

In this chapter the process of turgor regulation in *Vaucheria* is investigated. The oomycetes and *Vaucheria* share a relatively recent common ancestor, as shown by shared synapomorphic characters of compound flagellate cells and phylogenetic analysis of DNA sequences (Potter et al. 1997, Taylor 2003). Both belong to a wider group of protists called the Stramenopila. *Vaucheria* is characterized by siphonous (aseptate), coenocytic, tip-growing filaments which are similar to the hyphae of oomycetes (Ott and Brown 1974, Hulvey et al. 2007). *Vaucheria* provides an intriguing and novel experimental system for investigations of turgor regulation, because species grow in various habitats with different osmotic conditions, from freshwater through brackish conditions to fully marine (Chapter 2; Entwisle 1988).

The fact that *Vaucheria* shares a common lineage and several morphological characteristics with the Oomycota raises the question of whether, like the oomycetes tested, it is unable to turgor regulate. This would have consequences for those species that live in brackish

environments, as they would have to contend with changes in external osmotic potential. The fact that only euryhaline species of green algae regulate turgor, suggests that the ability to do this may be necessary for survival in such habitats. To investigate this, the responses of two species of *Vaucheria*, *Vaucheria repens* and *Vaucheria erythrospora*, to a variety of hyperosmotic shocks were studied.

## 3.2. Materials and methods

### 3.2.1. Culture maintenance

Two species of *Vaucheria* were chosen for this study from among seven species identified and described in Chapter 2. *Vaucheria repens* was obtained from Okeover Stream, a freshwater spring-fed stream on the campus of the University of Canterbury, Christchurch, New Zealand. *Vaucheria erythrospora* was obtained from intertidal sediments at Saltwater Creek, close to its outflow into the Pacific Ocean north of Christchurch, with salinity varying from 2 ppt during low tide up to 35 ppt during high tide (Fig. 3.1). Besides their contrasting habitats, they are also genotypically and morphologically distinct from one another (Chapter 2).

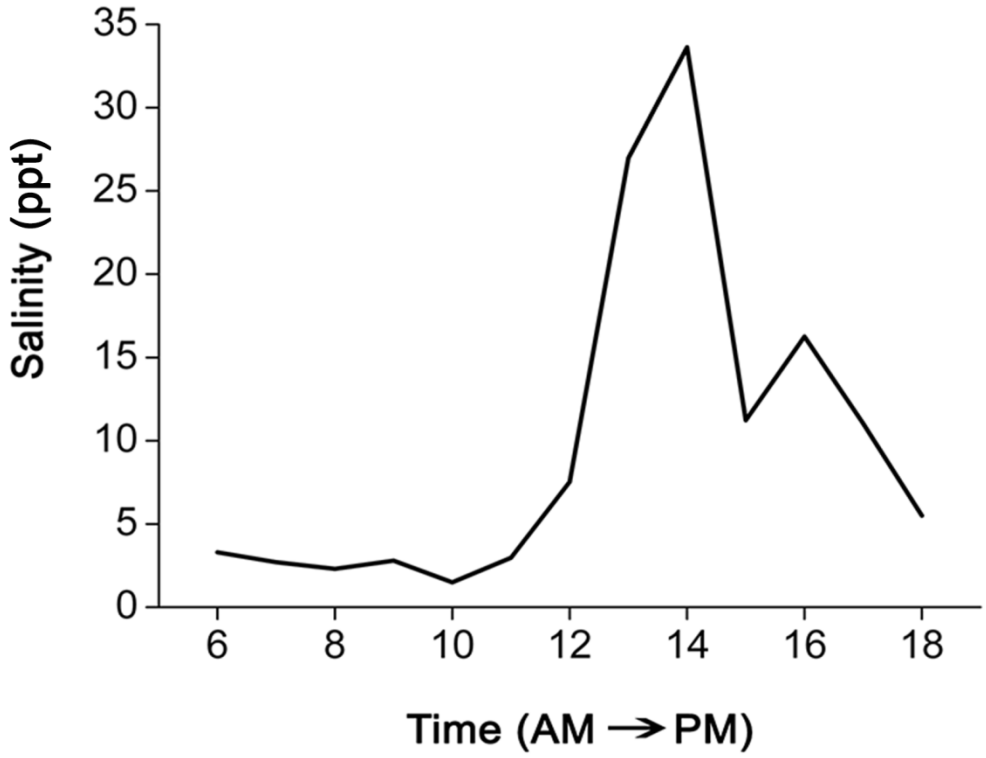


**Figure 3.1.** Salinity measurements over a period of 12 h from 6 a.m. to 6 p.m. on May 16, 2012 at Saltwater Creek, Sefton, Canterbury, New Zealand. Measurements were made close to the sampling location of the brackish water isolate, *Vaucheria erythrospora*. Salinity ranged between ~2 ppt and 35 ppt over the time period. Low tide was approximately at about 0930 h and high tide at about 1430 h.

*V. repens* was maintained in agarized (1% w/v) Bold's Basal Medium (BBM; Bischoff and Bold 1963) amended with vitamin solution (0.5 mL $L^{-1}$ from a stock of thiamine. HCl (200 mg $L^{-1}$), biotin (244.31 mg $L^{-1}$) and cyanocobalamin (1,355.4 mg $L^{-1}$). The osmolality of BBM was 62 mOsmol $kg^{-1}$. *V. erythrospora* was maintained in modified f/2 medium (Guillard and Ryther 1962), the salinity of which was adjusted to ~6 ppt by diluting natural seawater (osmolality 247 mOsmol $kg^{-1}$). Both *V. repens* and *V. erythrospora* were incubated on their respective media in 90 mm Petri dishes under standard conditions (16:8 h light:dark regime at 14°C and ~50 µmol photons $m^{-2}s^{-1}$ light intensity). Two-week-old growths of these cultures were used for pressure probe experiments. All osmolality measurements were made with a Wescor (model 5500, Wescor, Logan, UT, USA) vapor pressure osmometer.

### 3.2.2. Pressure probe measurements

Direct pressure measurements were made using a single cell pressure probe designed and built by Professor Stephen Tyerman, University of Adelaide, Australia. The pressure transducer in the probe was capable of measuring up to a maximum of 2 MPa (20 Bars). Micropipettes were pulled from borosilicate capillaries (1.2 mm OD, 0.69 mm ID, Harvard Apparatus, Kent, UK) on a Narashige pipette puller (Model PC-10, Narashige, Tokyo, Japan) and filled with low viscosity silicone oil (5 cst, Sigma Aldrich). Data acquisition for the probe experiments was conducted with PowerLab 4/20 (Model ML840, ADInstruments, Bella Vista, NSW, Australia) and read out using LabChart 7 (ver 7.2.1, ADInstruments). The pressure probe was attached to micromanipulators (Lang GMBH and Co. K6, Type STM3) which were in turn attached to a Zeiss IM35 microscope with a Zeiss F-LD20/O, 25 Phase objective.

Petri plates containing agarized medium (~0.5 cm thickness) with surface growths of *Vaucheria* siphons (BBM for *V. repens*, osmolality 62 mOsmol $kg^{-1}$; modified f/2 for *V. erythrospora*, osmolality 247 mOsmol $kg^{-1}$) were mounted on an inverted microscope (Zeiss IM35) and impaled with the micropipette. Upon impalement, the cytoplasm moved into the pipette forming a cytosplasm / oil meniscus as it pushed oil into the pipette away from the cell. Turgor measurements were made by recording the pressure that was required to push the meniscus back to the micropipette tip (Fig. 3.2). To ensure that the tip was not plugged during an experiment, oil was injected into siphon at the end of the experiment by increasing the pressure in the pipette. If oil would not enter the cell, the readings were discarded as this suggested that the tip was plugged and a wound response had likely occurred. Furthermore, in cases where there was release of oil into the siphon while applying pressure during an experiment, the experiment was stopped. A wound response upon impalement and plug formation around the pipette tip were a common occurrence with both strains (~50% of experiments). Also, any experiment where there was obvious damage to the siphon upon impalement or during the course of the experiment was discontinued and the data was discarded.

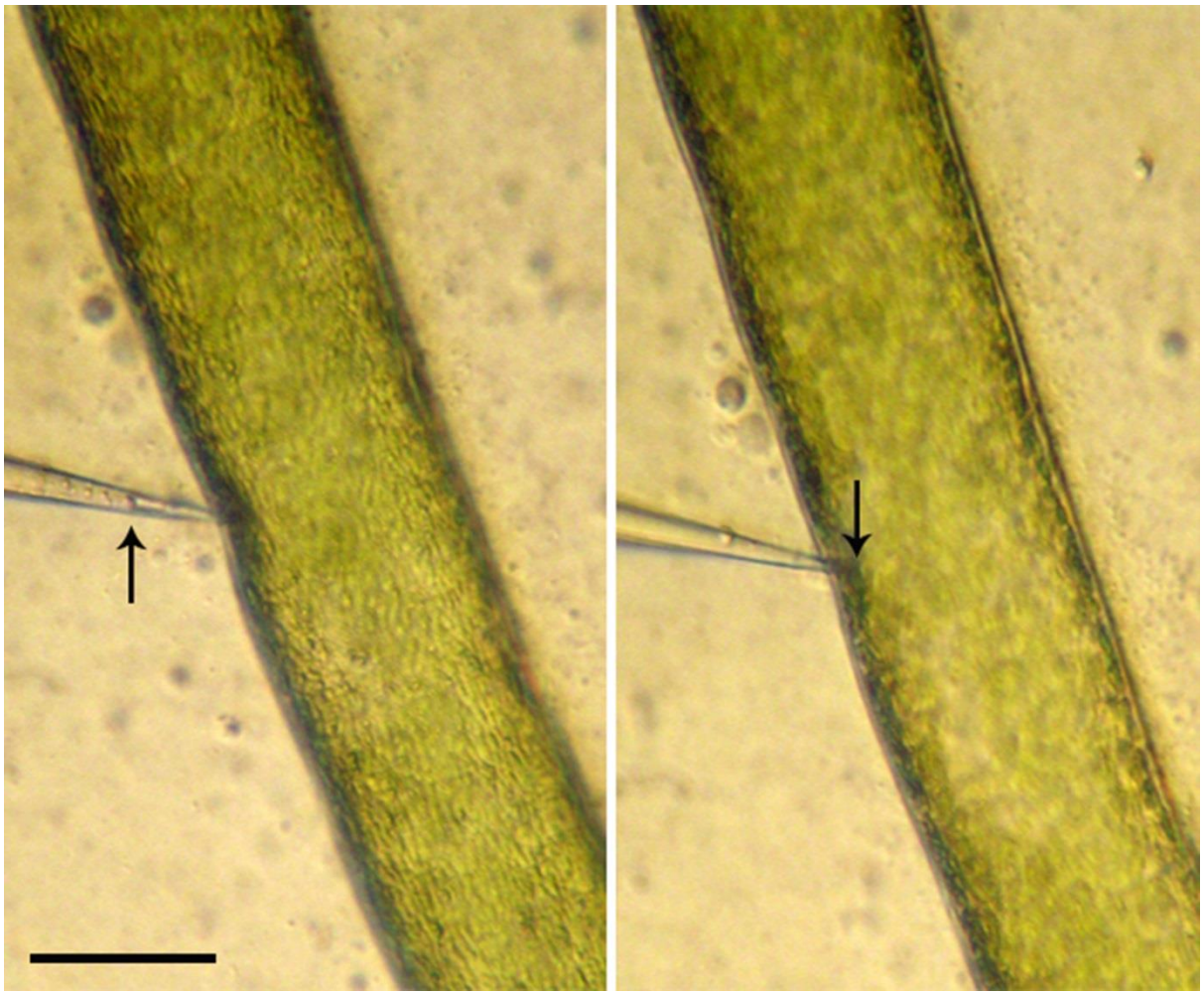

**Figure 3.2.** Example of impalement of a siphon of *Vaucheria repens* with the micropipette of the pressure probe. Upon impalement, the silicone oil was pushed back from the micropipette tip by the cytoplasm, visible as a meniscus (left arrow), due to turgor pressure. Pressure was then applied to push the meniscus back to the micropipette tip (right arrow). Bar = 50 µm.

### 3.2.3. Hyperosmotic treatments

Hyperosmotic shocks were imposed by exposure of siphons to aqueous solutions of NaCl or sorbitol. The concentrations used ranged from 0.1 to 0.5 M (NaCl), and from 0.2 to 1 M (sorbitol). For both NaCl and sorbitol, these concentrations raised the osmolalities to 148–580 mOsmol $kg^{-1}$ (as measured with the osmometer). As the two species were precultured on different media (as necessitated by their normal freshwater and estuarine habitats), different concentrations of NaCl or sorbitol were required in order to give them equivalent osmotic shocks. Thus, e.g., *V. repens* precultured on BBM media when exposed to 0.25 M NaCl solution gave an osmolality change of ~200 mOsmol $kg^{-1}$ translating into an osmotic shock of ~0.5 MPa. To experience the same osmotic shock, *V. erythrospora* precultured on f/2 media had to be exposed to a 0.4 M NaCl solution. This was approximated by converting the osmolarity change which was measured with the osmometer to an osmotic potential change, $\Delta\psi = -\Delta cRT$ (MPa = (mol . $kg^{-1}$) 0.00831 [(MPa L) . mol K] 293 K), where c is osmolality change, R is the universal gas constant and T is temperature in Kelvin. After impalement and initial turgor readings, 30–40 mL of hyperosmotic solution was added onto agarised media which completely flooded the surface growths of siphons. The osmolality of the shock solution was measured upon addition using the osmometer over the typical time course of an experiment for confirmation of the osmotic shock. Care was taken to pour and mix the solution gently to avoid dislodging the siphons from the agar and the pipette from the impaled siphon. Turgor was estimated at 1 min intervals by withdrawing the meniscus and reapplying pressure to push it back to the tip.

### 3.2.4. Measurement of growth rates and turgor under different salinities

Agarised (1% w/v) BBM and f/2 media containing different concentrations of NaCl were made up in 90 mm petri dishes, and *V. repens* and *V. erythrospora* were grown for 2 weeks under standard conditions (see culture maintanence). For measurement of growth rates, cultures were imaged daily in colour at 1,200 dpi using a flatbed scanner (Epson Perfection V700, Epson, Auckland, New Zealand). Growth rates were measured by overlaying images from each day and measuring siphon extension using the ruler tool in Adobe Photoshop (CS4 extended version 11.0; Adobe Systems Incorporated, San Jose, CA, USA). Mean growth rates and SD were calculated for 20 replicate siphons over 2 weeks.

For turgor measurements, two week old *V. repens* and *V. erythrospora* cultures growing on agarised BBM and f/2 media containing different concentrations of NaCl, were impaled using the pressure probe as described above. Mean turgor values and SD were calculated for a minimum of 15 replicates at each media NaCl concentration.

## 3.3. Results

### 3.3.1. Growth rates and turgor under different salinities

*V. repens* (Fig. 3.3) showed the most rapid growth (1.9 ± 0.06 mm $d^{-1}$) at ~0.002 M NaCl. Growth rates declined rapidly at higher concentrations of NaCl and did not occur above ~0.1 M NaCl. *V. erythrospora* grew at concentrations from ~0.04 M NaCl to as high as ~0.4 M NaCl. The optimum growth rate of 4.68 ± 0.14 mm $d^{-1}$ was observed at 0.13 M NaCl. Colonies of *Vaucheria* siphons covered more surface area on agar at optimal media NaCl concentrations of 0.002 M for *V. repens* (Fig. 3.4a) and 0.13 M for *V. erythrospora* (Fig. 3.4c). As NaCl concentrations were increased above optimum, the radial extension of the

colony was reduced. The morphology changed to more closely packed dense colonies with more branches per mm of agar surface (Fig. 3.4b and d).

The highest average turgor values in *V. repens* (0.98 ± 0.1 MPa; mean ± SD, n =16; range = 0.82–1.11 MPa) were recorded at 0.002 M NaCl, its optimal growth concentration (Fig. 3.5). As the NaCl concentration in the media increased, the turgor values decreased. Turgor dropped to 0.79 ± 0.04 MPa (mean ± SD; n = 15; range = 0.75–0.85 MPa) and 0.31 ± 0.04 MPa (mean ± SD; n =15; range = 0.23–0.37 MPa) at ~0.04 M and ~0.08 M NaCl respectively. Impalements were difficult in cultures growing above 0.08 M NaCl because of the low turgor. In contrast to *V. repens*, the highest average turgor values in *V. erythrospora* (1.05 ± 0.11 MPa; mean ± SD; n = 25) were recorded at ~ 0.04 M NaCl, which is lower than its optimal growth concentration. Though turgor values dropped at higher media NaCl concentrations, *V. erythrospora* maintained a turgor of 0.39 ± 0.06 (mean ± SD; n = 15; range = 0.34–0.49) even at ~ 0.4 M NaCl, its highest growth concentration.

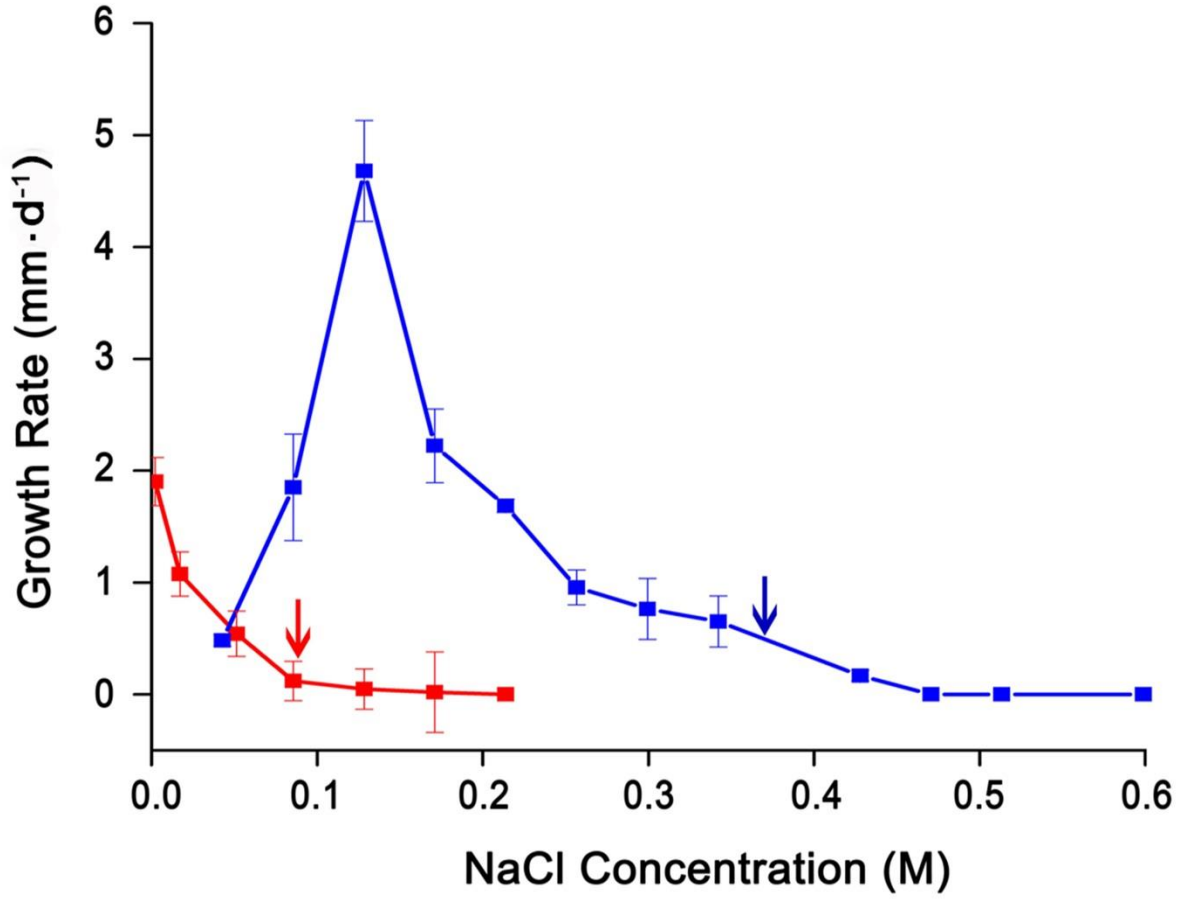


**Figure 3.3.** Growth rates in cultures of *V. repens* (red) and *V. erythrospora* (blue) grown at different NaCl concentrations. Optimal growth rates were observed at ~0.002 M (1.9 ± 0.06 mm $d^{-1}$; mean ± SD; n= 20) and ~0.13 M NaCl concentration (4.68 ± 0.14 mm $d^{-1}$; mean ± SD; n=20) in *V. repens* and *V. erythrospora*, respectively. *V. repens* did not grow above ~0.17 M and *V. erythrospora* above 0.5 M NaCl concentration. Arrows represent the highest NaCl concentrations in which the isolates showed turgor recovery in the pressure probe experiments following hyperosmotic shock.

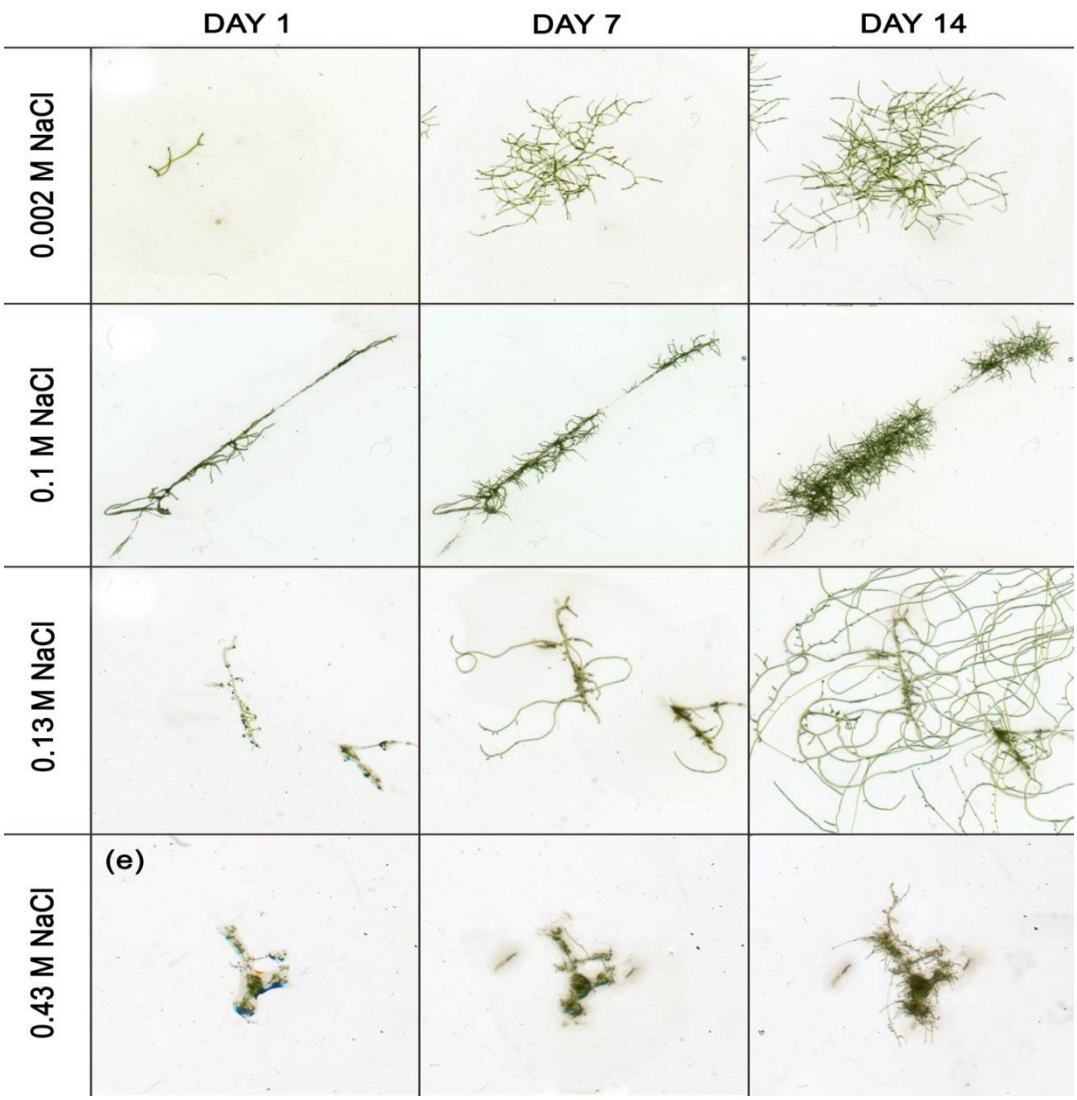


**Figure 3.4.** Growth of *V. repens* and *V. erythrospora* in media of different NaCl concentrations (a, b) *V. repens* after 1, 7, and 14 d of growth on optimal media (a) and at the highest NaCl concentration at which turgor recovery was observed in the pressure probe experiments (b). (c,d) *V. erythrospora* after 1, 7, and 14 d of growth on optimal media (c) and at the highest NaCl concentration at which turgor recovery was observed in the pressure probe experiments (d).

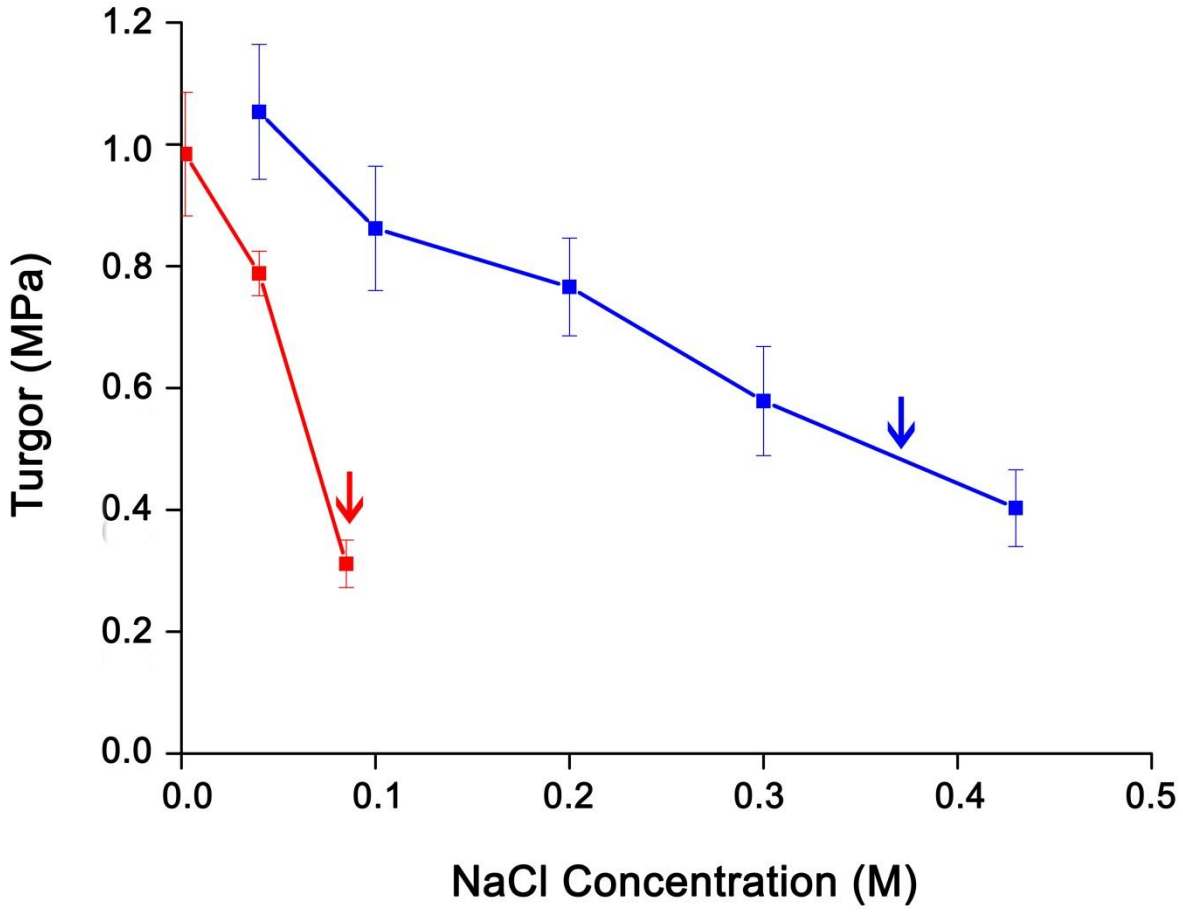


**Figure 3.5.** Turgor values in cultures of *V. repens* (red) and *V. erythrospora* (blue) that were grown at different NaCl concentrations. Highest turgor values were observed at ~0.002 M and ~0.04 M NaCl concentration in *V. repens* and *V. erythrospora*, respectively. Turgor values decreased with increasing media NaCl concentration in both *V. repens* and *V. erythrospora*. Arrows represent the highest NaCl concentrations in which the isolates showed turgor recovery in the pressure probe experiments following hyperosmotic shock.

### 3.3.2. Response to hyperosmotic shock

Before exposing the isolates to a hyperosmotic shock, their initial turgor pressure values were measured. The freshwater isolate, *V. repens*, had an average initial turgor pressure of 1.14–0.22 MPa (mean ± SD, n = 57; range: 0.73–1.57) whereas that of the brackish water isolate, *V. erythrospora* was marginally lower at 0.92 ± 0.17 MPa (mean ± SD, n = 41; range: 0.68–1.22). To investigate turgor recovery after osmotic challenge, siphons of *V. repens* were exposed to different concentrations of NaCl (Fig. 3.6a–c) and sorbitol (Fig. 3.6d-f) with equal osmolalities. Following an osmotic shock of -1.2 MPa (0.5 M NaCl), an initial average turgor pressure of 1.25 ± 0.17 MPa (mean ± SD, n = 7; range: 1.03–1.54) dropped to 0.37 ± 0.17 MPa (mean ± SD, n = 7; range: 0.18–0.59) on exposure and did not recover within 60 min. Plasmolysis was observed in all siphons a few minutes after exposure. A similar pattern was observed after a shock of -0.5 MPa (0.25 M NaCl). However, the siphons showed turgor recovery following a shock of -0.2 MPa (0.1 M NaCl). Turgor halved from 1.29 ± 0.19 MPa (mean ± SD, n = 5, range: 0.95–1.53) to 0.62 ± 0.11 MPa (mean ± SD, n = 5, range: 0.42–0.75), recovery started 20 min later, and was complete 60 min after exposure. Plasmolysis after hyperosmotic treatment was observed to be less marked and slower (~5-10 min) than that observed after the -1.2 MPa shock, with the siphons regaining turgidity during turgor recovery. Sorbitol treatments showed the same trends, with siphons showing turgor recovery up to an external osmotic shock of -0.2 MPa (0.2 M sorbitol; Fig. 3.3d), and no recovery with -0.5 and -1 MPa (0.5 M and 1 M sorbitol; Fig 3.6e and f) respectively.

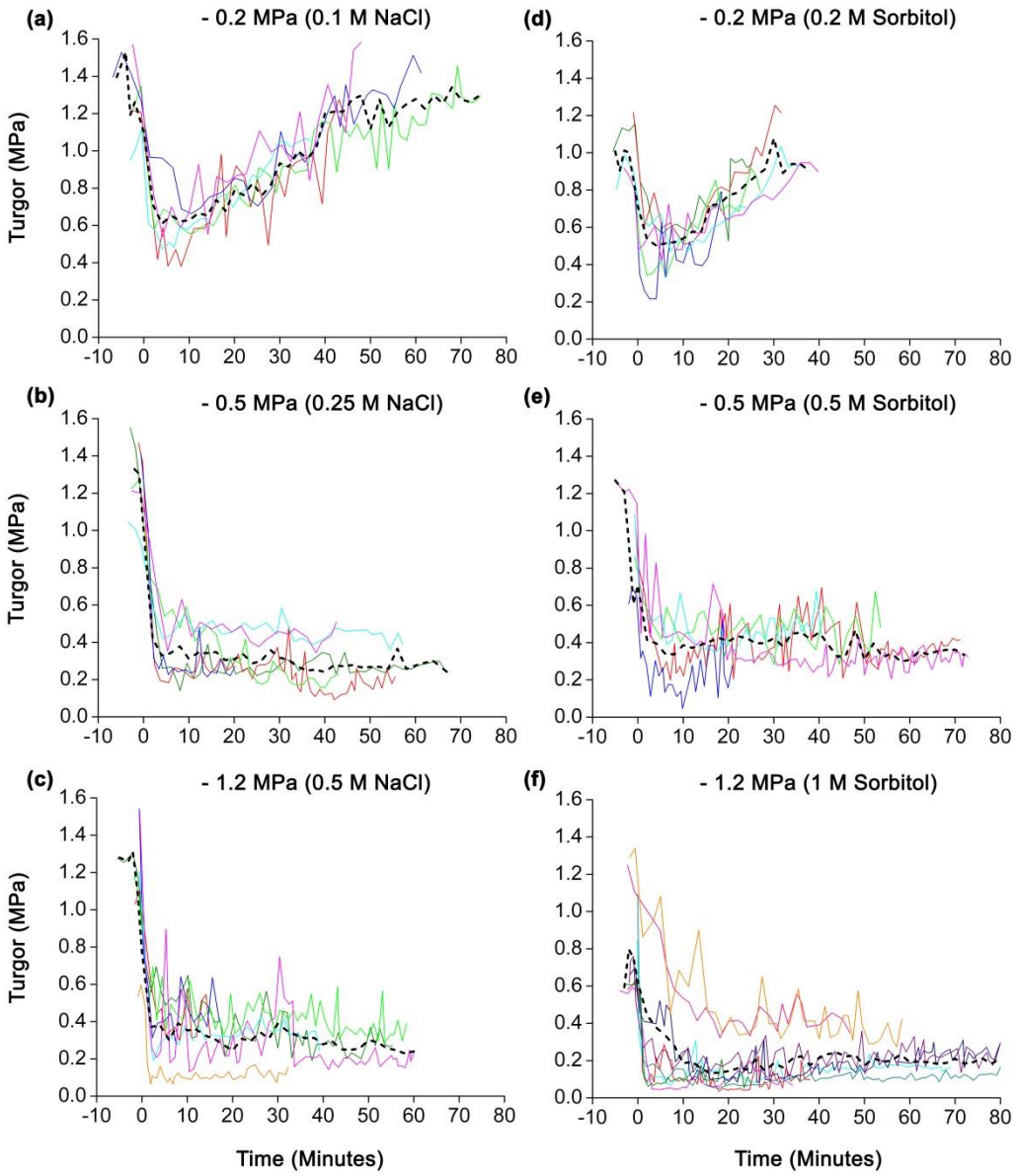


**Figure 3.6.** Turgor responses of *Vaucheria repens* to hyperosmotic stress. The graphs represent direct measurements of turgor (MPa) plotted against time relative to the osmotic shock (min). Each colored line represents a series of measurements from a single siphon. Individual measurements were taken at 1 min intervals. (a–c) Responses to different hyperosmotic shocks (MPa) provided by the concentrations of NaCl indicated in brackets. (d–f) Responses to different hyperosmotic shocks (MPa) provided by the concentrations of sorbitol indicated. The black dotted line in each graph is the trendline calculated as a moving average of turgor values from all experiments at a particular time point for each concentration. Turgor recovery as indicated by an increase in turgor toward original value after initial drop was observed in *V. repens* after a – 0.2 MPa hyperosmotic shock.

*Vaucheria erythrospora* was tested in a similar manner with different NaCl (Fig. 3.7a-c) and sorbitol (Fig. 3.7d) concentrations. Turgor recovery was observed after a hyperosmotic shock of -0.2 MPa (0.25 M NaCl), similar to the response observed in *V. repens* after a shock of the same magnitude. On exposure, turgor dropped from 0.90 ± 0.20 MPa (mean ± SD, n = 5; range; 0.72–1.19) to 0.41 ± 0.15 MPa (mean ± SD, n = 5; range: 0.19–0.57). Turgor recovery commenced ~15 min after exposure with complete recovery taking ~35–40 min. These times were quicker than observed with *V. repens* after the same magnitude osmotic shock. Significantly, turgor also recovered following exposure to a - 0.5 MPa shock (0.4 M NaCl; Fig. 3.7b), a response that we did not observe with *V. repens*. After the - 0.5 MPa shock, the onset of turgor recovery occurred after ~20–25 min with complete recovery at ~60 min. Turgor recovery was also observed in experiments after an ~ - 0.5 MPa shock imposed by 0.8 M sorbitol (Fig. 3.7d; the same shock imposed by 0.4 M NaCl). Plasmolysis was observed immediately after hyperosmotic treatment with siphons becoming turgid during recovery. Turgor did not recover when the magnitude of the shock was - 0.8 MPa (0.5 M NaCl; Fig. 3.7c).

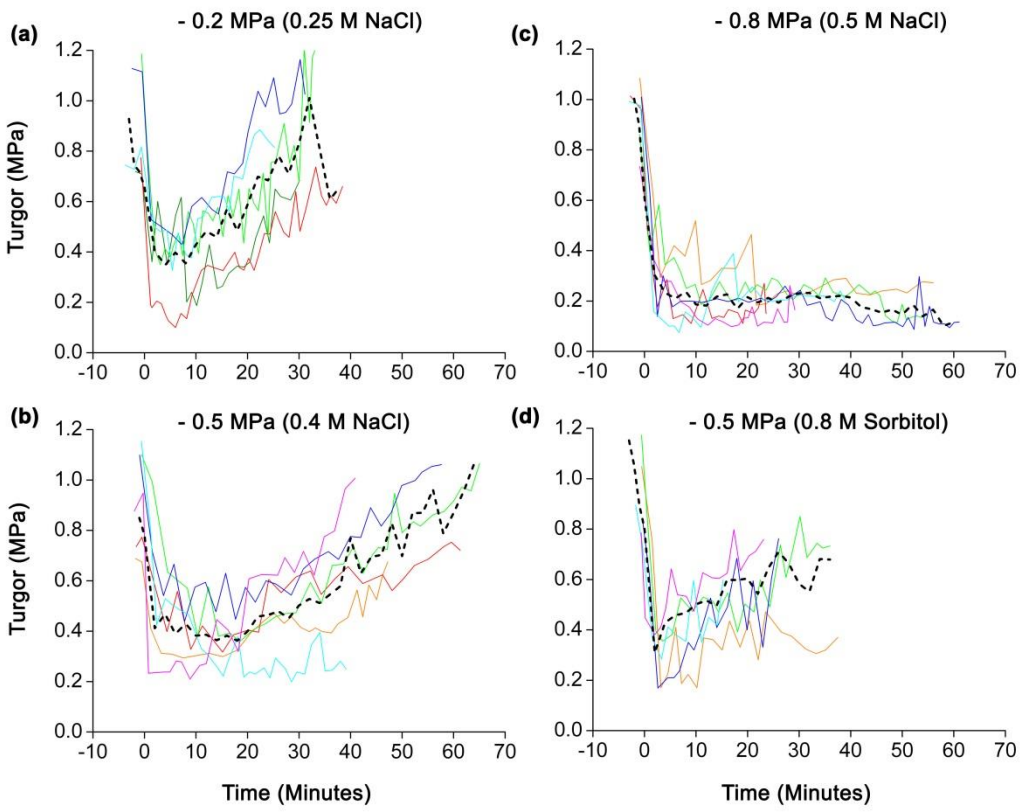


**Figure 3.7.** Turgor responses of *Vaucheria erythrospora* to hyperosmotic stress. The graphs represent direct measurements of turgor (MPa) plotted against time relative to the osmotic shock (min). Each colored line represents a series of measurements from a single siphon. Individual measurements were taken at 1 min intervals. (a–c) Responses to different hyperosmotic shocks (MPa) provided by the concentrations of NaCl indicated in brackets. (d) Response to a – 0.5 MPa hyperosmotic shock provided by 0.8 M sorbitol. The black dotted line in each graph is the trendline calculated as a moving average of turgor values from all experiments at a particular time point for each concentration. Turgor recovery as indicated by an increase in turgor toward original value after initial drop was observed in *V. erythrospora* after – 0.2 MPa and – 0.5 MPa hyperosmotic shocks.

## 3.4 Discussion

*Vaucheria repens* and *Vaucheria erythrospora* have been shown to respond differently to hyperosmotic shock. Though both isolates showed turgor recovery, each had its own threshold osmotic shock beyond which recovery did not occur. *V. erythrospora* was found to recover turgor after a larger shock than *V. repens* with threshold values for this ability of > 0.5 MPa for *V. erythrospora* and < 0.5 MPa for *V. repens*. Also, the quicker recovery responses of *V. erythrospora* indicated that it may be better adapted to variations in osmotic potential. Similarly, in the characean algae, *Chara longifolia*, a species found in saline habitats, has been shown to regulate turgor (Stento et al. 2000), while *Chara corallina*, an obligate freshwater species, does not (Bisson and Bartholomew 1984). *V. erythrospora* also grew on a wider range of media NaCl concentrations (~ 0.04 M to ~ 0.4 M NaCl) compared to *V. repens*, which did not grow beyond 0.1 M NaCl. Turgor values dropped with increasing media NaCl concentrations in both *V. erythrospora* and *V. repens*. While *V. erythrospora* maintained a turgor of ~ 0.3 MPa even at ~ 0.4 M NaCl, *V. repens* did not show any measureable turgor beyond 0.08 M NaCl. These different responses are likely to influence the type of habitats that can be occupied by the two species.

In *V. erythrospora*, the highest average turgor was recorded at ~ 0.04 M NaCl (~ 1 MPa) concentration in the media, while the highest average growth rate was recorded at ~ 0.1 M NaCl (~ 0.8 MPa). This observation that turgor does not influence average growth rate in a linear manner, is consistent with both model predictions and experimental observations in other tip-growing cells like fungi, oomycetes and pollen tubes (Kaminskyj et al. 1992; Kroeger et al. 2011).

The average initial turgor values of *V. repens* and *V. erythrospora* were 1.14 and 0.92 MPa, respectively. The higher turgor value for the freshwater species compared to the estuarine species mirrors what has been reported in *Chara* with values of 0.67 MPa for *C. corallina* (freshwater; Bisson and Bartholomew 1984) and 0.5 MPa for *C. longifolia* (saline; Stento et al. 2000). It should however be noted that direct comparison may not be valid as the two studies on *Chara* used different techniques to measure turgor, namely osmometer measurements on vacuolar sap for *C. corallina* and the pressure probe for *C. longifolia*. Irrespective of any differences between freshwater and saline species, the values are lower in the characean algae than in *Vaucheria*, and as indicated below, our values using the pressure probe are higher than those reported on other algae using the same technique. There has been a wide range of turgor values reported in other algae, although it is unclear whether this range reflects meaningful physiological differences, or is a result of the different techniques that were used to measure turgor. *Nitella* and *Valonia* have turgor values of 0.57 and 0.4 MPa respectively, measured using a pressure probe (Green and Stanton 1967, Zimmermann et al. 1976). Turgor has been estimated using osmometer measurements of the vacuolar sap of *Codium* and *Lamprothamnium*, giving values of 0.23 and 0.7 respectively (Bisson and Gutknecht 1975, Wichmann and Kirst 1989). Using incipient plasmolysis, two studies on *Klebsormidium* spp. from alpine habitats and *Zygnema* spp. from polar habitats reported higher turgor values ranging between 1.67 and 2.09 MPa in *Klebsormidium* spp and 0.8–1.67 MPa in *Zygnema* spp. (Kaplan et al. 2012, 2013).

The freshwater species, *V. repens*, showed turgor recovery after an osmotic shock of -0.2 MPa. Other studies of turgor responses of freshwater stramenopiles have used larger shocks. Lew et al. (2004) exposed the oomycete *Achlya bisexualis* to a hyperosmotic shock equivalent to a pressure change of - 0.59 MPa and observed no recovery of turgor. A similar

response was obtained with pressure changes of 0.3–0.4 MPa in *A. bisexualis* and up to ~0.8 MPa in another freshwater oomycete, *Saprolegnia ferax* (Money and Harold 1992, 1993). The contention from these results has been that oomycetes lack the ability to turgor regulate after hyperosmotic shock (Lew et al. 2004). Our data suggest that further studies may be warranted in which gentler osmotic shocks are used to confirm an absence of turgor regulation. Also, it should be noted that for comparative reasons the administration of the osmotic shock should be consistent between studies. In the study of Lew et al. (2004), the hyperosmotic shock may have taken longer to reach the cells than in this study, as solutions were not stirred when the shock was applied.

Though the oomycetes studied lack the ability to turgor regulate after hyperosmotic shock, they appear to have been shown to do so in response to a hypoosmotic shock (Lew et al. 2004). However, the absence of an initial change in turgor upon exposure to hypoosmotic solution may be due to experimental problems in raising the external osmotic potential. The responses of these *Vaucheria* isolates to a hypoosmotic shock have not been tested in this study.

If the oomycetes do indeed lack the ability to turgor regulate and, given that freshwater *V. repens* has been shown to regulate turgor, this raises interesting questions with respect to the possible evolution of turgor regulation. While *Achlya* and *Saprolegnia* belong to Saprolegniaceae, a family of the oomycetes restricted to freshwaters and non-saline soils (Hulvey et al. 2007), the genus *Vaucheria* includes different species in habitats ranging from freshwater, to brackish to fully marine. Recent phylogenetic studies on oomycete parasites of seaweeds suggest that eucarpic oomycetes like those encompassing Saprolegniaceae probably evolved from marine holocarpic ancestors (Beakes and Sekimoto 2008, Grenville-Briggs et

al. 2011). Based on this and considering the different responses to hyperosmotic shock of freshwater oomycetes (if indeed they are subsequently shown to be unable to turgor regulate after an osmotic shock of the order of -0.2 MPa) and the studied freshwater species of *Vaucheria*, it can be speculated that the ecology adopted by non-marine oomycetes might be more specialized. They might have colonized freshwaters prior to freshwater *Vaucheria* species, thus having longer to lose a vestigial property such as osmotic tolerance. This is implied by the current classification scheme, in which *Vaucheria* is a genus but Saprolegniaceae is a family. Alternatively, selection processes may be operating that favour the retention of turgor regulation in freshwater *Vaucheria*, such as the ability to opportunistically colonize brackish and saline habitats.

It should be noted that with some experiments with the probe, the magnitude of turgor loss was greater than the change in external osmotic pressure. This occurred in experiments involving both *V. repens* (with osmotic challenges of –0.2 and –0.5 MPa) and *V. erythrospora* (with an osmotic challenge of –0.2 MPa). Similar observations have been made with other organisms. In *Neurospora crassa* there was a turgor drop of 0.4 MPa after an osmotic shock of –0.2 MPa (Lew and Nasserifar 2009), in *Lilium* pollen grains a drop of 0.15 MPa after ashock of –0.1 MPa (Pertl et al. 2010) and in *Arabidopsis* epidermal root cells a drop of 0.4 MPa after a shock of –0.2 MPa (Shabala and Lew 2002). It is currently unclear why decreases of such magnitude occur. One possibility is that there could have been leakage around the probe due to stress-induced changes in the shape of the cells on addition of the hyperosmotic solution. Any leakage is likely to have been temporary, as in those experiments where turgor recovered it did so to approximately the original value prior to the osmotic shock. Alternately, some cells may have been damaged due to impalement, although as detailed in the Methods section, we discarded any recordings where there was obvious

evidence of cell damage. As a result, to the best of our abilities, we are confident that our recordings were made on undamaged cells and what is observed is actually turgor recovery and not damage recovery.

Turgor regulation under osmotic shock is likely to be a biphasic process (Kirst 1990). In the first phase, water flux caused by changing salinity leads to a change in turgor pressure. This change in pressure is possibly detected by an osmo-sensor. In the second phase, osmotically active solutes are used for osmotic adjustment to restore turgor back to normal. This osmotic adjustment can be brought about by an uptake of inorganic ions and/or synthesis of organic osmolytes. Turgor regulation through the uptake of inorganic ions has been seen in a wide range of organisms, e.g., in the salt tolerant characean algae *Chara longifolia* and *Lamprothamnium succinctum*, in the fungus *Neurospora crassa* and the angiosperm *Arabidopsis thaliana* (Stento et al. 2000; Shabala and Lew 2002; Lew et al. 2004). Only two members of Stramenopila have been reported to take up inorganic ions under hyperosmotic shock, these being a halotolerant, raphidophycean mixotrophic microalga, *Heterosigma akashiwo*, and a marine protist, *Thraustochytrium aureum* (Garrill et al. 1992; Gimmler 2000; Shabala et al. 2009). While osmotic adjustment in the former predominantly involves $K^+$ and $Cl^-$ uptake, the latter depends on $Na^+$ and $Cl^-$ uptake.

Ion movements have been shown to precede the adjustment of organic osmolytes in some algae, e.g., in halophilic chlorophytes, *Platymonas subcordiformis* and *Dunaliella parva* (Kirst 1990). In other algae, organic osmolytes are involved in the entire process of turgor recovery. In some cases, they are identical to the main photosynthetic products of algae (Kirst and Bisson 1979, Wegmann 1986, Fujii et al.1999). For example, a unicellular freshwater chrysophycean *Poterioochromonas malhamensis* (a stramenopile), synthesizes isofloridoside

under hyperosmotic shock (Kauss 1983; Bisson and Kirst 1995). Excess isofloridoside is then converted to osmotically inactive chrysolaminarin when normal conditions return. Chrysolaminarin is also produced as a storage product during photosynthesis. In response to hyperosmotic shock it is thought to be again broken down to osmotically active isofloridoside (Wegmann 1986; Stone and Clarke 1992). As *Vaucheria* species have abundant chrysolaminarin, this response, along with the movement of ions, could well underlie the turgor regulation observed in this study. The mechanistic basis of turgor regulation is examined further in Chapter 4.

Varying responses to osmotic shock in two species of *Vaucheria* from contrasting habitats have been reported in this study. The ability to regulate turgor over a wide range of osmotic shocks, makes *V. erythrospora* better suited to an estuarine habitat. *V. repens* is restricted to freshwater habitats, with little fluctuation in osmotic potential and hence does not need to regulate turgor over a wide range of osmotic shocks. The fact that *V. repens* can regulate turgor, albeit at low osmotic shocks, distinguishes it from freshwater characeans, which have been shown to lack this ability. The ability of both these *Vaucheria* species to regulate turgor also makes them fundamentally different from the morphologically similar oomycetes.

### 3.5. References

Andersen RA and Bailey JC 2002. Phylogenetic analysis of 32 strains of *Vaucheria* (Xanthophyceae) using the *rbc*L gene and its two flanking spacer regions. Journal of Phycology 38: 583–592.

Beakes GW and Sekimoto S 2008. The evolutionary phylogeny of oomycetes—insights gained from studies of holocarpic parasites of algae and invertebrates. In Lamour, K.

and Kamoun, S. [Eds.] Oomycete Genetics and Genomics: Diversity, Interactions, and Research Tools. John Wiley and Sons Inc., Hoboken, New Jersey, pp. 1–24.

Beilby MJ and Shepherd VA 1996. Turgor regulation in *Lamprothamnium papulosum*. I. I/V analysis and pharmacological dissection of the hypotonic effect. Plant, Cell and Environment. 19: 837–847.

Bischoff HW and Bold HC 1963. Phycological studies IV. Some soil algae from Enchanted Rock and related algal species. University of Texas Publication 6318:1–95.

Bisson MA and Bartholomew D 1984. Osmoregulation or turgor regulation in *Chara*? Plant Physiology 74: 252–255.

Bisson MA and Gutknecht J 1975. Osmotic regulation in the marine alga, *Codium decorticatum* I. Regulation of turgor pressure by control of ionic composition. Journal of Membrane Biology 24: 183–200.

Bisson MA and Kirst GO 1995. Osmotic acclimation and turgor pressure regulation in algae. Naturwissenschaften 82: 461–471.

Chitcholtan K, Harris E, Yu Y, Harland C and Garrill A. 2012. An investigation into plasmolysis in the oomycete *Achlya bisexualis* reveals that membrane–wall attachment points are sensitive to peptides containing the sequence RGD and that cell wall deposition can occur despite retraction of the protoplast. Canadian Journal of Microbiology 58: 1212–1220.

Entwisle TJ 1988. A monograph of *Vaucheria* (Vaucheriaceae, Chrysophyta) in south-eastern mainland Australia. Australian Systematic Botany. 1: 1–77.

Fujii S, Yamamoto R, Nakayama S, Yasui S and Broady PA 1999. Effects of salinity on growth and content of intracellular solutes in *Heterococcus* sp. (Tribonematales, Xanthophyceae) from Antarctica. Phycological Research. 47: 65–69.

Garrill A, Clipson, NJW and Jennings DH 1992. Preliminary observations on the monovalent cation relations of *Thraustochytrium aureum*, a fungus requiring sodium for growth. Mycological Research. 92: 295-304

Garrill, A., Findlay, G. P. and Tyerman, S. D. 1996. Mechanosensitive ion channels. In Smallwood, M., Knox, J. P. and Bowles, D. J. [Eds.]. Membranes: Specialized Functions in Plants. Bios scientific publishers, Oxford, UK, pp. 247–260.

Gimmler H 2000. Primary sodium plasma membrane ATPases in salt-tolerant algae: facts and fictions. Journal of Experimental Botany 51: 1171-1178

Green PB and Stanton FW 1967. Turgor pressure: direct manometric measurement in single cells of *Nitella*. Science 155: 1675–1676.

Grenville-Briggs L, Gachon CMM, Strittmatter M, Sterck L, Küpper FC and van West P 2011. A molecular insight into algal-oomycete warfare: cDNA analysis of *Ectocarpus siliculosus* infected with the basal oomycete *Eurychasma dicksonii*. PLoS ONE 6:e24500.

Guillard RRL and Ryther JH 1962. Studies on the marine planktonic diatoms: I. *Cyclotella nana* Hustedt, and *Detonula confervaceae* (Cleve) Gran. Canadian Journal of Microbiology. 8: 229–239.

Hulvey JP, Padgett DE and Bailey JC 2007. Species boundaries within *Saprolegnia* (Saprolegniales, Oomycota) based on morphological and DNA sequence data. Mycologia 99: 421–429.

Kaminskyj SGW, Garrill A and Heath IB 1992. The relation between turgor and tip growth in *Saprolegnia ferax*: turgor is necessary, but not sufficient to explain apical extension rates. Experimental Mycology 16: 64–75.

Kaplan F, Lewis LA, Herburger K and Holzinger A 2013. Osmotic stress in Arctic and Antarctic strains of the green alga *Zygnema* (Zygnematales, Streptophyta): effects on photosynthesis and ultrastructure. Micron 44: 317–330.

Kaplan F, Lewis LA, Wastian J and Holzinger A 2012. Plasmolysis effects and osmotic potential of two phylogenetically distinct alpine strains of *Klebsormidium* (Streptophyta). Protoplasma 249: 789–804.

Karsten U, Wienncke C and Kirst GO 1991. The effect of salinity changes upon the physiology of eulittoral green macroalgae from Antarctica and Southern Chile: II. Intracellular ions and organic compounds. Journal of Experimental Botany 42: 1533–1539.

Kauss H 1983. Volume regulation in *Poterioochromonas*. Plant Physiology. 71: 169–72.

Kirst GO 1990. Salinity tolerance of eukaryotic marine algae. Annual Review of Plant Physiology and Plant Molecular Biology 41: 21–53.

Kirst GO and Bisson MA 1979. Regulation of turgor pressure in marine algae: ions and low-molecular-weight organic compounds. Functional Plant Biology 6: 539–556.

Kroeger JH, Zerzour R and Geitmann A 2011. Regulator or driving force? The role of turgor pressure in oscillatory plant cell growth. PLoS ONE 6: e18549

Lew RR 1991. Electrogenic transport properties of growing *Arabidopsis* root hairs. Plant Physiology 97: 1527–1534.

Lew RR and Levina NN 2007. Turgor regulation in the osmosensitive cut mutant of *Neurospora crassa*. Microbiology 153: 1530–1537.

Lew RR, Levina NN, Walker SK and Garrill A 2004. Turgor regulation in hyphal organisms. Fungal Genetics and Biology 41:1007–1015.

Lew RR and Nasserifar S 2009. Transient responses during hyperosmotic shock in the filamentous fungus *Neurospora crassa*. Microbiology 155: 903–11.

Money NP 1997. Wishful thinking of turgor revisited: the mechanics of fungal growth. Fungal Genetics and Biology. 21: 173– 187.

Money NP and Harold FM 1992. Extension growth of the water mold *Achlya*: interplay of turgor and wall strength. Proceedings of National Academy of Sciences of the United States of America 89: 4245–4249.

Money NP and Harold FM 1993. Two water molds can grow without measurable turgor pressure. Planta 190: 426–430.

Ott DW and Brown RM 1974. Developmental cytology of the genus *Vaucheria* I. Organisation of the vegetative filament. British Phycological Journal 9: 111–126.

Pertl H, Pockl M, Blaschke C and Obermeyer G 2010. Osmoregulation in *Lilium* pollen grains occurs via modulation of the plasma membrane $H^+$ ATPase activity by 14-4-4 proteins. Plant Physiology 154: 1921–1928.

Potter D, Saunders GW and Andersen RA 1997. Phylogenetic relationships of the Raphidophyceae and Xanthophyceae as inferred from nucleotide sequences of the 18S ribosomal RNA gene. American Journal of Botany 84: 966–972.

Ray PM, Green PB and Cleland R 1972. Role of turgor in plant cell growth. Nature 239: 163–164.

Schleyer M, Schmid R and Bakker EP 1993. Transient, specific and extremely rapid release of osmolytes from growing cells of *Escherichia coli* K-12 exposed to hypoosmotic shock. Archives of Microbiology 160: 424–431.

Shabala SN and Lew RR 2002. Turgor regulation in osmotically stressed *Arabidopsis* epidermal root cells. Direct support for the role of inorganic ion uptake as revealed by concurrent flux and cell turgor measurements. Plant Physiology 129: 290–299.

Shabala L, McMeekin T and Shabala S 2009. Osmotic adjustment and requirement for sodium in marine protist thraustochytrid. Environmental Microbiology 11: 1835–1843.

Stento NA, Ryba NG, Kiegle EA and Bisson MA 2000. Turgor regulation in the salt-tolerant alga *Chara longifolia*. Plant, Cell and Environment 23: 629–637.

Stone BA and Clarke AE 1992. Chemistry and Biology of (1,3)-β-Glucans. La Trobe University Press, Victoria, Australia.

Taylor FJRM 2003. The collapse of the two-kingdom system, the rise of protistology and the founding of the international society for evolutionary protistology (ISEP). International Journal of Systematic and Evolutionary Microbiology 53:1707–1714.

Wegmann K 1986. Osmoregulation in eukaryotic algae. FEMS Microbiology Letters 39: 37–43.

Wichmann F and Kirst GO 1989. Adaptation of the euryhaline charophyte *Lamprothamnium papulosum* to brackish and freshwater: turgor pressure and vacuolar solute concentrations during steady-state culture and after hypo-osmotic treatment. Journal of Experimental Botany 40: 135–141.

Young AJ, Collins JC and Russell G 1987a. Solute regulation in the euryhaline marine alga *Enteromorpha prolifera* (O. F. Müll) J. Ag. Journal of Experimental Botany 38: 1298–1308.

Young AJ, Collins JC and Russell G 1987b. Ecotypic variation in the osmotic responses of *Enteromorpha intestinalis* (L.) Link. Journal of Experimental Botany 38:1309–24.

Zimmermann U, Steudle E and Lelkes PI 1976. Turgor pressure regulation in *Valonia utricularis*. Plant Physiology 58: 608–613.

# Chapter 4

## The contribution of ion uptake and osmolyte synthesis to turgor regulation after hyperosmotic shock in *V. erythrospora*

### 4.1. Introduction

The ability to respond to osmotic stress is likely to be a major determinant in the distribution of organisms in different aquatic habitats. Thus, those organisms that are able to keep turgor constant by altering their internal osmotic potential in response to changes in external osmotic potential may be better equipped to survive in a habitat such as an estuary that has an ever fluctuating osmotic potential.

Many euryhaline species of green algae have been shown to regulate turgor over a wide range of external osmotic potentials (Heidecker et al. 2003; Beilby et al. 2006; and references within). The regulation of turgor under hyperosmotic stress necessitates an increase in the internal osmotic potential, which will cause water to move into the cell and thus restore turgor. Algae that regulate turgor increase their internal osmotic potential either by an uptake of inorganic ions (e.g. $K^+$, $Na^+$), the synthesis of organic osmolytes (e.g. heterosides, polyols) or a combination of both (Bisson and Kirst 1995). Inorganic ions are likely to be readily available in the external environment and provide a rapid means of osmotic adjustment which could be crucial under varying osmotic potential. Turgor recovery by synthesis of organic osmolytes is slower and is likely to be energetically more costly, using ten times more ATP than ion uptake (Shabala and Lew 2002). The advantage of the synthesis of organic osmolytes, despite the energetic cost, is that they can accumulate to high concentrations in the cytosol without having any detrimental effect on cellular function (Yancey et al. 1982). In contrast, high concentrations of inorganic ions in the cytosol may impair cell function through effects on proteins and nucleic acids (Burg & Ferraris 2008).

The morphology of algae may dictate the kind of osmolytes that are employed for osmotic adjustment. Microalgae respond predominantly by synthesizing or degrading organic compounds, with ion uptake playing only a minor role (Kirst 1990). This preference for organic osmolytes is thought to be due to their high cytosol : vacuole ratio compared to giant-celled coenocytic macroalgae in which the vacuole occupies more than 95% of the cell (Kirst and Bisson 1979). This is however based on the assumption that organic compounds are synthesized and accumulated only in the cytosol. Salt tolerant species of the green chlophyte algae *Dunaliella* and *Tetraselmis*, rely on synthesis of glycerol and mannitol, respectively, under hyperosmotic stress (Kirst and Bisson 1979; Wegmann 1986). In macroalgae, an accumulation of inorganic ions in the vacuole would be necessary to bring about substantial osmotic adjustment. In these cells, organic osmolytes play a secondary role to the uptake of inorganic ions. For example, in the giant cell green alga, *Lamprothamnium succinctum*, a characean green alga with giant coenocytic cells, a cytosolic increase in sucrose has been shown to contribute to 40% of the osmotic potential during turgor recovery, with the remainder due to inorganic ion uptake (Kirst 1990). In coenocytes of the red alga *Griffithsia monilis,* most of the cell is occupied by the vacuole and the contribution of organic osmolytes to turgor recovery is negligible (Kirst 1990).

Much of our knowledge of the ion transport processes responsible for turgor regulation in algae comes from studies on green macroalgae belonging to two groups, the charophytes and the chlorophytes. The charophytes, which include the characean algae (e.g. *Chara* and *Lamprothamnium*), have been the most extensively studied owing to their large cells which have enabled electrophysiological studies. Among the chlorophytes, the large siphonous, coenocytic cells of *Valonia* and *Ventricaria* have received the most attention.

Characean algae and chlorophytes respond similarly to osmotic stress. Their euryhaline species are able to regulate turgor by taking up $K^+$ and $Cl^-$. $Na^+$ only plays a minor role in the

process and is actively extruded from the cytosol by a $Na^+/H^+$ antiporter (Bisson and Kirst 1980; Young et al. 1987; Kiegle and Bisson 1996; Bisson and Beilby 2002; Shepherd et al. 2004; Bisson et al. 2006). Species which colonise freshwater habitats appear to lack the ability to regulate turgor (Bisson and Bartholomew 1984; Frey et al. 1988). It is this inability, along with a comparatively less efficient $Na^+$ extrusion mechanism, that is thought to restrict these species to freshwater habitats.

Though both charophytes and chlorophytes employ $K^+$ and $Cl^-$ to regulate turgor, their electrophysiological responses to NaCl-induced hyperosmotic stress are thought to be different (Bisson et. al 2006). In the chlorophytes, the membrane potential has been shown to depolarize due to active uptake of $K^+$ into the vacuole through a tonoplast $K^+$ pump (Bisson and Beilby 2002; Bisson et al. 2006). The characean algae however, exhibit considerable variability in response to NaCl shock. Some studies have reported a depolarization of the membrane, while others have reported a hyperpolarization (Bisson and Kirst 1980; Okazaki et al. 1984; Reid et al. 1984; Al Khazaaly and Beilby 2007).

Very little is known of the physiological responses of other algal groups. The few investigations that have been carried out have been based on the analysis of cell contents. For example, a few species of red (Rhodophyceae) and brown (Phaeophyceae) algae regulate turgor by taking up $Na^+$, $K^+$ and $Cl^-$ ions (Kirst and Bisson 1979). *Vaucheria* is a yellow green alga (class Xanthophyceae) in the major phylogenetic group of eukaryotes called the heterokonts or stramenopiles (Heterokontophyta). This diverse group includes unicellular and multicellular algae, fungi-like organisms and marine parasites (Massana et al. 2004). The membrane transport processes involved in turgor regulation have been investigated in detail in only two stramenopiles - a raphidophycean, halotolerant microalga, *Heterosigma akashiwo* and a heterotrophic marine protist, *Thraustochytrium* (Garrill et al. 1992b; Gimmler 2000; Shabala et al. 2009). While the former extrudes $Na^+$ from the cytosol using a plasma

membrane $Na^+$-ATPase, the latter retains $Na^+$ and uses it to regulate turgor. Freshwater stramenopiles tested so far lack the ability to regulate turgor. These include the fungi-like oomycetes, *Achlya bisexualis* and *Saprolegnia ferax* and the chrysophycean alga *Poteriochromonas malhemensis*. The oomycetes respond to hyperosmotic stress by enabling growth under extremely low turgor, whereas *Poterioochromonas* regulates its volume by synthesizing an osmolyte, isofloridoside (Wegmann 1986; Money and Harold 1993; Bisson and Kirst 1995).

In Chapter 3, real time pressure measurements were used to show the ability of both a freshwater and an estuarine species of *Vaucheria* to regulate turgor in response to hyperosmotic stress. Turgor recovered more rapidly (within 60 min) in both *Vaucheria* species compared to charophytes and chlorophytes (3–6 days). *Vaucheria erythrospora*, the estuarine species, was able to tolerate a wider range of external solute concentrations both when cultured in the presence of those solutes over a long period and also when exposed to a sudden osmotic change. In the present chapter, investigations are reported on the mechanisms that underlie turgor regulation in this species. The role of inorganic ion uptake is studied, using: 1) pharmacological inhibition of specific membrane transport proteins and 2) measurement of ion fluxes using ion selective microelectrodes. Additionally, the metabolic profiles of this alga are analysed under stress to see if organic osmolyte synthesis contributes to turgor. Finally a model for turgor regulation in *V. erythrospora* in response to different hyperosmotic treatments is proposed on the basis of these investigations.

## 4.2. Materials and methods

### 4.2.1. Culture maintenance and sample preparation

*V. erythrospora* cultures were maintained in agarised f/2 medium as described in Chapters 2 and 3 under standard light and temperature conditions (16:8 h light:dark regime at 14°C and

~50 µmol photons $m^{-2}$ $s^{-1}$ light intensity). The pressure probe and GC-MS experiments were performed using two week old cultures that were growing in Petri dishes.

For MIFE experiments, *Vaucheria* siphons (1-2 mm long) were excised and immobilized onto a glass slide using thin strips of parafilm. Care was taken to secure the siphons gently without damaging them. The glass slide was placed in a 90mm Petri dish which was then filled with enough liquid f/2 medium to submerge the siphon entirely (usually 20 ml). The Petri dish was then incubated under standard light and temperature conditions for 24 hours before experimentation.

For membrane potential experiments, siphons were excised and immobilized onto plastic blocks using parafilm strips. The blocks were then gently placed in 10 mL Perspex measurement chambers filled with f/2 medium and incubated under standard light and temperature conditions.

### 4.2.2. Effect of ion channel inhibitors on turgor recovery

For inhibitor experiments, Gadolinium (III) chloride hexahydrate ($GdCl_3 . 6H_2O$; a mechanosensitive ion channel and non-selective cation channel inhibitor), tetraethylammonium chloride ($C_8H_{20}NCl$/ TEA; a $K^+$ channel inhibitor), verapamil hydrochloride ($C_{27}H_{38}N_2O_4 . HCl$; a calcium channel inhibitor) and sodium orthovanadate ($Na_3VO_4$: a $H^+$-ATPase inhibitor), were tested. Different concentrations of $Gd^{3+}$ (10–100 µM), TEA (10–50 mM), verapamil (10 µM) and orthovanadate (1mM) were added to the hyperosmotic solution made up in a NaCl solution that gave a shock of - 0.2 MPa. The NaCl concentration was adjusted such that the osmolality of each of the inhibitor containing solutions was the same. The response of the cell's turgor to osmotic shock and recovery in

the presence of the inhibitor was measured as described in the previous chapter. All chemicals were purchased from Sigma Aldrich.

### 4.2.3. Ion flux measurements

Net fluxes of $H^+$, $K^+$ and $Na^+$ were measured using the non-invasive Microelectrode Ion Flux Estimation (MIFE$^{TM}$) technique (ROCU, University of Tasmania, Hobart, Australia). For measurements microelectrodes were pulled from borosilicate glass capillaries (GC150-10, Harvard Apparatus Ltd., Kent, UK), oven dried overnight at 230 °C and silanized using tributylchlorosilane (Fluka, Buchs, Switzerland; catalogue no. 90796). The tips of the electrodes pulled and treated in this way were 2-3 µm in diameter. The electrodes were back-filled with the different solutions in order to select for different ions: for $H^+$ a solution of 0.15 mM NaCl + 0.4 mM $K_2HPO_4$ was used; for $K^+$ a solution of 0.5 M KCl was used and for $Na^+$ a solution of 500 mM NaCl was used. The tips were then front-filled with commercially available ionophore cocktails (Fluka catalogue no. 95297 for $H^+$, 60031 for $K^+$ and 71178 for $Na^+$). The ion-selective electrodes thus prepared were mounted on a 3D-micromanipulator (MX-2, Narshige, Tokyo, Japan) with the tips close to one another (~ 5 µm) and calibrated using a set of standards. Any that gave Nernst slope responses of < - 50 mV per decade were discarded due to low ion specificity.

For ion flux measurements, the tips were positioned about 5-10 µm from the siphon (Fig. 4.1). A computer-controlled stepper motor moved the electrodes between two positions (5 µm and 45 µm) from the surface of the siphon in a 10 s square-wave manner. The potential differences between the two positions were recorded and converted into electrochemical potential differences with CHART software (Newman 2001), using the calibrated Nernst slope of each electrodes. Net ion fluxes were calculated using the MIFEFLUX software for cylindrical diffusion geometry (Newman 2001). A higher electrochemical gradient measure

for an ion at the closer position (5 µm from the siphon) meant a greater concentration of the ion at that point than at the distant position (45 µm from the siphon). This was interpreted as ion efflux. Similarly a higher electrochemical gradient for the ion at the distant position (45 µm) than the closer one (5 µm) meant an ion influx. The reference electrode, consisting of a plastic tube filled with 1000 mol $m^{-3}$ KCl in 2% agar (w/v) was placed close to the siphon in the experimental solution.

The immobilized siphons were initially transferred from the f/2 medium to a basic salt medium (BSM) containing 0.1 mM $CaCl_2$, 0.2 mM KCl and different NaCl (1-100 mM) or sorbitol (150 mM) concentrations, depending on the experiment. The low NaCl (1mM) BSM was used for resolution of $Na^+$ fluxes, as these cannot be measured at high $Na^+$ concentrations using MIFE. The siphons were left to adapt for 1 hour before measurements. Net ion fluxes were measured for 5-10 min to ensure steady initial values before applying the hyperosmotic shock. For hyperosmotic treatments, isosmotic NaCl and sorbitol treatments were used (150 mM and 225 mM, respectively) to provide an osmotic shock of - 0.6 MPa. The first 60 s of measurements after addition of hyperosmotic solution was ignored to account for the establishment of diffusion gradients and mixing of solutions. Transient ion fluxes were then recorded for up to 60 min.

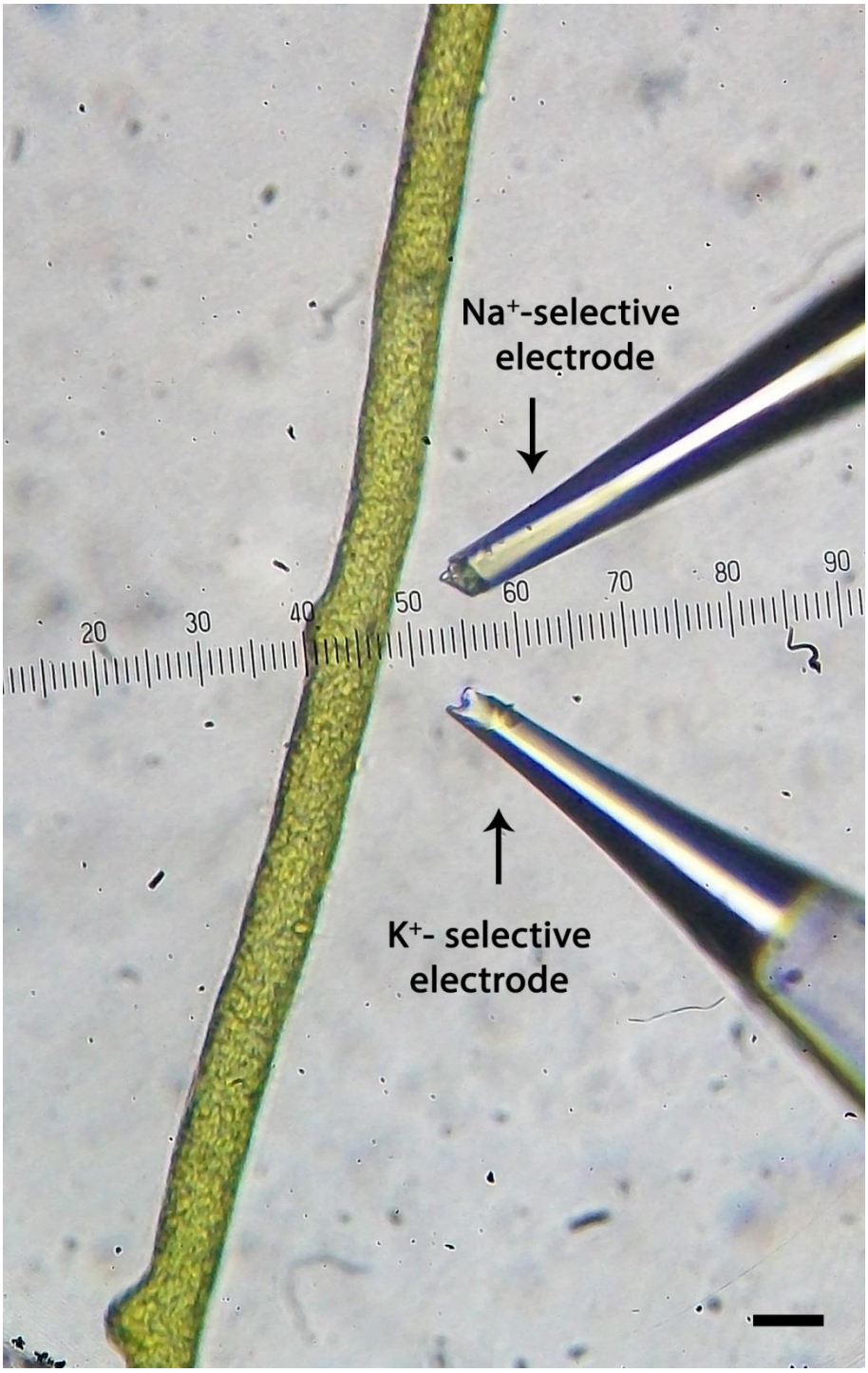


**Figure 4.1.** Example of a MIFE experiment, where transient $Na^+$ and $K^+$ fluxes in *Vaucheria erythrospora* are being measured simultaneously using ion selective microelectrodes.

### 4.2.4. Membrane potential ($E_m$) measurements

Perspex chambers with immobilized *Vaucheria* siphons were emptied of the growth medium which was then replaced with an isosmotic solution with low NaCl (0.2–1 mM; osmotically adjusted using sorbitol) and left to adapt for 1 hour before measurements. For $E_m$ measurements, borosilicate glass microelectrodes (Harvard Apparatus Ltd, Kent, UK) pulled to a tip diameter of ~ 0.5 µm, were filled with 1 M KCl and connected via an Ag/AgCl half-cell to the MIFE electrometer. For these experiments a vertical MIFE configuration was used, with a manually operated micromanipulator (MMT-5, Narshige, Tokyo, Japan) to impale the siphons. $E_m$ was monitored using the CHART software. For hyperosmotic treatments, BSM solutions with 100 mM NaCl and 170 mM sorbitol were used. After a stable $E_m$ measurement (over ~ 1 min) was obtained, the respective hyperosmotic solutions were added gently to avoid dislodging the microelectrode from the siphons. $E_m$ was recorded for 15–25 min after treatment. The reference electrode used was as described above.

### 4.2.5. $Na^+$ flux reversal experiments

Immobilized siphons were transferred from growth solution (f/2 medium) with a high $Na^+$ concentration (100 mM) to a low $Na^+$ solution (100 µM) of the same osmolality (adjusted using sorbitol), leading to $Na^+$ efflux down the gradient. The external $Na^+$ concentration was increased in a step wise manner to 150 µM, 200 µM, 500 µM and 1000 µM. Fluxes were recorded at each of these concentrations for 2–3 min before increasing the external $Na^+$ concentration to the next level. To detect the possible role of a $Na^+/H^+$ exchanger in mediating $Na^+$ fluxes in *V. erythrospora*, the above experiment was repeated in the presence of amiloride hydrochloride ($C_6H_8ClN_7O$. HCl; 0.5 mM) which is an inhibitor of the $Na^+/H^+$ exchanger in plant and animal cells. Fluxes were also compared in experiments where the $Na^+$ concentration was kept constant at 1000 µM, in the presence and absence of amiloride. In

all these experiments, siphons were pre-treated with amiloride, dissolved in the growth solution for 1h prior to changing to low $Na^+$ solution.

### 4.2.6. Imaging plasmolysis and turgor recovery

Petri dishes with siphons of *V. erythrospora* immobilized on glass slides were exposed to hyperosmotic stress (as described above) under different $Na^+$ concentrations (1mM-100 mM). The Petri dishes were mounted on a Zeiss IM 35 inverted microscope (Carl Zeiss, Jena, Germany) and micrographs of different stages of turgor recovery were observed using a Nikon E5400 camera using a 10x objective lens (Nikon Corporation, Tokyo, Japan).

### 4.2.7. Metabolic profiling under hyperosmotic stress

The protocol used for metabolic profiling was based on one previously used for plant cells (Lisec et al. 2006). Two week old surface growths of *V. erythrospora* on Petri dishes with agarised f/2 medium were subjected to a hyperosmotic shock of - 0.2 MPa (provided by NaCl as above). Siphons were gently removed from different Petri dishes, 0, 15, 30, 45, 60, 75 and 90 min after applying the shock. They were then snap frozen with liquid nitrogen and transferred to 2 ml Eppendorf tubes and weighed. The samples were then homogenized after adding 1 ml 100% methanol (pre-cooled at - 20 °C) for enzyme inactivation and mixed at 70 °C for 10 min in a thermomixer (Thermomixer 5436, Eppendorf, Hamburg, Germany) at 950 rpm. This was followed by centrifugation for 10 min at 11,000 rpm. The supernatant was then subjected to a 1:2 chloroform : distilled water extraction and centrifuged at 3,200 rpm. The polar phase (water soluble metabolites) was concentrated overnight in a vacuum concentrator (Savant$^{TM}$ SPD131DDA SpeedVac$^{TM}$ Concentrator, Thermo Fisher Scientific, Wltham, MA, USA) without any heating. For derivatization, 40 µl of methoxyamine hydrochloride (Sigma Aldrich; 20 mg $ml^{-1}$) was added and mixed at 37 °C in the thermomixer for 2 h at 950 rpm.

Then, 70 µl of *N*-methyl-*N*-(trimethylsilyl) trifluoroacetamide (MSTFA reagent; Sigma Aldrich) was added followed by mixing at 37 °C for 30 min. For standard curves, samples of commercially available compounds (obtained from Sigma Aldrich) were prepared at concentrations ranging from 1 mM–10 µM, in the same way as the biological samples as described below.

The derivatized samples were then transferred to autosampler vials and analysed on a QP2010 Plus GC-MS (Shimadzu Corp., Kyoto, Japan). One µl of each sample was injected at 150 °C with a linear velocity control of 37.5 cm $sec^{-1}$. The split ratio on injection was kept at 50 : 1 for a lower concentration run and 700 : 1 for a higher concentration run (to get a dynamic range of concentrations). Chromatography was performed with an Rxi-5ms fused silica column – 30 m long, 0.25 mm internal diameter, 0.25 µm film thickness (Restex Corp., Bellefonte, PA, USA). The temperature was kept isothermal for 2 min at 80 °C, followed by a 15 °C $min^{-1}$ increase to 300 °C. It was then held at 300 °C for 8 s. Both ion source and interface temperatures were set at 250 °C. The recorded mass range was between 50–550 m/z at 20 scans $s^{-1}$. Post run analysis was performed using the GCMSsolution software (Shimadzu Corp., Kyoto, Japan). Chromatographic peaks were identified using the NIST library. Areas under the peaks were estimated for the different compounds in the samples and concentrations were calculated using standard curves.

## 4.3. Results

### 4.3.1. The effect of ion channel inhibitors on turgor recovery

To investigate the possible role of ion movements in turgor recovery after a hyperosmotic shock, *V. erythrospora* siphons were exposed to different concentrations of $Gd^{3+}$, TEA, verapamil and orthovanadate in the hyperosmotic solution. Turgor recovery showed a dose-dependent sensitivity to $Gd^{3+}$ (Fig 4.2) and TEA (Fig. 4.3). At a concentration of 10 µM,

$Gd^{3+}$ did not have any effect on the turgor recovery of the siphons. After dropping from an initial value of 0.75 ± 0.08 MPa (mean ± SD, n = 5; range: 0.66–0.87 MPa) to 0.28 ± 0.06 MPa (mean ± SD, n = 5; range: 0.21–0.35 MPa), turgor recovery started after 15 min and recovered completely within 50 min in all experiments (Fig 4.2 A). On exposure to 50 µM $Gd^{3+}$, turgor recovery was inhibited in a few experiments (two out of seven experiments; Fig. 4.2 B), with turgor dropping from 0.82 ± 0.18 MPa (mean ± SD, n = 5; range: 0.98–0.51 MPa) to 0.28 ± 0.05 MPa (mean ± SD, n = 5; range: 0.16–0.31 MPa). At the highest concentration of $Gd^{3+}$ tested (100 µM), turgor recovery was inhibited in five of six experiments. In the experiments where inhibition occurred, turgor dropped from 0.77 ± 0.15 MPa (mean ± SD, n = 5; range: 0.43–0.92 MPa) to 0.24 ± 0.12 MPa (mean ± SD, n = 5; range: 0.12–0.41) and did not recover within 60 min.

Turgor recovery was observed within 50 min in all experiments where siphons were exposed to 10 mM TEA (Fig. 4.3 A). However, recovery was inhibited in six of seven experiments at 50 mM TEA (Fig 4.3 B). In those experiments where recovery was inhibited turgor dropped from an initial value of 0.85 ± 0.15 MPa (mean ± SD, n = 6; range: 0.66–1.06 MPa) to 0.32 ± 0.05 MPa (mean ± SD, n = 6; range: 0.26–0.46 MPa) and did not recover within 60 min.

Turgor recovery was also inhibited by orthovanadate (Fig 4.4 A) and verapamil (Fig. 4.4. B). On exposure to 1 mM orthovanadate, turgor dropped from 0.85 ± 0.20 MPa (mean ± SD, n=7; range: 0.47–1.05 MPa) to 0.25 ± 0.12 MPa (mean ± SD, n=7; range: 0.12–0.49 MPa). Similarly, on exposure to 10 µM verapamil, turgor dropped from 1.02 ± 0.17 MPa (mean ± SD, n=6; range: 0.83–1.24 MPa) to 0.32 ± 0.05 MPa (mean ± SD, n=6; range: 0.24–0.37). Turgor did not recover within 60 min under both treatments.

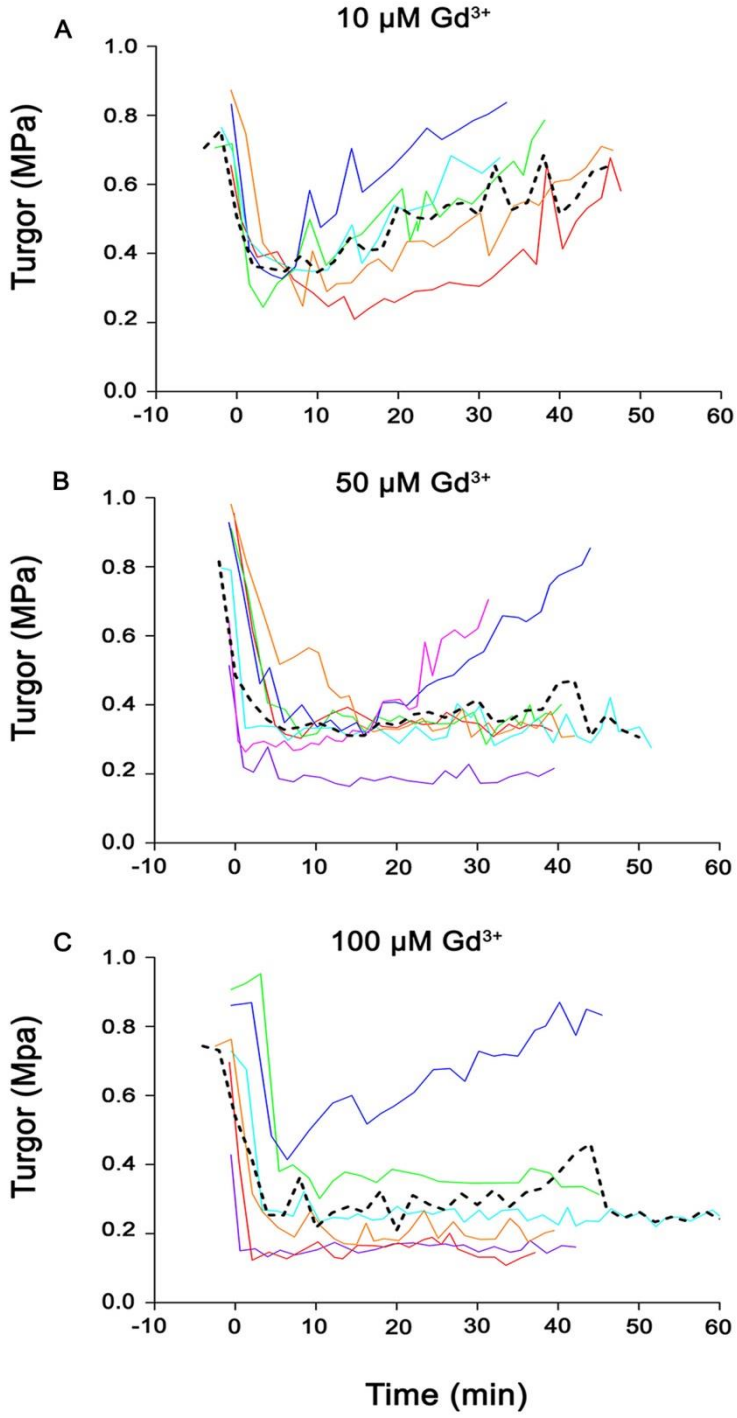


**Figure 4.2.** The effect of $Gd^{3+}$ on turgor recovery in *Vaucheria erythrospora* after a hyperosmotic shock of - 0.2 MPa, generated by adding different concentrations of $Gd^{3+}$ to the hyperosmotic solution made up with NaCl. The graphs represent direct measurements of turgor (MPa) plotted against time relative to the osmotic shock (min). Each coloured line represents a series of measurements from a single siphon. Individual measurements were taken at 1 min intervals. The black dotted line in each graph is the trend line calculated as a moving average of turgor values from all experiments at a particular time point for each concentration. Turgor recovery was inhibited by 50 and 100 µM $Gd^{3+}$, as indicated by the observation that turgor did not return toward its original value after the initial drop.

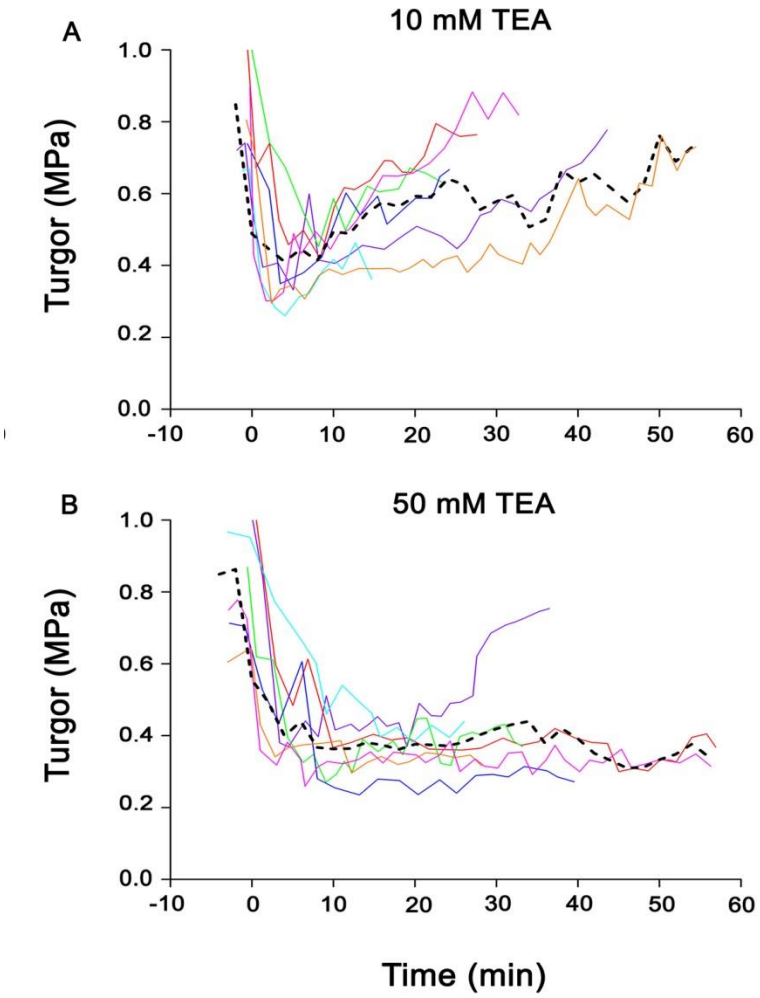


**Figure 4.3.** The effect of TEA on turgor recovery in *Vaucheria erythrospora* after a hyperosmotic shock of - 0.2 MPa, generated by adding different concentrations of TEA to the hyperosmotic solution made up with NaCl. The graphs represent direct measurements of turgor (MPa) plotted against time relative to the osmotic shock (min). Each coloured line represents a series of measurements from a single siphon. Individual measurements were taken at 1 min intervals. The black dotted line in each graph is the trend line calculated as a moving average of turgor values from all experiments at a particular time point for each concentration. Turgor recovery was inhibited by 50 mM TEA, as indicated by the observation that turgor did not return toward its original value after the initial drop.

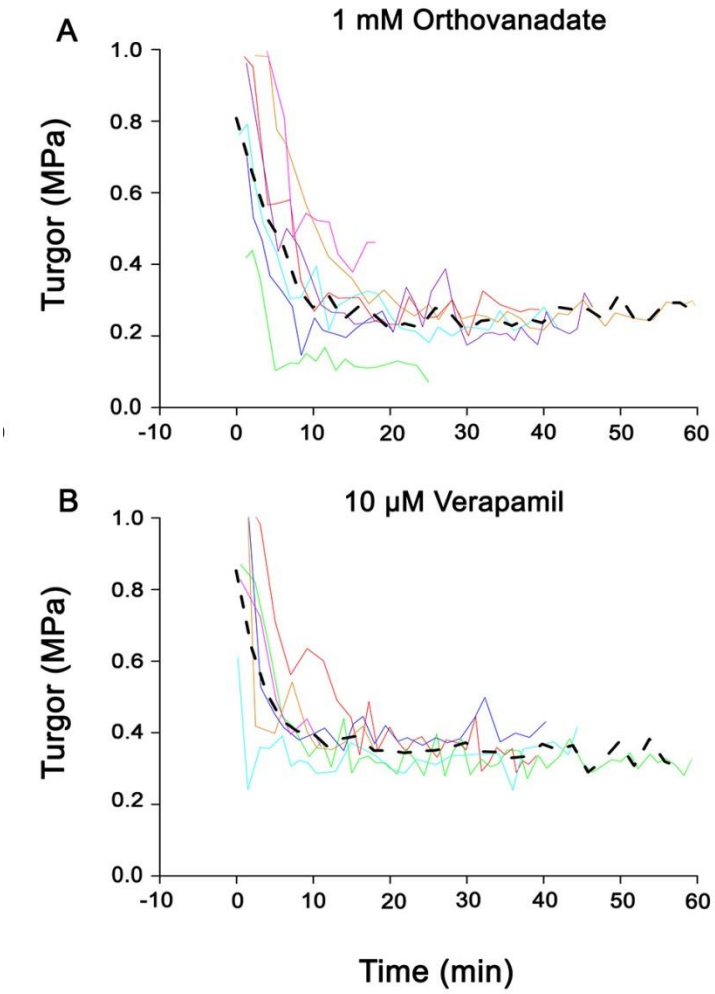


**Figure 4.4.** The effect 1 mM orthovanadate (A) and 10 µM verapamil (B) on turgor recovery in *Vaucheria erythrospora* after a hyperosmotic shock of - 0.2 MPa, generated by adding these concentrations of orthovanadate and verapamil to the hyperosmotic solution made up with NaCl. The graphs represent direct measurements of turgor (MPa) plotted against time relative to the osmotic shock (min). Each coloured line represents a series of measurements from a single siphon. Individual measurements were taken at 1 min intervals. The black dotted line in each graph is the trend line calculated as a moving average of turgor values from all experiments at a particular time point for each concentration. Turgor recovery was inhibited under both these treatments as indicated by the observation that turgor did not return toward its original value after the initial drop.

### 4.3.2. Net $K^+$ and $Na^+$ flux kinetics

The results described in 4.3.1 suggest the importance of membrane transport proteins and thus ion movements in the recovery of turgor after a hyperosmotic shock. Given this, ion fluxes and membrane potentials were investigated using the MIFE technique.

Net flux kinetics were first estimated under an ionic hyperosmotic shock imposed by NaCl (-0.6 MPa). There was an increased efflux of $K^+$ under NaCl hyperosmotic stress, with the net flux changing from - 0.48 ± 8.81 nmol $m^{-2}$ $s^{-1}$ before stress to - 9.79 ± 13.9 nmol $m^{-2}$ $s^{-1}$ (mean ± SE, n= 5) within 30 min after stress (Fig. 4.5 A and B). Sodium fluxes could not be resolved in these experiments because of the high NaCl concentration in the bathing solution and the hyperosmotic solution (a total concentration of 250 mM).

To enable resolution of $Na^+$ fluxes under hyperosmotic stress, the siphons were instead treated with a 220 mM sorbitol stress in a bathing solution with low $Na^+$ (1mM). This provided the same stress as 150 mM NaCl (~ - 0.6 MPa). Immediately upon exposure to the hyperosmotic sorbitol solution, an uptake of $K^+$ was observed, in contrast to the efflux that was observed under NaCl stress (Fig. 4.6 A and B). The net $K^+$ flux changed from - 14.88 ± 1.62 nmol $m^{-2}$ $s^{-1}$ before stress to 14.906 ± 2.01 nmol $m^{-2}$ $s^{-1}$ (mean ± SD, n=7) after. Also, there was $Na^+$ uptake, with the net flux changing from - 23.18 ± 1.2 nmol $m^{-2}$ $s^{-1}$ before stress to 6.66 ± 1.98 nmol $m^{-2}$ $s^{-1}$ (mean ± SE, n=7) within 30 min after stress (Fig 4.6 C and D).

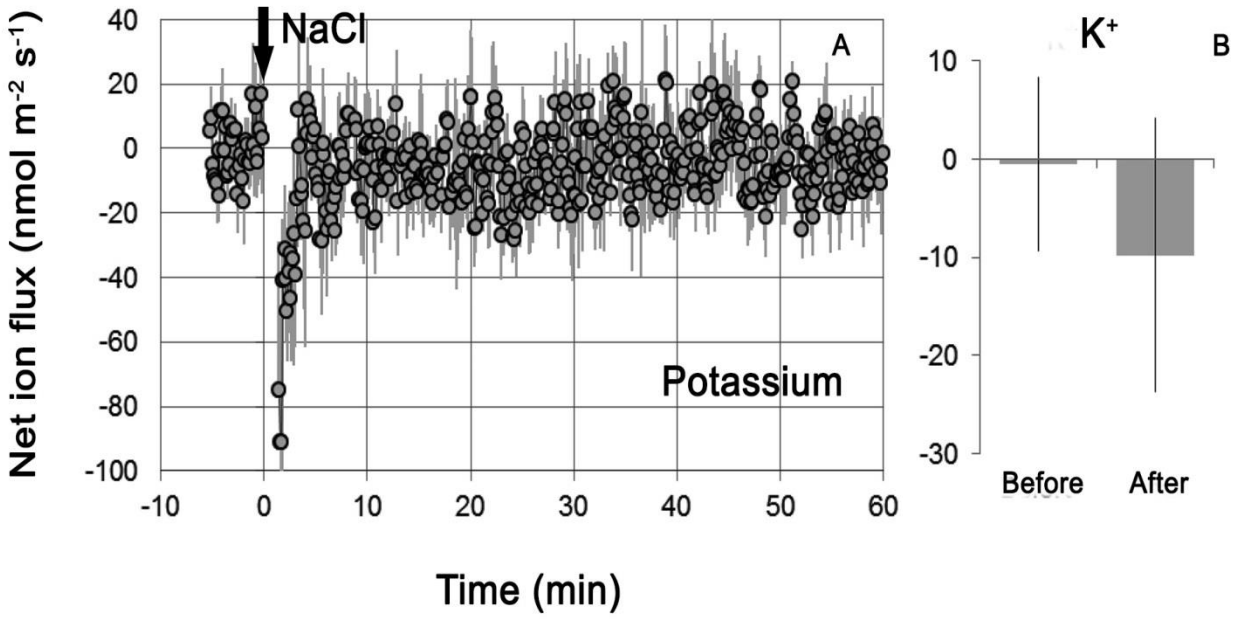


**Figure 4.5.** $K^+$ fluxes of *Vaucheria erythrospora* in response to NaCl hyperosmotic challenge. A- Net $K^+$ flux kinetics measured under a - 0.6 MPa shock provided by 150 mM NaCl. Siphons were grown and measured under high sodium (100 mM) conditions. B- Net average $K^+$ fluxes over a 30 min period before and after hyperosmotic challenge. Mean ± SE (n = 5 siphons).

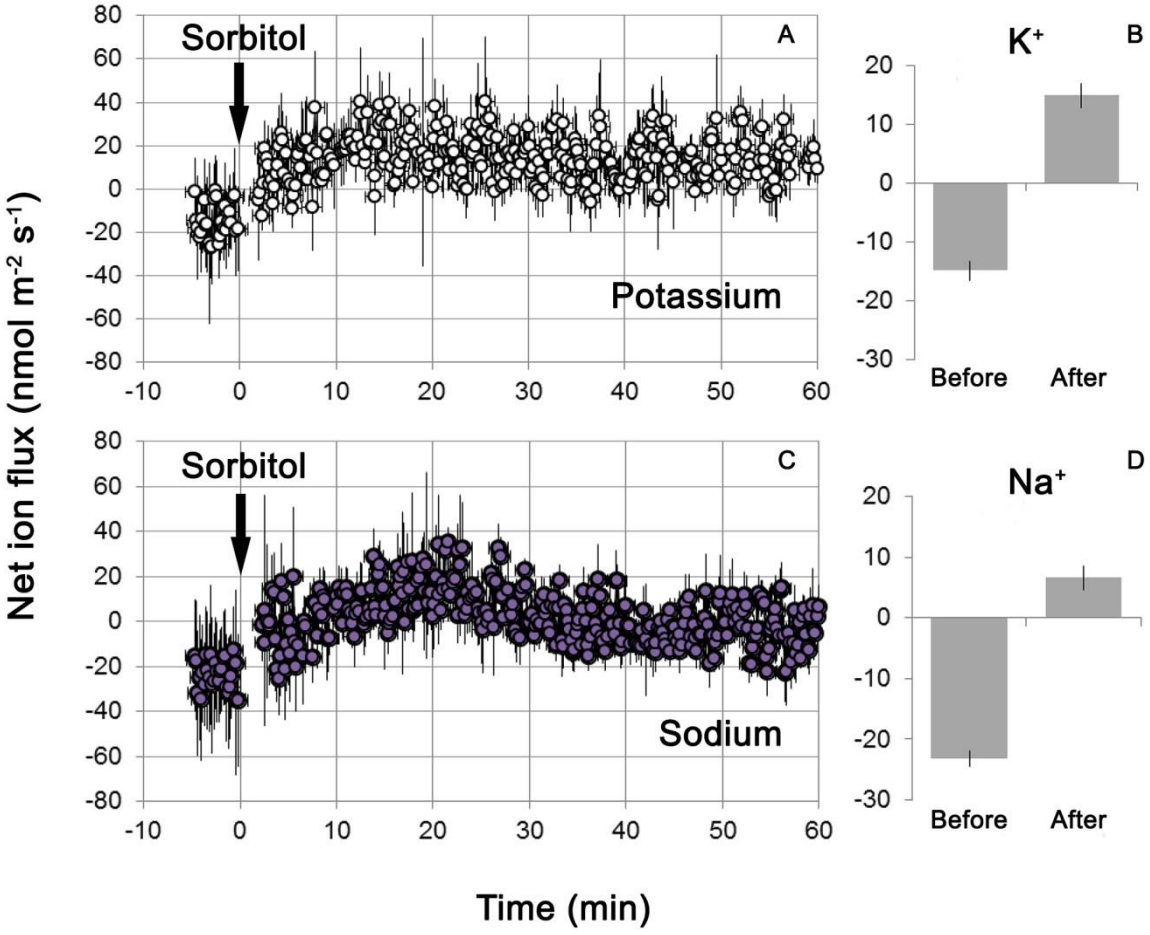


**Figure 4.6.** Ion fluxes of *Vaucheria erythrospora* in response to sorbitol hyperosmotic challenge. A and C- Net flux kinetics of $K^+$ and $Na^+$ measured under a - 0.6 MPa shock provided by 220 mM sorbitol. Siphons were transferred to low (1 mM) sodium conditions 1h prior to measurements to enable resolution of net $Na^+$ fluxes. B and D- Net average fluxes of $K^+$ and $Na^+$ over a 30 min period before and after hyperosmotic challenge. Mean ± SE (n = 7 siphons).

### 4.3.3. Effect of external $Na^+$ concentration and amiloride on net $Na^+$ fluxes

The results described in 4.3.1 suggests that $Na^+$ was taken up both in response to sorbitol hyperosmotic shock (discussed in later sections). To estimate how much of this $Na^+$ remains in the cytosol and how much of it is sequestered possibly in the vacuole, the cytosolic $Na^+$ concentration was estimated under control conditions.

For this, siphons were subjected to stepwise increases in $Na^+$ concentration (as described in the methods). As siphons were transferred from a high $Na^+$ environment (100mM) to a low $Na^+$ environment (100 µM), $Na^+$ ions moved out of the cytosol, down a concentration gradient. This translated into an efflux of - 61.16 nmol $m^{-2}$ $s^{-1}$ (mean ± SE, n=5; Fig 4.7 A and B). Efflux reduced to - 13.83 ± 10.80 nmol $m^{-2}$ $s^{-1}$ following an increase in external $Na^+$ concentration to 150 µM. After a further increase to 200 µM $Na^+$, net $Na^+$ flux was found to be almost zero. Increasing $Na^+$ influx was observed at 500 µM and 1000 µM external $Na^+$. In experiments where siphons were treated with 0.5 mM amiloride, flux reversal, i.e., the change from efflux to influx, occurred at a higher $Na^+$ concentration of about 300 µM compared to 200 µM in the absence of amiloride (Fig. 4.8 A).

Net $Na^+$ fluxes were also measured from siphons incubated for 30 min under a constant external $Na^+$ concentration of 1000 µM, both in the presence or absence of 0.5 mM amiloride (Fig 4.8). The control siphons (no amiloride) showed a $Na^+$ influx of 57.05 ± 11.66 nmol $m^{-2}$ $s^{-1}$ (mean ± SE, n= 21). In contrast, a significant efflux of - 80.06 ± 22.84 nmol $m^{-2}$ $s^{-1}$ (mean ± SE, n=16) was observed in siphons that were treated with amiloride.

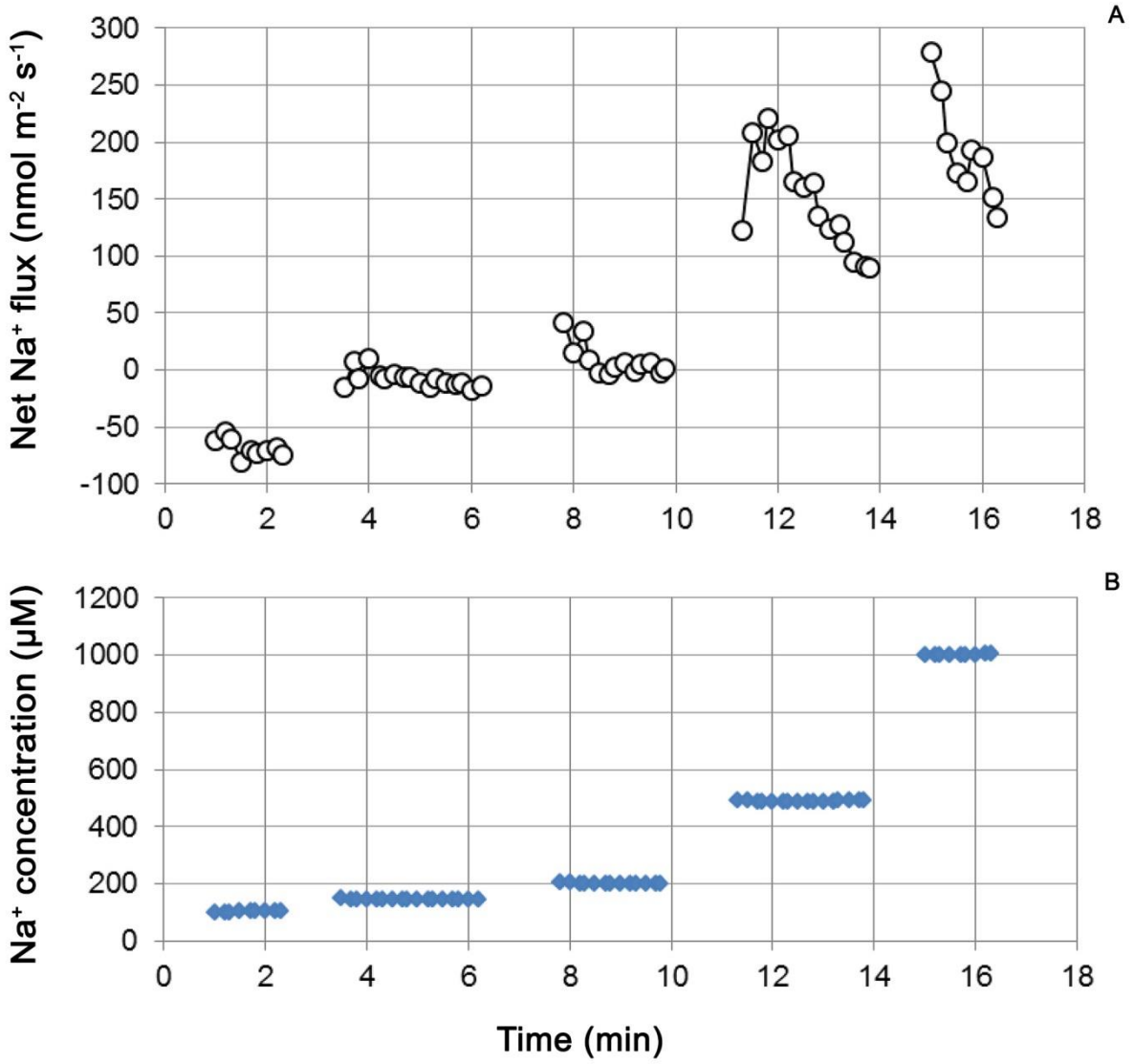


**Figure 4.7.** $Na^+$ fluxes in *Vaucheria erythrospora*. A - Net $Na^+$ fluxes measured in response to the step-wise increase in external $Na^+$ concentrations (depicted in B). One (of four) typical examples are shown. Net zero $Na^+$ flux is observed at external $Na^+$ of around 200 µM.

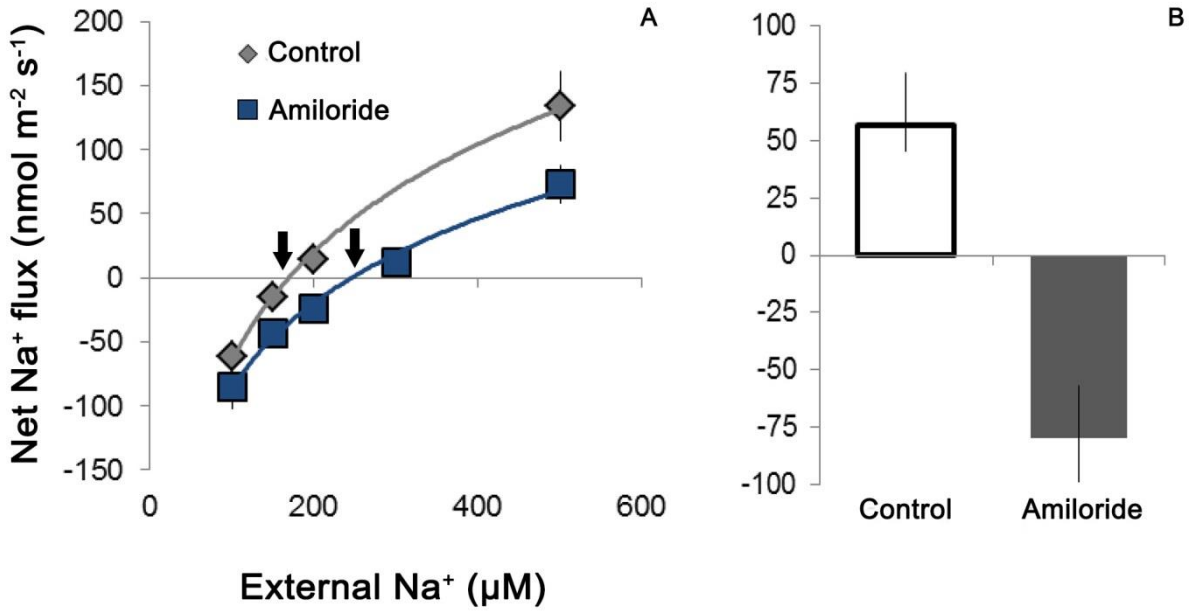


**Figure 4.8.** A - Dose-dependency of net $Na^+$ fluxes in the presence (blue line) and absence of amiloride (grey line). Arrows in the figure indicate external $Na^+$ concentrations at which flux reversal occurs. Mean ± SE (n = 4-5). B - Effect of amiloride treatment (0.5 mM) on mean net $Na^+$ fluxes measured from siphons incubated in 1mM NaCl solution. Mean ± SE (n = 16 to 21).

### 4.3.4. Membrane potential under hyperosmotic stress

Membrane potential ($E_m$) recordings were made to study how this may change due to hyperosmotic stress. Adding 100 mM NaCl to the external solution led to a depolarization (i.e. moving to a less negative $E_m$) of $E_m$ to - 20 mV (Fig 4.9 A), followed by repolarization (i.e. moving to to a more negative $E_m$). The $E_m$ continued to repolarize before settling at a steady value of - 65 ± 13.5 mV within 15–20 min. In contrast, exposure to an iso-osmotic solution of sorbitol (170 mM) led to hyperpolarization of $E_m$ by 5 mV, followed by rapid depolarization back to the original $E_m$ value within 10 min (Fig 4.9 B). No significant difference in the steady state $E_m$ values was found in siphons exposed to varying $Na^+$ concentrations of 200 µM and 1 mM (- 104 ± 5 mV and - 106 ± 3.5 mV respectively; Fig 4.9 C). In siphons treated with amiloride (0.5 mM), $E_m$ was slightly lower at - 97.5 ± 6 mV.

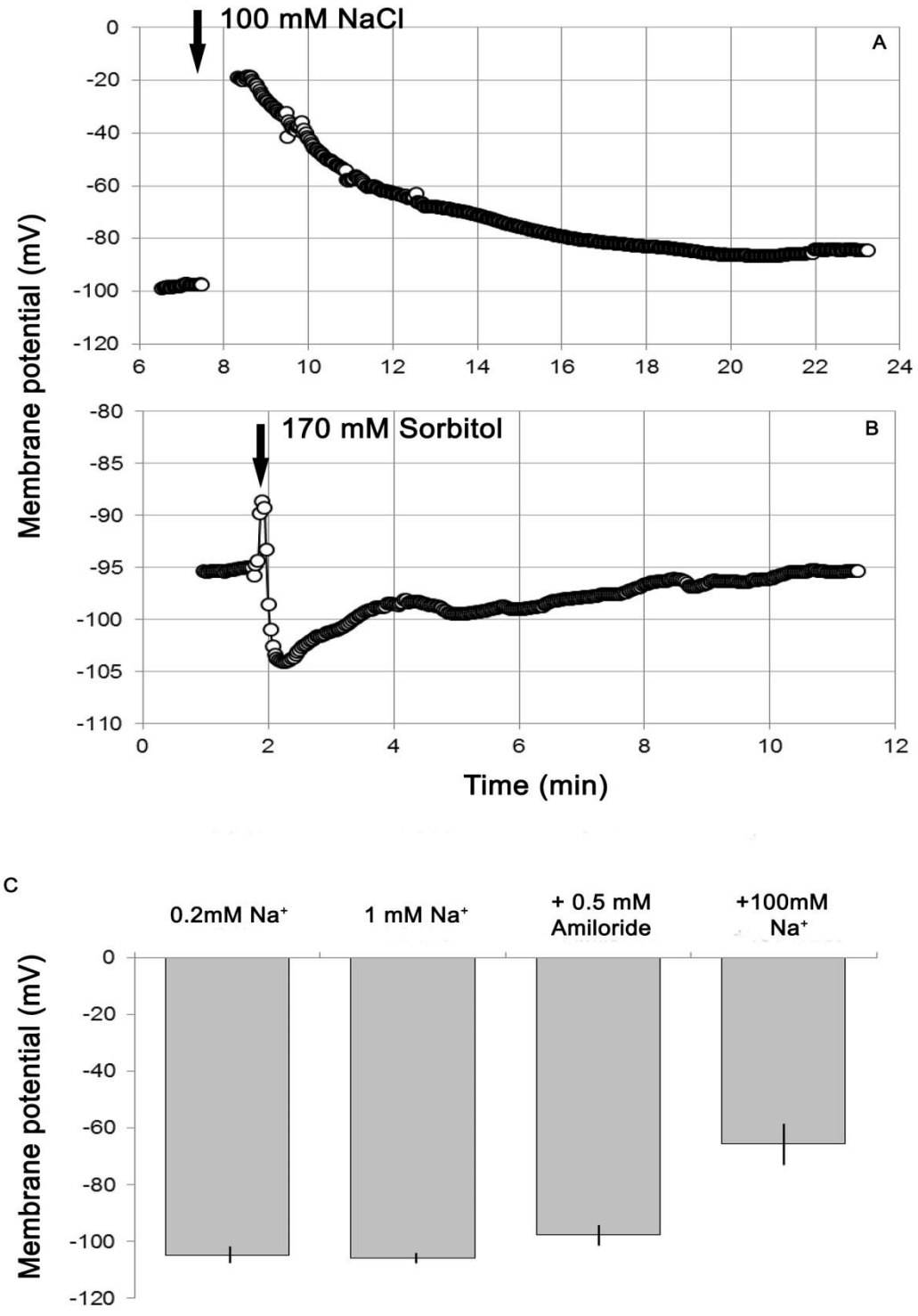


**Figure 4.9.** Membrane potential of *Vaucheria erythrospora* siphons. A and B - Kinetics of membrane potential changes in response to hyperosmotic NaCl and sorbitol challenge. One (of 4) typical examples is shown. C - Steady-state membrane potential values for cells exposed to different amount of $Na^+$. Mean ± SE; n= 4 for each treatment.

### 4.3.5. Turgor recovery at varying external $Na^+$

To study if external $Na^+$ concentration had an impact on turgor recovery in response to a -0.6 MPa hyperosmotic shock, *Vaucheria* siphons were imaged at 1mM, 10 mM and 100 mM $Na^+$. The hyperosmotic shock caused visible plasmolysis. Turgor recovery as indicated by deplasmolysis was complete within 360 min in the presence of 1mM NaCl (Fig. 4.10), 90 min in the presence of 10 mM NaCl (Fig. 4.11) and 60 min in the presence of 100mM NaCl (Fig. 4.12).

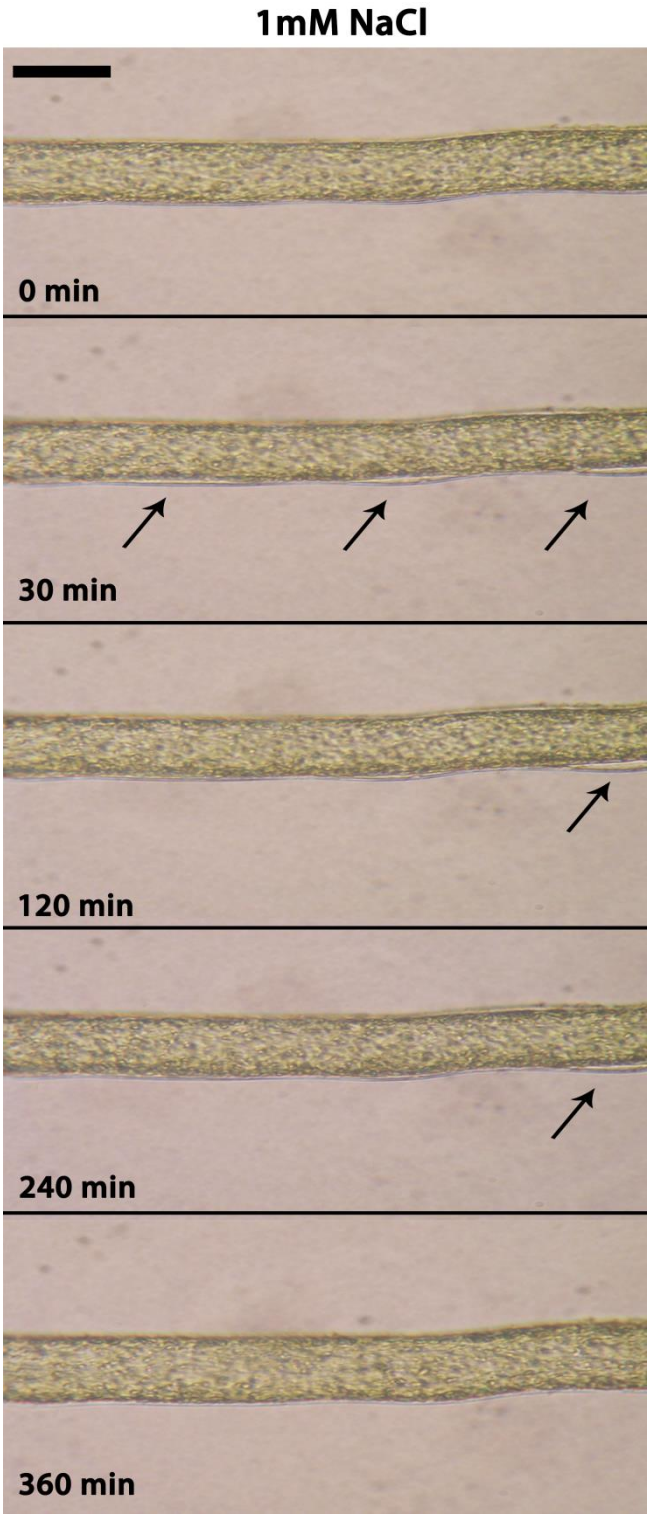


**Figure 4.10.** Micrographs of *Vaucheria erythrospora* siphons at external 1 mM external $Na^+$ concentration in response to a -0.6 MPa hyperosmotic shock. Turgor recovery was observed within 360 min as indicated by visible deplasmolysis following plasmolysis (arrows) induced by the hyperosmotic shock. Bar = 50 µm.

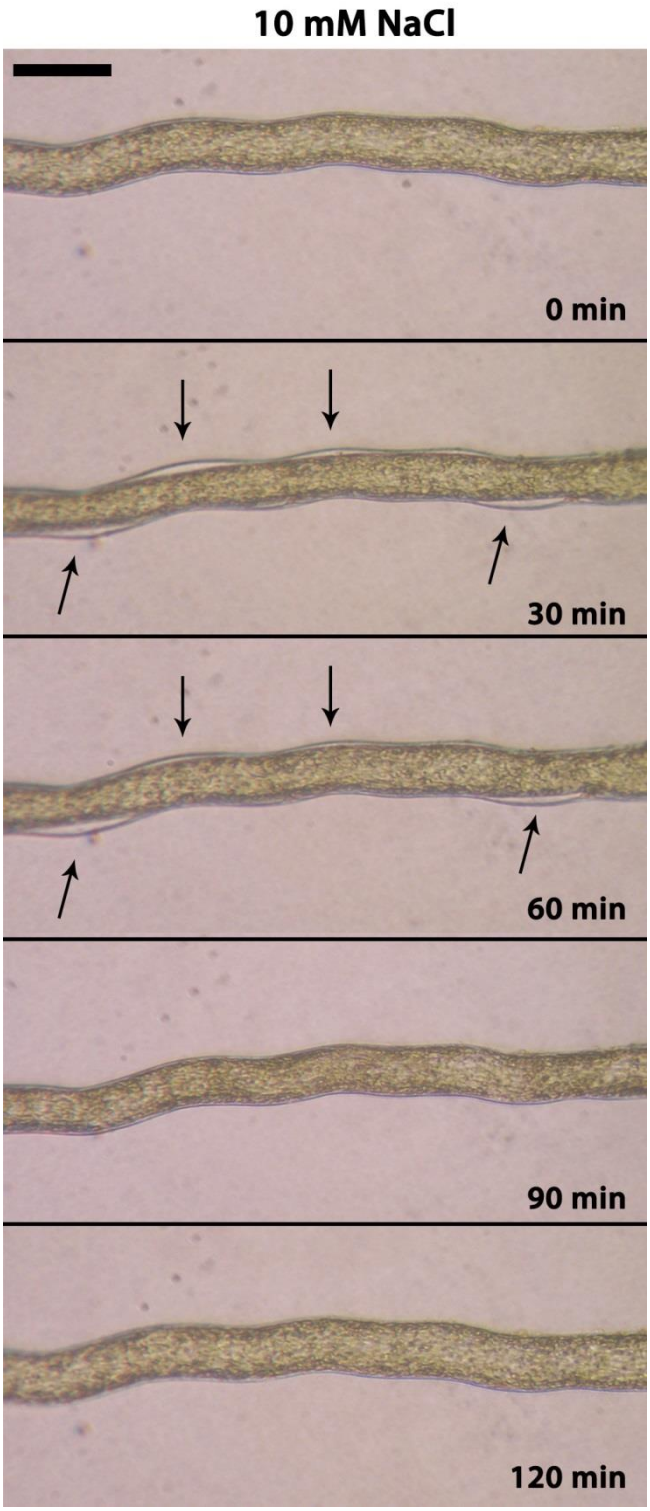


**Figure 4.11.** Micrographs of *Vaucheria erythrospora* siphons at external 10 mM external $Na^+$ concentration in response to a -0.6 MPa hyperosmotic shock. Turgor recovery was observed within 120 min as indicated by visible deplasmolysis following plasmolysis (arrows) induced by the hyperosmotic shock. Bar = 50 µm.

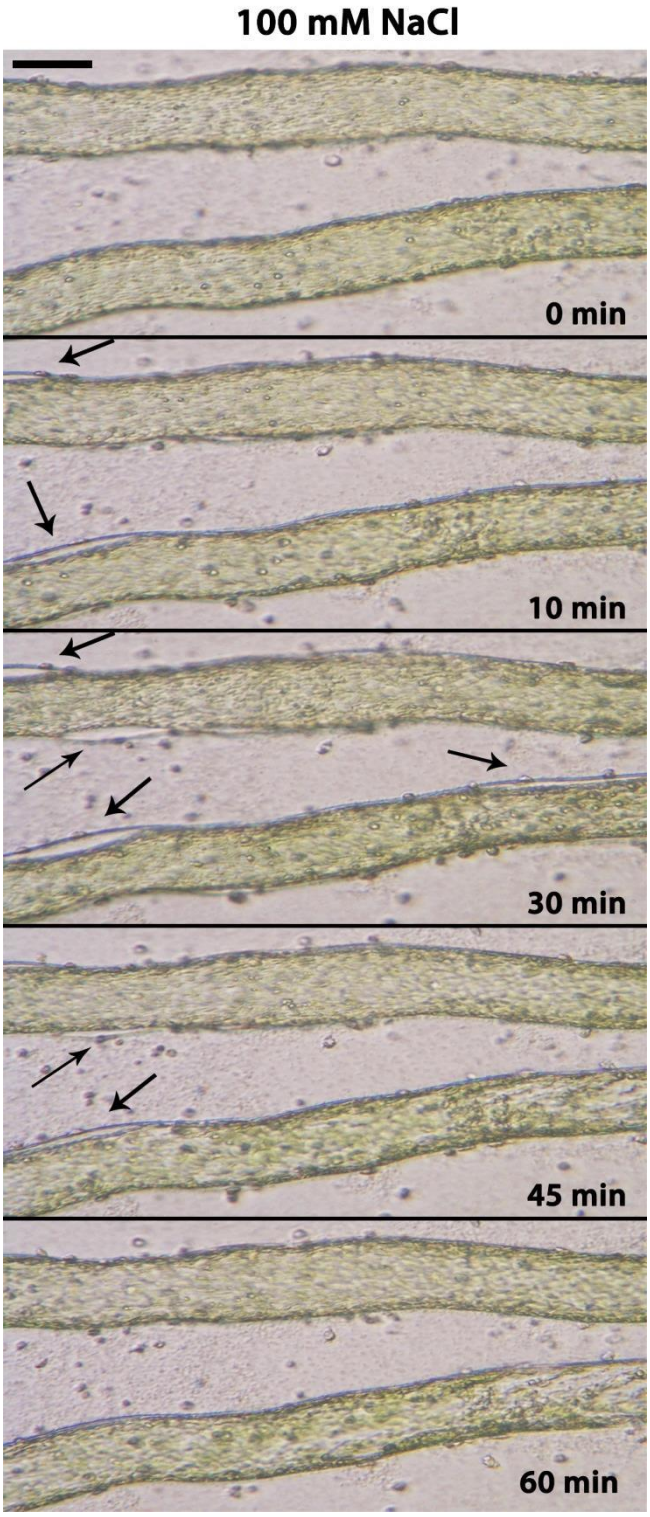


**Figure 4.12.** Micrographs of *Vaucheria erythrospora* siphons at external 100 mM external $Na^+$ concentration in response to a -0.6 MPa hyperosmotic shock. Turgor recovery was observed within 60 min as indicated by visible deplasmolysis following plasmolysis (arrows) induced by the hyperosmotic shock. Bar = 50 µm.

### 4.3.6. Metabolic profiles under hyperosmotic stress

The results described above suggest a role for the uptake of ions in turgor regulation after a hyperosmotic shock. The concentrations of four organic osmolytes were measured at various stages after a hyperosmotic shock to see if they may play a complementary role in the process.

Four compounds were identified from the metabolic profiling of the alga in response to NaCl shock (- 0.2 MPa). These were- glycerol, sorbitol/D-glucitol, L- proline and maltose. These compounds were detected both before and after exposure to NaCl shock with no significant change in concentration over 90 min after stress (Fig 4.13). There was a large variation in concentrations of replicates of the same compounds, which resulted in large error values. The concentrations of maltose were the highest at 407.1 ± 220.85 μM (mean ± SD, n= 10; range: 125–770 μM) before stress and 430.19 ± 144.37 μM (mean ± SD, n= 10; range: 259–608 μM) 90 min after stress (Fig. 4.13 D). Sorbitol was at the lowest concentrations (Fig 4.13 C) – 0.58 ± 0.25 μM (mean ± SD, n= 10; range: 0.19–0.98 μM) before stress and 1.28 ± 1.19 μM (mean ± SD, n= 10; range: 0.29–3.51 μM).

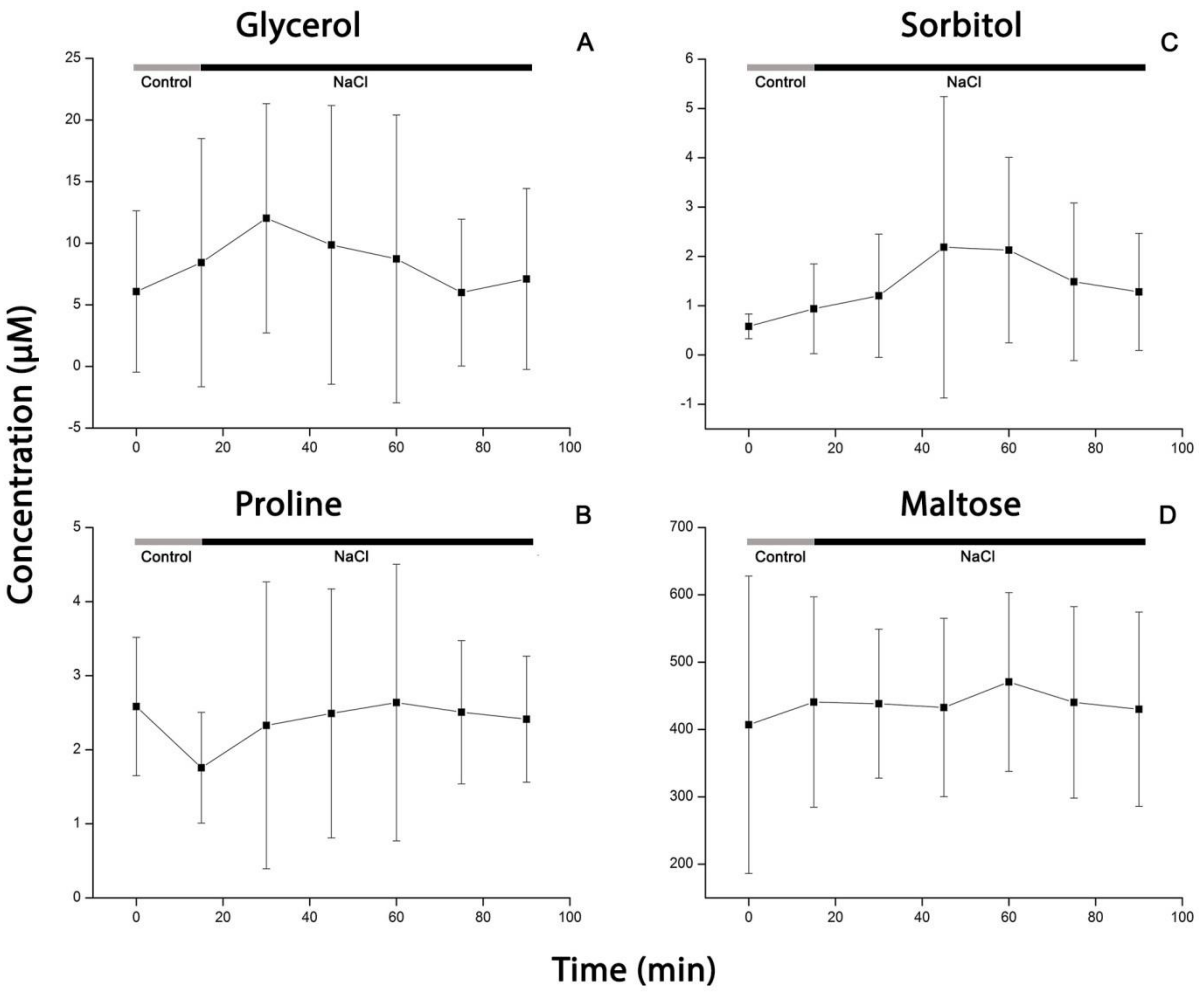


**Figure 4.13.** Concentrations of polar metabolites in response to hyperosmotic stress provided by NaCl. Changes in glycerol (A), proline (B), sorbitol (C) and maltose (D) 15- 90 min after hyperosmotic stress. Mean ± SD; n= 10.

## 4.4. Discussion

This study reports on the mechanisms underlying turgor regulation after a hyperosmotic shock in the estuarine alga *Vaucheria erythrospora*. Investigations have focused on the involvement of both ion uptake and organic osmolyte synthesis.

### 4.4.1. Turgor recovery after NaCl-induced hyperosmotic shock

#### 4.4.1.1. Changes in $E_m$

Under NaCl shock, the $E_m$ initially depolarized by ~ 80 mV to -20 mV in *V. erythrospora* followed by a repolarization (Fig 4.9). After 20 min of repolarization, the $E_m$ recovered to ~ -80 mV. This is similar to responses of the siphonous green alga, *Ventricaria ventricosa*, which also regulates turgor (Bisson and Beilby 2002; Bisson et al. 2006). The characean algae exhibit different responses to NaCl shock. A rapid transient hyperpolarization of ~ 50 mV has been reported in the euryhaline *Chara longifolia* (Hoffmann and Bisson 1988). Rapid hyperpolarization followed by depolarization has also been reported in the closely related euryhaline characean *Lamprothamnium succinctum* (Okazaki et al. 1984; Al Khazaaly and Beilby 2007). Other studies have reported contradictory results. In *L. succintum*, an initial depolarization of $E_m$ for the first 10 min was followed by hyperpolarization by 20 mV (Reid et al. 1984) whereas Bisson and Kirst (1980) found variable responses , with some cells exhibiting depolarization of $E_m$ and others hyperpolarization under NaCl shock.

#### 4.4.1.2. Depolarization phase

It is possible that the rapid depolarization observed in this study (80mV; Fig. 4.9 A) may be due to a passive influx of $Na^+$ into the cytosol through nonselective cation channels (NSCC). While $Na^+$ fluxes after a hyperosmotic shock with NaCl could not be measured, a dose dependant inhibition of turgor recovery by $Gd^{3+}$ has been demonstrated (50 and 100 µM; Fig.

4.2), which is an inhibitor of NSCCs (Demidchik and Tester 2002). This is consistent with $Na^+$ uptake through these channels being involved in turgor recovery after NaCl shock. NSCCs are known to be major routes for $Na^+$ uptake in green algae and higher plants (Tyerman et al. 1997; Demidchik et al. 2002; Demidchik and Maathuis 2007; Amtmann and Beilby 2010). Based on this, the inhibition of turgor recovery in our experiments could be due to the inhibition of $Na^+$ uptake through NSCC, considering that $Na^+$ uptake was shown to be the major contributor to cell turgor in a marine species of the stramenopile *Thraustochytrium* (Shabala et al. 2009).

#### 4.4.1.3. Repolarization phase

The repolarization of $E_m$ observed in our experiments (to -80 mV; Fig. 4.9 A) could be due to increased activity of the $H^+$-ATPase. This is based on the observed inhibition of turgor recovery in siphons treated with orthovanadate (1mM; Fig. 4.4 A) an inhibitor of the $H^+$-ATPase. Increased proton pumping under NaCl hyperosmotic shock has been reported in both *C. longifolia* and *L. succinctum* (Yao et al. 1992; Bisson and Shepherd 2001; Beilby et al. 2006; Al Khazaaly and Beilby 2007; Amtmann and Beilby 2010). This process has been studied in detail in *L. succinctum* which responds to a decrease in turgor and increase in external $Na^+$ by pumping protons out of the cytosol at a greater rate to compensate for the depolarization caused by $Na^+$ entry, thus maintaining a negative $E_m$ (Al Khazaaly and Beilby 2007; Amtmann and Beilby 2010). Vanadate-sensitive $H^+$ efflux under NaCl shock has also been reported in both glycophyte and halophyte plants using the MIFE technique (Shabala and Bose 2012).

Anion ($Cl^-$) uptake could also be involved in the repolarization of $E_m$ in *V. erythrospora*. The electrochemical gradient generated by the $H^+$-ATPase has been shown to drive transport of

ions through channels and transporters (Michelet and Boutry 1995). For example, this gradient may be used to drive uptake of $Cl^-$ through a $H^+/Cl^-$ symporter. $H^+/Cl^-$ symporters moving one or two protons per $Cl^-$ ion have been reported in both euryhaline characean algae and higher plant cells (Hoffmann and Bisson 1988; Felle 1994; Shabala and Lew 2002). Other pathways for entry of $Cl^-$ could be through depolarization activated or $Ca^{2+}$-dependant $Cl^-$ channels like the ones known to operate in characean algae (Teakle & Tyerman 2010). This would lead to balancing of positive charge generated by $Na^+$ entry and contribute to the repolarization. Due to time constraints $Cl^-$ fluxes were not measured in this study.

$K^+$ uptake contributes little to turgor recovery under NaCl-induced hyperosmotic shock in *V. erythrospora*. This is apparent from the $K^+$ flux recordings in response to a NaCl shock of -0.6 MPa (Fig. 4.5 A and B). An efflux of -10 nmol $m^{-2}$ $s^{-1}$ was observed over 30 min after administering the shock. The leakage of $K^+$ out of the cell due to exposure to high external NaCl has been well documented in higher plants and has also been reported in algae (Pottosin and Andjus 1994; Shabala et al. 2005; Bose et al. 2013; Jayakannan et al. 2013). This is thought to be brought about by the entry of $Na^+$ into the cell through NSCCs, leading to a depolarization of $E_m$ (reviewed in Shabala and Cuin 2008). This then leads to $K^+$ efflux through depolarization-activated, $K^+$ outward-rectifying channels (KORCs). The $K^+$ loss observed in this study (10 nmol $m^{-2}$ $s^{-1}$), was lower than that reported from all higher plants studied, aside from root epidermal cells of wheat (Fig. 4.5; Table 4.1). This low amount could be due to the activity of inward rectifying $K^+$ channels (KIRCs), counteracting the $K^+$ loss. This scenario is supported by the observation of the inhibition of turgor recovery under NaCl shock when siphons were treated with TEA (50 mM; Fig. 4.3 B), an inhibitor of $K^+$ channels (Blatt 1992). This suggests the possible role of net $K^+$ uptake, possibly through KIRCs, which is driven by $H^+$-ATPase-mediated hyperpolarization. KIRCs are major pathways for low-

affinity uptake of $K^+$ in plants and algae (Blatt 1992; Sauer et al. 1993; Cushman 2001). In the case of *V. erythrospora*, the $K^+$ loss through KORCs possibly masks the influx through KIRCs, leading to net $K^+$ efflux observed in our experiments. It should be noted that TEA has been reported to inhibit the aquaporin AQP1in humans, a major pathway mediating water flux (Detmers et al. 2006). A binding site for TEA in AQP1 was identified using molecular docking by Müller et al. (2008). This study also estimated a 50% reduction of water flux on exposure to TEA. This raises the question as to whether TEA also inhibits aquaporins in other systems. If this is the case, the inhibition of turgor recovery seen here could also be explained by reduced water fluxes.

**Table 4.1.** Comparison of NaCl stress-induced $K^+$ loss in *V. erythrospora* and in reports of higher plant tissues in the literature. The next lowest $K^+$ efflux values after *V. erythrospora* are seen in wheat root epidermal cells (bold).

| **Species** | **Tissue** | **NaCl stress (mM)** | **Average $K^+$ efflux over 30 min, (nmol $m^{-2}$ $s^{-1}$ )** | **Reference** |
|---|---|---|---|---|
| ***Vaucheria erythrospora*** | **Siphons** | **150** | **10*** | **This work** |
| Arabidopsis | Root epidermis | 50 | 450 | Shabala et al (2005) |
| | Root epidermis | 100 | 380 | Jayakannan et al (2013) |
| | Leaf mesophyll | 50 | 120 | Shabala et al (2006) |
| Barley | Root epidermis | 160 | 350 | Chen et al (2005) |
| | Leaf mesophyll | 20 | 260 | Shabala et al (2005) |
| **Wheat** | **Root epidermis** | **150** | **20** | **Cuin et al (2009)** |
| | Leaf mesophyll | 100 | 180 | Wu et al (2013) |
| Broad bean | Leaf mesophyll | 90 | 150 | Shabala (2000) |
| Maize | Root epidermis | 50 | 120 | Pandolfi et al (2010) |
| Quinoa | Root epidermis | 100 | 140 | Hariadi et al (2011) |
| Lucerne | Root epidermis | 80 | 300 | Smethurst et al (2008) |
| Poplar | Root epidermis | 50 | 70 | Sun et al (2009) |
| Cotton | Root epidermis | 150 | 300 | Li et al (2013) |

* Not significantly different from zero.

### 4.4.2. Turgor recovery after sorbitol-induced hyperosmotic shock

Experimental conditions necessitated the use of low external $Na^+$ conditions (1mM) in order to resolve $Na^+$ fluxes. Thus in addition to NaCl shock, experiments were carried out looking at the fluxes that follow a hyperosmotic shock imposed by sorbitol.

#### 4.4.2.1. Changes in $E_m$

The sorbitol-induced shock (~ 0.5 MPa) caused a hyperpolarization of $E_m$ by -20 mV, followed by a relatively rapid depolarization (of the order of several minutes) (Fig. 4.9 B; the initial depolarization seen in the trace in this figure is an artefact of adding the hyperosmotic solution). The $E_m$ returned to the resting membrane potential 10 min after the initial depolarization. This response is similar to that observed in both characean algae and higher plants (Shabala and Lew 2002; Al Khazaaly and Beilby 2010). In turgor regulating *Arabidopsis* roots which were exposed to the same hyperosmotic shock, $E_m$ only depolarized by 5 mV in 30 min after hyperpolarizing by -20 mV (Shabala and Lew 2002). The process takes longer in characean algae, for example in *L. succinctum* the maximum hyperpolarization by about -50 mV is achieved after 2 h (Al Khazaaly and Beilby 2007). In the turgor-regulating fungus *Neurospora crassa* a transient depolarization of $E_m$ lasting 2–3 min has been observed, followed by sustained hyperpolarization (Lew et al. 2004). The $E_m$ was found to recover to the level of the resting membrane potential in 10 min, as was the case in our study.

#### 4.4.2.2. Hyperpolarization phase

The hyperpolarization of $E_m$ may be indicative of $H^+$-ATPase activation, something which has been widely documented in algae, plants and fungi (Shabala and Lew 2002; Lew et al. 2004; Beilby et al. 2006). Because of the low concentration of $Na^+$ in the external solution,

the gradient for passive influx is lower, which is possibly why there was no observation of significant depolarization.

#### 4.4.2.3. Depolarization phase

Net flux kinetics recorded under sorbitol-induced hyperosmotic shock (-0.6 MPa) showed that there was increased uptake of both $Na^+$ and $K^+$ (~ 30 nmol $m^{-2}$ $s^{-1}$ for both ions; Fig. 4.6) 30 min after shock. The hyperpolarization caused by activation of the proton pump could contribute to depolarization by driving the $K^+$ influx, possibly through KIRCs. This is supported by our demonstration of inhibition of turgor recovery by $H^+$-ATPase and $K^+$ channel inhibitors (Fig. 4.4A, 4.3). Chloride uptake may also contribute to this depolarization. The pathways for $Cl^-$ and Na+ uptake are likely to be the same in response to hyperosmotic treatments with both NaCl and sorbitol. When exposed to sorbitol shock, a $Na^+$ gradient may be involved in driving passive uptake through NSCCs, but under these low $Na^+$ conditions this gradient would be lower. This could explain the slower repolarization observed here (Fig 4.10B) relative to the depolarization observed in response to NaCl shock (Fig. 4.10A).

### 4.4.3. The importance of $Na^+$

While uptake of both $Na^+$ and $K^+$ in *V. erythrospora*, turgor recovery was not complete within one hour under low $Na^+$ conditions (1mM $Na^+$). This was apparent as siphons were still visibly plasmolysed 1 h after adding sorbitol (Fig 4.10). In contrast, our turgor recovery experiments with the pressure probe showed that turgor recovered within 40 min under a - 0.2 MPa shock and within 60 min under a - 0.5 MPa shock (Chapter 3; Fig 3.7). Our net flux measurements under low $Na^+$ conditions also support the observation of slower recovery times. The major ions, $Na^+$, $K^+$ and $Cl^-$ (assuming that $Cl^-$ is taken up to counter both $Na^+$ and

$K^+$ uptake), were found to be taken up at 120 nmol $m^{-2}$ $s^{-1}$. Based on our model calculations of net flux measurements (Fig 4.14), we estimated that at this rate of influx, complete turgor recovery from a -0.6 MPa hyperosmotic shock would take about 5.6 h, assuming that recovery is mediated entirely by inorganic ion uptake.

The quicker recovery times in the turgor recovery experiments can be explained by the different conditions the alga was exposed to in these experiments. When using the pressure probe, siphons were in agarised f/2 medium and had a higher concentration of $Na^+$ (100mM) in the external medium compared to the 1mM $Na^+$ that was present in the flux experiments. Based on this, it was hypothesized that the recovery would be quicker under higher concentrations of $Na^+$ in the external solution. Micrographs of hyperosmotically stressed siphons exposed to increasing concentrations of $Na^+$ (1-100 mM) confirmed this (Fig. 4.10-4.12). Turgor recovered within 360 min, 90 min and 60 min in the presence of 100 mM, 10 mM and 1 mM $Na^+$ respectively. These results suggest that the speed of turgor recovery is directly related to the concentration of $Na^+$ in the external medium. $Na^+$ has been shown to be the chief contributor to turgor regulation in a marine species of the stramenopile *Thraustochytrium* but it is not indispensable as turgor regulation occurs, even in its absence, by the use of compatible solutes (Shabala et al. 2009).

## MODEL CALCULATIONS OF TURGOR RECOVERY TIME BASED ON FLUX MEASUREMENTS

Considering a segment of *Vaucheria* siphon 100 µm long and 40 µm in diameter

The surface area of this segment would be:

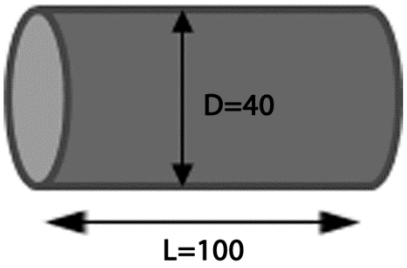


$S = 2 * \pi * R * L$, where R = 20 µm (radius)
$S = 2 * 3.14 * 20 * 100 = 1.25 * 10^4$ µm²
$S = 1.25 * 10^{-8}$ m²

The segment's volume would be:

$V = \pi * R^2 * L$
$V = 3.14 * 400 * 100 = 1.25 * 10^5$ µm³
$V = 1.25 * 10^{-13}$ m³

The relationship between total amount of accumulated ions (ΔN) in this segment and flux would be

$$\Delta N = \text{Flux} * \text{Surface Area} * \text{Time}$$

Hence,

$$\text{Flux} = \Delta N / (\text{Surface Area} * \text{Time})$$

According to van't Hoff's law, the relationship between ion accumulation and cell turgor is (Shabala, 2000):

$$\Delta\psi = \Delta N * R * T / V$$

Where R = 8.31 (universal gas constant); T = 296 K

Therefore,

$$\text{Flux} = \Delta\psi * V/(R*T*S*\text{Time})$$

Addition of 150 mM NaCl requires increase in cell turgor by ~ 0.6MPa, or $6*10^5$ Pa

Turgor recovery was observed in pressure probe experiments within 1h (Chapter 3; Fig. 3.7). Given this, the flux required for turgor recovery in 1 h (3600 s) would be:

Flux = $6 * 10^5 * 1.25 * 10^{-13}/(296 * 8.31 * 1.25 * 10^{-8} * 3600)$ mol m$^{-2}$ s$^{-1}$
Flux = 680 nmol m$^{-2}$ s$^{-1}$

Thus, to be able fully recover their turgor within 1 h by means of inorganic osmolytes, cells have to take up major ions ($Na^+$, $Cl^-$, and $K^+$) at the average rate of **680 nmol m$^{-2}$ s$^{-1}$**.

From the MIFE measurements in low-sodium conditions (Fig 4.6), the average increase in $Na^+$ and $K^+$ uptake is 30 nmol m$^{-2}$ s$^{-1}$ each

Assuming $Cl^-$ is also taken up as a counter ion to $Na^+$ and $K^+$, uptake would possible be double that amount. The total net ion flux would then be:
30 + 30+ 60 = **120 nmol m$^{-2}$ s$^{-1}$**

Thus, the approximate estimated time for this siphon segment to recover turgor in low external sodium (1 mM) conditions would be:

**680/120 = 5.6 h**

**Figure 4.14.** Model calculations for recovery of turgor on exposure to NaCl-induced hyperosmotic stress based on MIFE flux measurements. Based on flux experiments in low external $Na^+$ concentration (1mM; Fig. 4.6), we estimated that recovery would take 5.6 h.

$Na^+$ is likely to be an energetically cheap osmoticum for *V. erythrospora*, considering its abundance in the external environment. However, metabolically detrimental effects could be caused by a higher concentration of $Na^+$ over $K^+$ in the cytosol. $K^+$ is a major nutrient vital for various biochemical processes, e.g., balancing the negative charge of DNA and proteins and for enzyme activation (Maathuis and Amtmann 1999). Concentrations of $Na^+$ > 100 mM are thought to inhibit *in-vitro* protein synthesis which requires cytosolic $K^+$ concentrations of 100–150 mM (Blumwald et al. 2000). Because of their similar physicochemical structures, $Na^+$ is thought to compete for binding sites occupied by $K^+$, affecting crucial $K^+$- dependant metabolic processes (Maathuis and Amtmann 1999; Zhu 2003). Our flux data showed that a $Na^+$ flux reversal, i.e. change from efflux to influx, took place at an external $Na^+$ concentration of 200 µM. Based on this reversal flux value and the measurements of steady state $E_m$ (-100 to -145 mV), the internal cytosolic $Na^+$ concentration was estimated to be 20–30 mM. These results suggest that the alga is likely to be able to sequester $Na^+$ in its vacuole. This ability possibly enables the use of $Na^+$ for turgor regulation and could be a key determinant of its survival under the conditions of varying osmotic potential that would be found in an estuary. The large central vacuole, occupying most of the siphon, could possibly allow for accumulation of high concentrations of $Na^+$, keeping it below toxic levels in the cytosol. This process of vacuolar $Na^+$ compartmentalization could possibly be carried out by $Na^+/H^+$ antiporters (NHXs) in the tonoplast, powered by the electrochemical gradient generated by a vacuolar $H^+$-ATPase. $Na^+/H^+$ antiporter-mediated vacuolar $Na^+$ compartmentalization is thought to be important with respect to salt tolerance in higher plants (Blumwald et al. 2000; Flowers and Colmer 2008).

### 4.4.4. A possible plasma membrane $Na^+$/ $H^+$ antiporter in *V. erythrospora*

Higher plants maintain $Na^+$ concentrations below toxic levels in the cytosol by extruding it into the external medium. Studies with radioactive $Na^+$ isotopes and amiloride have shown that both the salt-tolerant *C. longifolia* and the salt sensitive *C. corralina*, actively extrude $Na^+$ through $Na^+/H^+$ antiporters (Clint and MacRobbie 1987; Kiegle and Bisson 1996). A major pathway for $Na^+$ extrusion in higher plants is the SOS1 (Salt Overly Sensitive gene) encoded $Na^+/H^+$ antiporter which was initially identified in *Arabidopsis thaliana* and subsequently in other plants, including the halophyte *Thellungiella salsuginea* (Shi et al. 2000; Oh et al. 2009; Quintero et al. 2011). These antiporters are sensitive to amiloride, which inhibits $Na^+/H^+$ exchangers in algal, plant and animal systems (Kleyman and Cragoe 1988; Kiegle and Bisson 1996; Cuin et al. 2011). These extrusion mechanisms are thought to be crucial for the survival of these organisms in high salinity habitats.

In our flux reversal experiments, where $Na^+$ and $H^+$ fluxes were recorded simultaneously at low $Na^+$ concentrations (1 mM), the ions were observed to be in opposite phases (Fig. 4.15). In consequence, an influx of $Na^+$ was occurring simultaneously with $H^+$ efflux, which would be consistent with the operation of a $Na^+/H^+$ exchanger. Additionally it was observed that this flux reversal took place at a higher external $Na^+$ concentration of about 300 μM in the presence of amiloride (0.5mM; Fig. 4.7 A). This points to an antiporter operating in the opposite direction to that of the SOS1 encoded NHXs in higher plants, i.e., mediating active $Na^+$ uptake rather than extrusion. The habitat of *V. erythrospora* suggests an adaptive significance for this type of active $Na^+$ uptake mechanism. The alga was collected from the banks of an estuary with waters of varying salinity in addition to being exposed to the air at low tide with the subsequent possibility of increased salinity due to evaporation or decreased salinity during rainfall (Chapter 3). This mechanism possibly serves as a means of $Na^+$ uptake

against the electrochemical gradient during low salinity. Such an antiporter would not impact the $E_m$ if it was taking up 1 $Na^+$ for each $H^+$ extruded and would depend on the electrochemical gradient of $H^+$. This would require the cytosolic pH to be more acidic relative to that of the external medium. Additionally, the alga would be exposed to a hypoosmotic stress during freshwater exposure when it would have to extrude ions to regulate turgor. This suggests that $Na^+$ is possibly taken up as a nutrient through the $Na^+$/ $H^+$ antiporter under low external $Na^+$ concentrations.

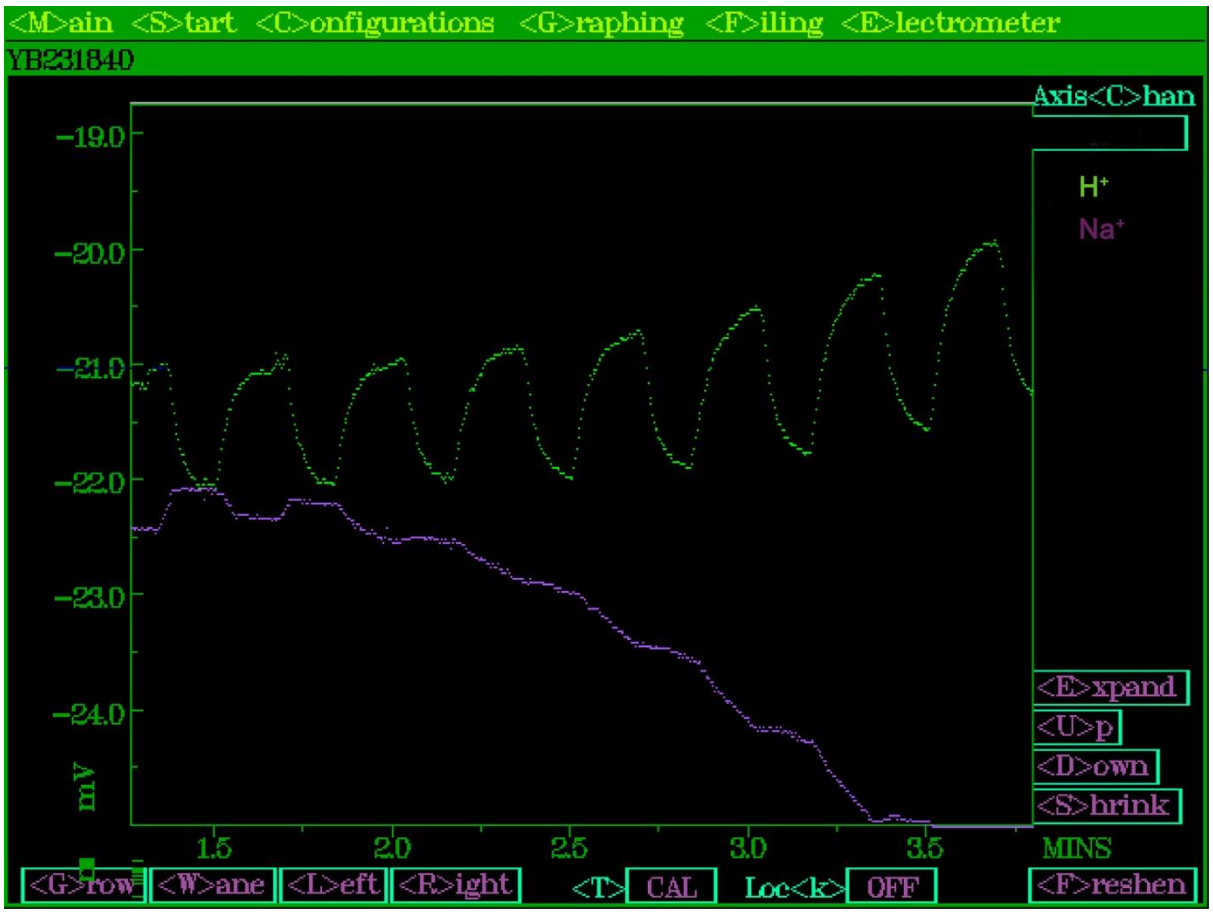


**Figure 4.15.** MIFE screenshot illustrating relationship between $Na^+$ and $H^+$ fluxes measured from *Vaucheria erythrospora* filaments. While the magnitude of $H^+$ flux (green trace) is increasing, $Na^+$ flux is decreasing (pink trace), so the flux changes occur in an opposite phase.

### 4.4.5. Role of $Ca^{2+}$ in turgor regulation

The inhibition of turgor regulation seen in this study by the $Ca^{2+}$ channel inhibitor, verapamil (10 µM; Fig 4.4 B), suggests that $Ca^{2+}$ may be important for the process in *V. erythrospora*. Calcium has been noted to control ion transport during turgor regulation by acting as a signalling molecule, for example through the regulation of $Ca^{2+}$ dependent $Cl^-$ channels in *C. longifolia* (Bisson et al. 1995). Greater $H^+$-ATPase pumping rates have been reported in *C. corralina* under high external $Ca^{2+}$ concentrations in response to NaCl shock (Amtmann and Beilby 2010). In the salt tolerant charophytes, *Lamprothamnium succinctum* and *Chara longifolia*, an influx of $Ca^{2+}$ into the cytosol was found to be necessary for turgor regulation under hypotonic stress (Okazaki and Tazawa 1990; Bisson et al. 1995; Okazaki et al. 2002). Stretch-activated $Ca^{2+}$ channels are also thought to play a role in turgor regulation in diverse organisms, for example, in hyphae of the oomycete *Saprolegnia ferax* and guard cells of higher plants (Cosgrove and Hedrich 1991; Garrill et al. 1992a; Garrill et al. 1993; Zhang et al. 2007). An increase in cytosolic $Ca^{2+}$, which is dependent on extracellular $Ca^{2+}$ concentrations, has been reported to either directly or indirectly limit $K^+$ efflux and $Na^+$ entry, and activate $Na^+$ extrusion in plants on exposure to NaCl shock (Shabala et al. 2006). $Ca^{2+}$ fluxes were not measured in this study.

It should however be noted that verapamil has been shown to directly inhibit outward rectifying $K^+$ channels in plant cells (Terry et al. 1992; Thomine et al. 1994). This raises questions with respect to the specificity of the inhibitor, thus the inhibition of turgor recovery observed in our study with verapamil could be $Ca^{2+}$-independent and occur due to its effects on other channels.

### 4.4.6. Role of organic osmolytes in turgor recovery

The presence of some polar organic compounds (glycerol, sorbitol, proline and maltose; Fig. 4.13) were detected in this study, which have been reported as osmolytes in diverse algae

(Ben-Amotz and Avron 1983; Kirst 1990). However, the rapid turgor recovery in *V. erythrospora* within 60 min in both pressure probe experiments (Chapter 3; Fig. 3.7) and from micrographs of stressed siphons (Fig. 4.10– 4.12) in response to NaCl shock is probably too quick for *de novo* synthesis of organic osmolytes (Shabala and Lew 2002). Such rapid recovery has been used to suggest in other systems that the process of turgor regulation is mediated predominantly by inorganic ions.

### 4.4.7. Conclusions

To the best of my knowledge, this is the first detailed investigation of the mechanisms of turgor regulation in a Xanthophycean alga and one of the few studies on algae other than charophytes and chlorophytes. *Vaucheria erythrospora* responds differently to hyperosmotic shocks induced by NaCl and sorbitol. The alga responds to a hyperosmotic shock imposed by NaCl with the passive entry of $Na^+$ into the cell through non-selective cation channels (NSCCs) which will depolarise the *E*m. This is followed by a repolarization and recovery to resting membrane potential possibly by increased proton extrusion by the $H^+$-ATPase and/or subsequent entry of $Cl^-$ possibly through anion channels and $H^+$ symport. Therefore in response to NaCl shock, the alga regulates turgor by taking up $Na^+$ and possibly $Cl^-$ (Fig. 4.16). A sorbitol-induced shock on the other hand, hyperpolarizes the membrane, which could be explained by the activation of the $H^+$-ATPase. This is followed by a depolarization which could be explained by $K^+$ uptake through inward rectifying channels (KIRCs) triggered by the hyperpolarization. $Na^+$ is also taken up possibly through NSCCs and $Cl^-$ through anion channels and $H^+$ symport. Hence, in addition to $Na^+$ and $Cl^-$, $K^+$ uptake also plays a role in turgor recovery in response to a sorbitol-induced shock (Fig. 4.17). The large vacuole in *Vaucheria,* which occupies most of the siphon could enable the uptake of large amounts of $Na^+$ as it could act as a compartment for $Na^+$ sequestration through the action of $Na^+/H^+$

antiporters in the tonoplast. This strategy allows for utilization of $Na^+$, which is available in the external environment, to regulate turgor, while keeping cytosolic $Na^+$ concentrations below toxic levels. During freshwater exposure in an estuary, when the external $Na^+$ is low, $Na^+$ is possibly taken up actively as a nutrient through an amiloride sensitive $Na^+/H^+$ antiporter. Also, by limiting $K^+$ efflux under high salinity, the alga retains $K^+$, vital for proper functioning of cellular processes. Its ability to regulate turgor by quickly taking up and efficiently compartmentalizing inorganic ions possibly helps *V. erythrospora* survive in an estuarine habitat.

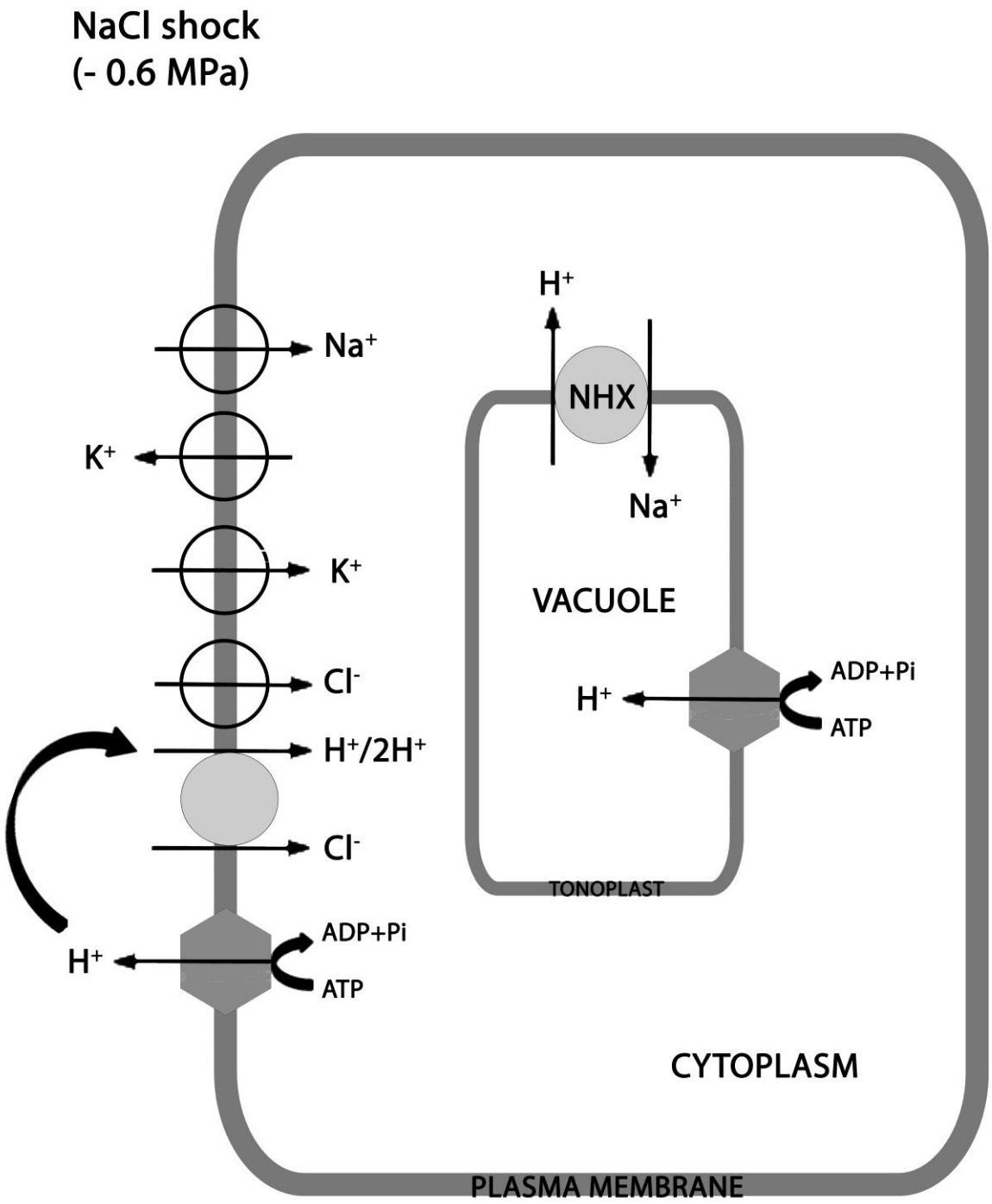


**Figure 4.16.** A model illustrating possible pathways of inorganic ion transport involved in turgor regulation after a NaCl-induced hyperosmotic shock (-0.6 MPa) in *Vaucheria erythrospora*. $Na^+$ is taken up passively through NSCCs depolarizing the $E_m$. Vacoular $Na^+$ compartmentalization is mediated by a tonoplast NHX. The plasma membrane $H^+$-ATPase is activated by drop in turgor, hyperpolarizating the $E_m$. $Cl^-$ is then taken up through a $H^+/Cl^-$ symporter which is driven by the $H^+$-ATPase generated $H^+$ gradient or through anion channels. $K^+$ efflux is limited under high salinity through KORCs. There is also a possibility of $K^+$ entry through KIRCs.

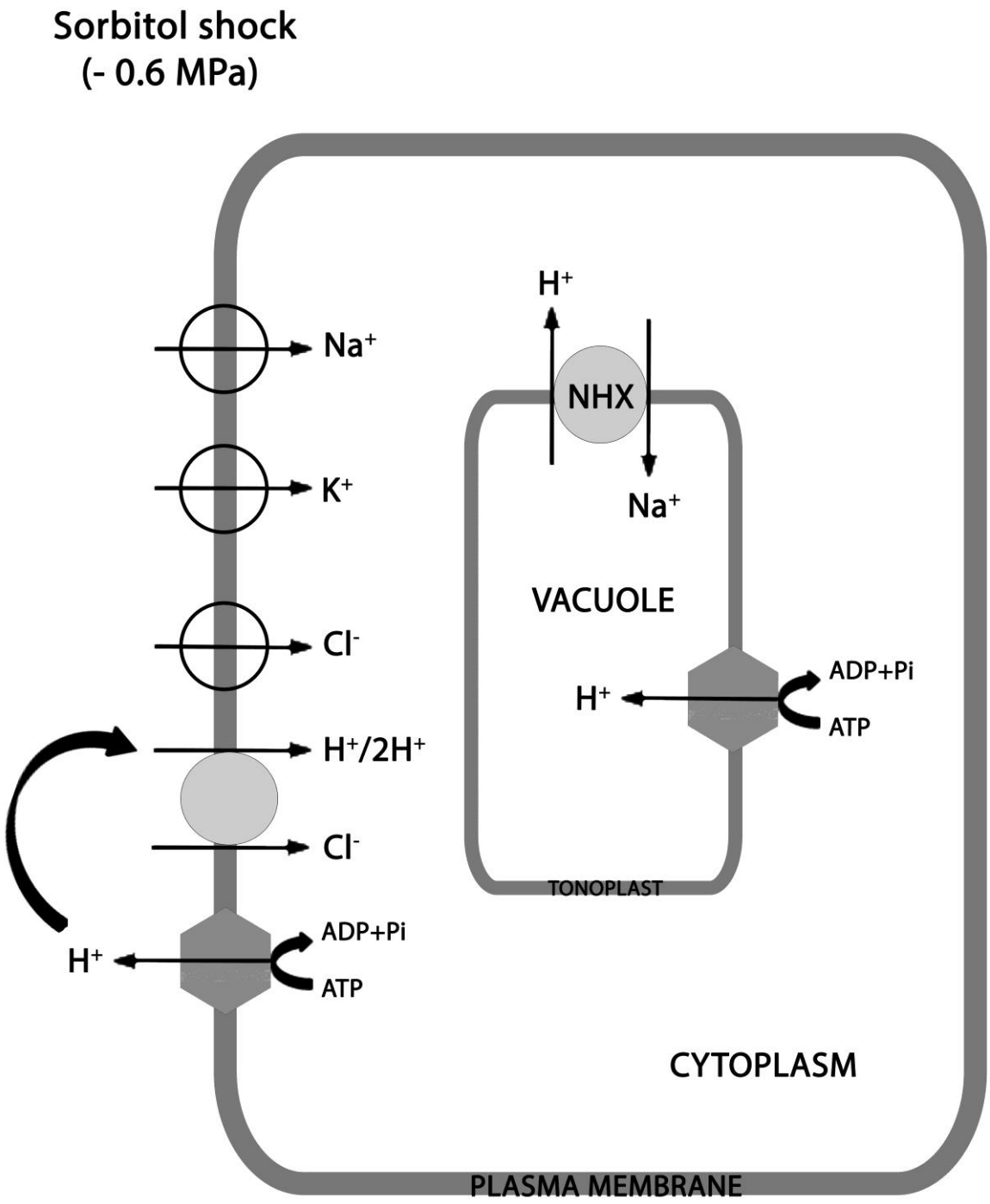


**Figure 4.17.** A model illustrating possible pathways of inorganic ion transport involved in turgor regulation after a sorbitol-induced hyperosmotic shock (-0.6 MPa) in *Vaucheria erythrospora*. The $H^+$- ATPase is activated by a drop in turgor and hyperpolarizes the $E_m$. $K^+$ is taken up through KIRCs, acxtivated by the hyperpolarization of $E_m$. $Cl^-$ is taken up through a $H^+/Cl^-$ symporter which is driven by the $H^+$-ATPase generated $H^+$ gradient or through anion channels. $Na^+$ is taken up passively through NSCCs. Vacoular compartmentalization of $Na^+$ is mediated by a tonoplast NHX.

## 4.5. References

Al Khazaaly S, Beilby MJ 2007. Modelling ion transporters at the time of hypertonic regulation in *Lamprothamnium succinctum* (Characeae, Charophyceae). Charophytes 1: 28-47

Amtmann A, Beilby M 2010. The Role of Ion Channels in Plant Salt Tolerance. In: Demidchik V, Maathuis F Ed. Ion Channels and Plant Stress Responses, Springer Berlin Heidelberg. Pp. 23-46.

Ben-Amotz A, Avron M 1983. Accumulation of metabolites by halotolerant algae and its industrial potential. Annual Review of Microbiology 37: 95-119.

Beilby MJ, Bisson MA, Shepherd VA 2006. Electrophysiology of Turgor Regulation in Charophyte Cells. In: Volkov A Ed. Plant Electrophysiology, Springer Berlin Heidelberg. Pp. 375-406.

Beilby MJ, Shepherd VA 2001. Modeling the current-voltage characteristics of charophyte membranes. II. The effect of salinity on membranes of *Lamprothamnium papulosum*. The Journal of Membrane Biology 181: 77-89.

Bisson MA, Beilby MJ 2002. The transport systems of *Ventricaria ventricosa*: hypotonic and hypertonic turgor regulation. The Journal of Membrane Biology 190: 43-56.

Bisson MA, Beilby MJ, Shepherd VA 2006. Electrophysiology of turgor regulation in marine siphonous green algae. The Journal of Membrane Biology 211: 1-14.

Bisson MA, Kirst GO 1980. *Lamprothamnium*, a euryhaline charophyte: I. Osmotic relations and membrane potential at steady state. Journal of Experimental Botany 31: 1223-1235.

Bisson MA, Kirst GO 1995. Osmotic acclimation and turgor pressure regulation in algae. Naturwissenschaften 82: 461-471.

Bisson MA, Bartholomew D 1984. Osmoregulation or turgor regulation in *Chara*? Plant Physiology 74: 252-255.

Bisson MA, Beilby MJ 2002. The transport systems of *Ventricaria ventricosa*: hypotonic and hypertonic turgor regulation. The Journal of Membrane Biology 190: 43-56.

Bisson MA, Beilby MJ, Shepherd VA 2006. Electrophysiology of turgor regulation in marine siphonous green algae. Journal of Membrane Biology 211: 1-14.

Bisson MA, Kiegle E, Black D, Kiyosawa K, Gerber N 1995. The role of calcium in turgor regulation in *Chara longifolia*. Plant, Cell and Environment 18: 129-137.

Blatt MR 1992. $K^+$ channels of stomatal guard cells. Characteristics of the inward rectifier and its control by pH. The Journal of General Physiology 99: 615-644.

Blumwald E, Aharon GS, Apse MP 2000. Sodium transport in plant cells. Biochimica et Biophysica Acta (BBA) - Biomembranes 1465: 140-151.

Bose J, Xie Y, Shen W, Shabala S 2013. Haem oxygenase modifies salinity tolerance in *Arabidopsis* by controlling $K^+$ retention via regulation of the plasma membrane $H^+$-ATPase and by altering SOS1 transcript levels in roots. Journal of Experimental Botany 64: 471-481.

Burg MB, Ferraris JD 2008. Intracellular organic osmolytes: function and regulation. Journal of Biological Chemistry 283: 7309-7313.

Chen Z, Newman I, Zhou M, Mendham N, Zhang G, Shabala S 2005. Screening plants for salt tolerance by measuring $K^+$ flux: a case study for barley. Plant, Cell and Environment 28: 1230-1246.

Clint GM, MacRobbie EAC 1987. Sodium efflux from perfused giant algal cells. Planta 171: 247-253.

Cosgrove D, Hedrich R 1991. Stretch-activated chloride, potassium, and calcium channels coexisting in plasma membranes of guard cells of *Vicia faba* L. Planta 186: 143-153.

Cuin TA, Tian Y, Betts SA, Chalmandrier R, Shabala S 2009. Ionic relations and osmotic adjustment in durum and bread wheat under saline conditions. Functional Plant Biology 36: 1110-1119.

Cuin TA, Bose J, Stefano G, Jha D, Tester M, Mancuso S, Shabala S 2011. Assessing the role of root plasma membrane and tonoplast $Na^+/H^+$ exchangers in salinity tolerance in wheat: in planta quantification methods. Plant, Cell and Environment 34: 947-961.

Cushman JC 2001. Osmoregulation in plants: implications for agriculture. American Zoologist 41: 758-769.

Demidchik V, Maathuis FJM 2007. Physiological roles of nonselective cation channels in plants: from salt stress to signalling and development. New Phytologist 175: 387-404.

Demidchik V, Davenport RJ, Tester M 2002. Non selective cation channels in plants. Annual Review of Plant Biology 53: 67-107.

Detmers FJM, de Groot BL, Müller EM, Hinton A, Konings IBM, Sze M, Flitsch SL, Grubmüller H, Deen PMT 2006. Quaternary ammonium compounds as water channel

blockers: specificity, potency and site of action. Journal of Biological Chemistry 281: 14207-14214

Faraday CD, Spanswick RM, Bisson MA 1996. Plasma membrane isolation from freshwater and salt-tolerant species of *Chara*: antibody cross-reactions and phosphohydrolase activities. Journal of Experimental Botany 47: 589–594.

Felle HH 1994. The $H^+/Cl^-$ symporter in root-hair cells of *Sinapis alba* (an electrophysiological study using ion-selective microelectrodes). Plant Physiology 106: 1131-1136.

Flowers TJ, Colmer TD 2008. Salinity tolerance in halophytes. New Phytologist 179: 945-963.

Frey N, Büchner KH, Zimmermann U 1988. Water transport parameters and regulatory processes in *Eremosphaera viridis*. The Journal of Membrane Biology 101: 151-163.

Garrill A, Clipson NJW, Jennings DH 1992a. Preliminary observations on the monovalent cation relations of *Thraustochytrium aureum*, a fungus requiring sodium for growth. Mycological Research 96: 295-304.

Garrill A, Lew RR, Heath IB 1992b. Stretch-activated $Ca^{2+}$ and $Ca^{2+}$-activated $K^+$ channels in the hyphal tip plasma membrane of the oomycete *Saprolegnia ferax*. Journal of Cell Science 101: 721-730.

Garrill A, Findlay GP, Tyerman SD 1996. Mechanosensitive ion channels. In: Smallwood M, Knox, JP and Bowles, DJ Eds. Membranes: Specialized Functions in Plants. Oxford, UK, Bios scientific publishers. Pp. 247-60.

Garrill A, Jackson S, Lew R, Heath IB 1993. Ion channel activity and tip growth: tip localized stretch-activated channels generate an essential $Ca^{2+}$ gradient in the oomycete *Saprolegnia ferax*. European Journal of Cell Biology 60: 358-365.

Gimmler H 2000. Primary sodium plasma membrane ATPases in salt-tolerant algae: facts and fictions. Journal of Experimental Botany 51: 1171-1178.

Hariadi Y, Marandon K, Tian Y, Jacobsen S-E, Shabala S 2011. Ionic and osmotic relations in quinoa (*Chenopodium quinoa* Willd.) plants grown at various salinity levels. Journal of Experimental Botany 62: 185-193.

Heidecker M, Wegner LH, Binder KA, Zimmermann U 2003. Turgor pressure changes trigger characteristic changes in the electrical conductance of the tonoplast and the plasmalemma of the marine alga *Valonia utricularis*. Plant, Cell & Environment 26: 1035-1051.

Hoffmann R, Bisson MA 1988. The effect of divalent cations on $Na^+$ tolerance in charophytes. I: *Chara buckellii*. Plant, Cell & Environment 11: 461-472.

Jayakannan M, Bose J, Babourina O, Rengel Z, Shabala S 2013. Salicylic acid improves salinity tolerance in *Arabidopsis* by restoring membrane potential and preventing salt-induced $K^+$ loss via a GORK channel. Journal of Experimental Botany 64: 2255-2268.

Kiegle EA, Bisson MA 1996. Plasma membrane $Na^+$ transport in a salt-tolerant charophyte (isotopic fluxes, electrophysiology, and thermodynamics in plants adapted to saltwater and freshwater). Plant Physiology 111: 1191-1197.

Kirst GO 1990. Salinity tolerance of eukaryotic marine algae. Annual Review of Plant Physiology and Plant Molecular Biology 41: 21-53.

Kirst GO, Bisson MA 1979. Regulation of turgor pressure in marine algae: ions and low molecular-weight organic compounds. Functional Plant Biology 6: 539-556.

Kleyman T, Cragoe E, Jr. 1988. Amiloride and its analogs as tools in the study of ion transport. The Journal of Membrane Biology 105: 1-21.

Lew RR, Levina NN, Walker SK & Garrill A 2004. Turgor regulation in hyphal organisms. Fungal Genetics and Biology 41:1007–1015.

Li M-y, Li F-j, Yue Y-s, Tian X-l, Li Z-h, Duan L-s 2013. NaCl-induced changes of ion fluxes in roots of transgenic *Bacillus thuringiensis* (Bt) cotton (*Gossypium hirsutum* L.). Journal of Integrative Agriculture 12: 436-444.

Lisec J, Schauer N, Kopka J, Willmitzer L, Fernie AR 2006. Gas chromatography mass spectrometry-based metabolite profiling in plants. Nature Protocols 1: 387-396.

Maathuis FJM, Amtmann A 1999. $K^+$ Nutrition and $Na^+$ Toxicity: The basis of cellular $K^+/Na^+$ ratios. Annals of Botany 84: 123-133.

Massana R, Castresana J, Balagué V, Guillou L, Romari K, Groisillier A, Valentin K, Pedrós Alió C 2004. Phylogenetic and ecological analysis of novel marine stramenopiles. Applied and Environmental Microbiology 70: 3528-3534.

Michelet B, Boutry M 1995. The plasma membrane $H^+$-ATPase: a highly regulated enzyme with multiple physiological functions. Plant Physiology 108: 1-6.

Money N, Harold F 1993. Two water molds can grow without measurable turgor pressure. Planta 190: 426-430.

Müller EM, Hub JS, Grubmüller H, de Groot BL. Is TEA an inhibitor for human aquaporin 1?

Newman IA 2001. Ion transport in roots: measurement of fluxes using ion-selective microelectrodes to characterize transporter function. Plant, Cell and Environment 24: 1-14.

Oh D-H, Leidi E, Zhang Q, Hwang S-M, Li Y, Quintero FJ, Jiang X, D'Urzo MP, Lee SY, Zhao Y and others 2009. Loss of halophytism by interference with SOS1 expression. Plant Physiology 151: 210-222.

Okazaki Y, Ishigami M, Iwasaki N 2002. Temporal Relationship between cytosolic free $Ca^{2+}$ and membrane potential during hypotonic turgor regulation in a brackish water charophyte *Lamprothamnium succinctum*. Plant and Cell Physiology 43: 1027-1035.

Okazaki Y, Shimmen T, Tazawa M 1984. Turgor regulation in a brackish charophyte, *Lamprothamnium succinctum* II. Changes in $K^+$, $Na^+$ and $Cl^-$ concentrations, membrane potential and membrane resistance during turgor regulation. Plant and Cell Physiology 25: 573-581.

Okazaki Y, Tazawa M 1990. Calcium ion and turgor regulation in plant cells. The Journal of Membrane Biology 114: 189-194.

Pandolfi C, Pottosin I, Cuin T, Mancuso S, Shabala S 2010. Specificity of polyamine effects on NaCl-induced ion flux kinetics and salt stress amelioration in plants. Plant and Cell Physiology 51: 422-434.

Pottosin II, Andjus PR 1994. Depolarization-activated $K^+$ channel in *Chara* droplets. Plant Physiology 106: 313-319.

Quintero FJ, Martinez-Atienza J, Villalta I, Jiang X, Kim W-Y, Ali Z, Fujii H, Mendoza I, Yun D-J, Zhu J-K and others 2011. Activation of the plasma membrane $Na^+/H^+$

antiporter salt-overly-sensitive 1 (SOS1) by phosphorylation of an auto-inhibitory C-terminal domain. Proceedings of the National Academy of Sciences 108: 2611-2616.

Ray PM, Green PB, Cleland R 1972. Role of turgor in plant cell growth. Nature 239: 163-164.

Reid RJ, Jefferies RL, Pitman MG 1984. *Lamprothamnium*, a euryhaline charophyte: IV. Membrane potential, ionic fluxes and metabolic activity during turgor adjustment. Journal of Experimental Botany 35: 925-937.

Sauer G, Simonis W, Schönknecht G 1993. An inwardly rectifying cation current across the plasma membrane of the green alga *Eremosphaera viridis*. Plant and Cell Physiology 34: 1275-1282.

Shabala L, McMeekin T, Shabala S 2009. Osmotic adjustment and requirement for sodium in marine protist thraustochytrid. Environmental Microbiology 11: 1835-1843.

Shabala L, Cuin T, Newman I, Shabala S 2005a. Salinity-induced ion flux patterns from the excised roots of *Arabidopsis* SOS mutants. Planta 222: 1041-1050.

Shabala S 2000. Ionic and osmotic components of salt stress specifically modulate net ion fluxes from bean leaf mesophyll. Plant, Cell and Environment 23: 825-837.

Shabala S, Cuin TA 2008. Potassium transport and plant salt tolerance. Physiologia Plantarum 133: 651-669.

Shabala S, Shabala L, Van Volkenburgh E, Newman I 2005. Effect of divalent cations on ion fluxes and leaf photochemistry in salinized barley leaves. Journal of Experimental Botany 56: 1369-1378.

Shabala S, Demidchik V, Shabala L, Cuin TA, Smith SJ, Miller AJ, Davies JM, Newman IA 2006. Extracellular $Ca^{2+}$ ameliorates NaCl-induced $K^+$ loss from *Arabidopsis* Root and Leaf cells by controlling plasma membrane $K^+$-permeable channels. Plant Physiology 141: 1653-1665.

Shabala SN, Bose J 2012. Application of non-invasive microelectrode flux measurements in plant stress physiology. In: Volkov AG Ed. Plant Electrophysiology. Springer Berlin Heidelberg. Pp. 91–126.

Shabala SN, Lew RR 2002. Turgor regulation in osmotically stressed *Arabidopsis* epidermal root cells. Direct support for the role of inorganic ion uptake as revealed by concurrent flux and cell turgor measurements. Plant Physiology 129: 290–299.

Shepherd VA, Beilby MJ, Bisson MA 2004. When is a cell not a cell? A theory relating coenocytic structure to the unusual electrophysiology of *Ventricaria ventricosa* (*Valonia ventricosa*). Protoplasma 223: 79-91.

Shi H, Ishitani M, Kim C, Zhu J-K 2000. The *Arabidopsis thaliana* salt tolerance gene SOS1 encodes a putative $Na^+/H^+$ antiporter. Proceedings of the National Academy of Sciences 97: 6896-6901.

Smethurst CF, Rix K, Garnett T, Auricht G, Bayart A, Lane P, Wilson SJ, Shabala S 2008. Multiple traits associated with salt tolerance in lucerne: revealing the underlying cellular mechanisms. Functional Plant Biology 35: 640-650.

Sun J, Dai S, Wang R, Chen S, Li N, Zhou X, Lu C, Shen X, Zheng X, Hu Z and others 2009. Calcium mediates root $K^+/Na^+$ homeostasis in poplar species differing in salt tolerance. Tree Physiology 29: 1175-1186.

Teakle NL, Tyerman SD 2010. Mechanisms of $Cl^-$ transport contributing to salt tolerance. Plant, Cell and Environment 33: 566-589.

Teodoro AE, Zingarelli L, Lado P 1998. Early changes of $Cl^-$ efflux and $H^+$ extrusion induced by osmotic stress in *Arabidopsis thaliana* cells. Physiologia Plantarum 102: 29-37.

Terry BR, Findlay GP, Tyerman SD 1992. Direct effects of $Ca^{2+}$ channel blockers on plasma membrane cation channels of *Amaranthus tricolor* protoplasts. Journal of Experimental Botany 43: 1457-1473.

Thomine S, Zimmermann S, Van Duijn B, Barbier-Brygoo H, Guern J 1994. Calcium channel antagonists induce direct inhibition of the outward rectifying potassium channel in tobacco protoplasts. FEBS Letters 340: 45-50.

Tyerman SD, Skerrett M, Garrill A, Findlay GP, Leigh RA 1997. Pathways for the permeation of $Na^+$ and $Cl^-$ into protoplasts derived from the cortex of wheat roots. Journal of Experimental Botany 48: 459-480.

Wegmann K 1986. Osmoregulation in eukaryotic algae. FEMS Microbiology Letters 39: 37-43.

Wu H, Shabala L, Barry K, Zhou M, Shabala S 2013. Ability of leaf mesophyll to retain potassium correlates with salinity tolerance in wheat and barley. Physiologia Plantarum 149: 515-527.

Yancey P, Clark M, Hand S, Bowlus R, Somero G 1982. Living with water stress: evolution of osmolyte systems. Science 217: 1214-1222.

Yao X, Bisson MA, Brzezicki LJ 1992. ATP-driven proton pumping in two species of *Chara* differing in salt tolerance. Plant, Cell & Environment 15: 199-210.

Young AJ, Collins JC, Russell G 1987. Solute regulation in the euryhaline marine alga *Enteromorpha prolifera* (O. F. Müll) J. Ag. Journal of Experimental Botany 38: 1298-1308.

Zhang W, Fan L-M, Wu W-H 2007. Osmo-sensitive and stretch-activated calcium-permeable channels in *Vicia faba* guard cells are regulated by actin dynamics. Plant Physiology 143: 1140-1151.

Zhu J-K 2003. Regulation of ion homeostasis under salt stress. Current Opinion in Plant Biology 6: 441-445.

Zingarelli L, Teresa Marrè M, Massardi F, Lado P 1999. Effects of hyper-osmotic stress on $K^+$ fluxes, $H^+$ extrusion, transmembrane electric potential difference and comparison with the effects of fusicoccin. Physiologia Plantarum 106: 287-295.

# Chapter 5

## Summary and Future Directions

The aim of this study was to look at the responses to hyperosmotic stress of different species of the xanthophycean alga, *Vaucheria*. Other than the chlorophytans and charophyceans, our knowledge of the responses of algae to osmotic stress is limited.

Chapter 2 presents the morphological and phylogenetic characterization of *Vaucheria* specimens collected from contrasting habitats in New Zealand. Seven species were identified based on the morphology of their reproductive structures. Two were described as new species, *V. aestuarii* from an estuary and *V. edaphica* from moist soil. Two from brackish habitats, *V. erythrospora* and *V. litorea*, were reported for the first time in New Zealand. *V. repens* (= *V. bursata*), a freshwater species and *V. erythrospora* were selected for further study.

Chapters 3 and 4 describe the ability of these two species to regulate turgor in response to hyperosmotic shock. *V. erythrospora* was found to regulate after greater hyperosmotic shocks and grow over a wider range of media salinities than *V. repens*. These different responses may underlie the ability of *V. erythrospora* to survive in an estuary and restrict *V. repens* to freshwater. Experiments using inhibitors of membrane transport proteins and measurements of ion fluxes and membrane potentials suggest that *V. erythrospora* may regulate turgor after a hyperosmotic shock. The mechanism involves the uptake of $Na^+$ and other inorganic ions, compartmentalization of $Na^+$ in the vacuole and limitation of $K^+$ loss. The role of organic osmolyte synthesis in the process was considered to be negligible because of the rapidity of recovery.

While this study has added to current knowledge on *Vaucheria*, it has raised many questions that warrant further investigation.

Do marine species of *Vaucheria* that are subject to little osmotic variation, have a reduced ability to regulate turgor? If so, is the mechanism similar to that of freshwater *V. repens*?

Future research could also determine whether other freshwater and estuarine *Vaucheria* and indeed other stramenopile algae like the large brown seaweeds share the same abilities and mechanisms as the ones reported here. Species growing on moist soil like *V. edaphica*, likely to be exposed to dessication stress, could also be tested.

Earlier studies which reported the inability of freshwater oomycetes to regulate turgor used hyperosmotic shocks of greater magnitude (-0.6 MPa) than those used on *V. repens* in this study (-0.2 MPa). Would oomycetes be able to turgor regulate after milder osmotic shocks? Oomycetes from marine environments could also be tested.

$Cl^-$ fluxes in *V. erythrospora* are worthy of investigation in order to test the hypothesis that $Cl^-$ plays a role in turgor recovery.

The preliminary results of this study suggest the operation of a $Na^+/H^+$ antiporter in the plasma membrane of *V. erythrospora*. This possibly mediates $Na^+$ uptake for nutritional purposes. Molecular and electrophysiological investigations are needed to confirm the presence of this antiporter.

Finally, this study reported two new species from a just a small collection of strains. This suggests that the diversity of *Vaucheria* in New Zealand is poorly known. Extensive collections and the application of morphological and molecular phylogenetic approaches could extend their known diversity considerably as well as providing opportunity to test the currently accepted taxonomy of the genus.

# Recipes for media used for growth of *Vaucheria* strains

## 1. BBM medium (Bold's Basal Medium with vitamins) composition

**Stock solution ($L^{-1}$)**

| Chemical | Concentration (g $L^{-1}$) |
|---|---|
| **Main elements** | |
| $NaNO_3$ | 25 |
| $MgSO_4$. $7H_2O$ | 7.5 |
| NaCl | 2.5 |
| $K_2HPO_4$ | 7.5 |
| $KH_2PO_4$ | 17.5 |
| $CaCl_2$. $2H_2O$ | 2.5 |
| **Trace elements** | |
| $ZnSO_4.7H_2O$ | 8.82 |
| $MnCl_2.4H_2O$ | 1.44 |
| $MoO_3$ | 0.71 |
| $CuSO_4.5H_2O$ | 1.57 |
| $Co(NO_3)_2.6H_2O$ | 0.49 |
| **Vitamins mix** | |
| Cyanocobalamin (Vitamin B12) | 0.0005 |
| Thiamine.HCl (Vitamin B1) | 0.1 |
| Biotin (Vitamin H) | 0.0005 |

**Medium ($L^{-1}$)**

| Chemical | ml $l^{-1}$ |
|---|---|
| Main elements from stock | 10 (each element) |
| Trace elements from stock | 1 |
| Vitamin mix from stock | 1 |

The media was made up in distilled water and pH was adjusted using 1M HCl and 1M NaOH to 7. The vitamin mix was filter sterilized and added after autoclaving.

2. **Modified f/2 medium composition**

**Stock solution ($L^{-1}$)**

| Chemical | Concentration (g $l^{-1}$) |
|---|---|
| **Trace elements** | |
| $Na_2$ EDTA | 4.16 |
| $FeCl_3.6H_2O$ | 3.15 |
| $ZnSO_4.7H_2O$ | 0.022 |
| $CuSO_4.5H_2O$ | 0.01 |
| $CoCl_2.6H_2O$ | 0.01 |
| $MnCl_2.4H_2O$ | 0.18 |
| $Na_2MoO_4.2H_2O$ | 0.006 |
| **Vitamin mix** | |
| Cyanocobalamin (Vitamin B12) | 0.0005 |
| Thiamine.HCl (Vitamin B1) | 0.1 |
| Biotin (Vitamin H) | 0.0005 |

**Medium ($L^{-1}$)**

| Chemical | Composition ($l^{-1}$) |
|---|---|
| $NaNo_3$ | 0.075 g |
| $NaH_2PO_4.2H_2O$ | 0.00565 g |
| Trace elements from stock | 1 ml |
| Vitamin mix from stock | 1 ml |

The medium was made up with 1 litre of diluted filtered seawater to give a salinity of 1.2 ‰. The pH was adjusted to 7 with 1M NaOH or HCl. The vitamin mix was filter sterilized and added after autoclaving.

A copy of the following published manuscript containing some data from Chapters 2, 3 and 4 is attached in the pages that follow:

Muralidhar, A, Novis, PM, Broady, PA, Collings, DA, Garrill, A. (2013) An estuarine species of the alga *Vaucheria* (Xanthophyceae) displays an increased capacity for turgor regulation when compared to a freshwater species. Journal of Phycology 49: 967-978.

Published manuscript not available due to copyright restrictions.